

DEPARTMENT OF MINES AND ENERGY
SOUTH AUSTRALIA

SCANNED

REPT. BK. NO. 91/61
REPORT ON THE 12TH BIENNIAL
CONFERENCE, AUSTRALIAN CLAY
MINERALS SOCIETY, BALLARAT
4-7 FEBRUARY, 1991 AND TEXT OF
PAPER PRESENTED ON THE MOUNT
HOPE KAOLIN DEPOSIT, EYRE
PENINSULA, SOUTH AUSTRALIA.

GEOLOGICAL SURVEY

by

J.L. KEELING
MINERAL REOSURCES

and

M.D. RAVEN
CSIRO - DIVISION OF SOILS

JUNE, 1991

DME 50/83

**ABSTRACT
COMPLETE**

<u>CONTENTS</u>	<u>PAGE</u>
ABSTRACT	1
INTRODUCTION	2
TEXT OF TALK	3
Introduction	3
Geology	3
Exploration and Testing	4
Recent Studies	7
Concluding Remarks	13
REFERENCES	14

<u>FIGURES</u>	<u>Plan No.</u>
1. Eyre Peninsula - Tectonic Map	S22085
2. Eyre Peninsula - Geological Map	S22086
3. Mount Hope Kaolin deposit - Geology and location	S21044
4. Mount Hope Kaolin deposit - Drillhole Location	89-383
5. X-ray diffraction traces - MH54 (formamide)	S22087
6. X-ray diffraction traces - MH54, 64 and 67	S22087

<u>PLATES</u>	<u>Slide/Photo No.</u>
1. Mount Hope kaolin deposit - shaft site.	39494
2. Thin section of kaolin ore from the shaft site.	39495
3. Shaft sample, thin section showing remnant mica flakes interleaved in coarse crystal stacks of kaolinite.	39496
4. Scanning electron micrograph of coarse kaolinite platelets in the <2 μ m size fraction.	38894
5. Scanning electron micrograph of coarse stacks of kaolinite crystals from the shaft sample.	38898

6.	Detail of a coarse kaolinite stack showing open structure.	38899
7.	Transmission electron micrograph of a coarse kaolinite platelet.	38906
8.	Dehydrated tubular halloysite in the <2 μ m fraction of a kaolin sample from hole MH54.	39497
9.	Disrupted halloysite tube together with well crystalline fine-grained kaolinite.	38903
10.	Detail of tubes showing flattened ends due to collapse.	39498
11.	Detail of a rolled tube showing regular terminations on the tube end (top of photo).	38908

APPENDICES

APPENDIX A	List of conference delegates	A1-A3
APPENDIX B	Conference programme Abstracts of papers and posters	Bi-Bv B1-B44
APPENDIX C	Notes for mid-conference excursion to heavy clay industries in the Ballarat area.	C1-C22

FIGURES

Fig. No.	
1.	Vitclay - Ballarat plant
2.	Selkirk Brick
3.	Enfield Claypit
4-12.	XRD results, Enfield Pit

PLATES

Plate No.		Neg. No
C1	Vitclay Pipes Pty Ltd, Ballarat plant	39499
C2	Vitclay Pipes, Ballarat, Sewer pipes	39500
C3	Selkirk Brick, Ballarat North pit	39501
C4	Selkirk Brick, extrusion plant	39502
C5	Enfield Clay Pit	39503
C6	Enfield Clay Pit, detail of plastic clay	39504
C7	Buninyong Clay Pit	39505

APPENDIX D Field guide for post-conference
 excursion of kaolin mining at Lal Lal
 and Pittong.

D1-D16

FIGURES

Fig. No.

1. Geology of the Lal Lal area
2. Block diagram of the Lal Lal area
3. Lal Lal Iron Company Mines

PLATES

Plate No.

D1	Lal Lal Kaolin Pit
D2	Lal Lal Dyke Kaolin Deposit
D3	Pittong Kaolin Deposit

Neg. No.

39506
39507
39508

DEPARTMENT OF MINES AND ENERGY
SOUTH AUSTRALIA

REPT BK NO 91/61
DME NO 50/83
DISK NO G02521

THE MOUNT HOPE KAOLIN DEPOSIT, EYRE PENINSULA,
SOUTH AUSTRALIA

ABSTRACT

A large primary kaolin deposit was outlined, during 1972-73, in deeply weathered gneiss and schist south of Mount Hope township on southwestern Eyre Peninsula. Although sampling indicated well-crystallised kaolinite of moderate to good brightness, the yield of $<2\mu\text{m}$ size fraction was low and the rheological properties were poor. Subsequent evaluation of bulk samples in West Germany suggested that viscosity could be improved to meet paper-coating specifications. Recent mineralogical studies show a variety of kaolin morphologies, from broad ragged-edged sheets to thin platelets and rolled sheets or tubes.

For some samples, dispersion in water results in a high proportion of coarse thin platelets which may comprise the bulk of, or be difficult to separate from the $<2\mu\text{m}$ fraction, and probably contribute to the poor rheological properties. Production of a coating-grade kaolin will require beneficiation which improves the yield and effective separation of the $<2\mu\text{m}$ size particles. Where the $<2\mu\text{m}$ fraction comprises predominantly tubular forms, the kaolin may be suitable only for filler grades.

INTRODUCTION

The Australian Clay Minerals Society is an informal grouping of mineralogist, geologists, chemists, physicists, geomorphologists, engineers and soil scientists interested in clay minerals. The only organised function of the society is a biennial conference. Attendance at a conference confers membership of the society for a period of two years.

The 12th Biennial Conference was held in Ballarat at Ballarat University College from 4 to 7 February, 1991. The conference comprised two days of formal paper and poster presentation separated by a one day mid-conference field excursion of heavy clay industries in the Ballarat area. A one day post-conference field excursion was held which included a visit to kaolin mining operations at Lal Lal and Pittong.

Seventy seven delegates, see Appendix A, registered for the first three days of the conference and about 40 people attended the post-conference excursion.

Text of the paper on Mount Hope Kaolin Deposit presented at the conference is reproduced here in full.

The programme and abstracts of papers presented at the conference are given in Appendix B.

Field notes for the one day mid-conference excursion and post-conference excursion are reproduced in Appendices C and D respectively.

At the Business Meeting held on 6 February, details were announced on progress with preparations to hold the 10TH INTERNATIONAL CLAY CONFERENCE in Adelaide from 18-26 July 1993. The venue will be Adelaide University. S. A. Department of Mines and Energy has indicated support and assistance, in particular with field excursions.

TEXT OF TALK

Introduction

* SLIDE 1 (tectonic map, Fig.1)

The Mount Hope deposit was one of three large kaolin deposits on Eyre Peninsula which were investigated during the early 1970s. The other deposits were at Kimba (CSR-Pechiney, 1969-70) and Mount Sturt (Sadex Pty Ltd, 1971-75). Despite claims published in the local press at the time that the area would become a major world source of high-grade kaolin for the paper industry, none of the deposits were subsequently developed. Investigations have continued at Mount Hope, and more recently, interest in exploration for kaolin in the area has been renewed following the discovery, in 1984, of large deposits in the Inkster area, east of Streaky Bay.

Geology

There is considerable potential for large areas of kaolinized bedrock to be preserved on Eyre Peninsula. The tectonic map (Fig.1) shows that most of western Eyre Peninsula is underlain by granitic and gneissic bedrock. The more favourable units are the Archean Sleaford Complex gneiss and granite (~2300 Ma) and the younger Middle Proterozoic Hiltaba Suite granite (~1450 Ma). These are amongst some of the oldest rocks on the

Australian continent and for the most part, have had long and complex weathering histories.

* SLIDE 2 (Geological map, Fig.2)

The geological map of the same area, more accurately reflects our knowledge of the distribution of basement rocks. Most of western and southern Eyre Peninsula are covered by Quaternary deposits. These include Bridgewater Formation calcareous dunes along the western and southern margins of the Peninsula, and quartz dune sand and fluvial deposits in the interior. With the exception of a few prominent topographic highs of mainly unweathered granite or metasediments, this cover effectively masks the basement rocks. Although this blanket of younger sediments has helped to preserve areas of deeply weathered bedrock, it has also proved to be a major impediment to exploration and possibly to mining.

* SLIDE 3 (Mt Hope Geol Map, Fig.3)

In the Mount Hope area, basement geology is best exposed along the coast at Drummond Point and as a discontinuous range of low hills which include Mount Hope and Mount Drummond. The remainder of the area is covered mainly by calcareous dunes and interdunal clay and calcrete. The basement outcrops are all Sleaford Complex granite, and, in the absence of any bedrock outcrop in the area of the kaolin deposit, it was assumed that this area was also underlain by granite.

Exploration and Testing

* SLIDE 4 (Mount Hope kaolin deposit Fig.4)

Exploration for kaolin at Mount Hope commenced in 1971 following the intersection of a thick interval of white kaolinized bedrock in a well, drilled for stock water, on the property "Allerton

Hills". Encouraging results were obtained in early company drilling by Exploration Drilling and Blacker Motors. Samples contained between 40 - 60%, well-crystalline, white kaolinite showing good to excellent brightness. An agreement to explore and develop the deposit was made with Abaleen Minerals No Liability. During 1972 - 73, 52 rotary/air holes were drilled which outlined a large residual kaolin deposit. Indicated resources of 11 million tonnes of ore averaging 10m thickness were delineated below 5 to 12m thickness of overburden which comprised mainly Bridgewater Formation and iron-stained kaolin.

Development of the deposit was always contingent on the kaolin product being acceptable for paper coating markets. The need to produce a product which could be offered for sale at this top end of the kaolin market was, and still is, considered essential to the economics of opening up the deposit. Broadly, the requirements for this market include:

- . a high degree of brightness, typically above 85% reflectance and preferably above 87%
- . fine particle size: 100% < 5 μ m with 80 - 92% < 2 μ m
- . good rheological properties such that slurries remain fluid at solids contents of around 70%.

Test work on the < 2 μ m fraction confirmed acceptable brightness which varied between 83 to 90% reflectance for the raw product. However, the yield of < 2 μ m fraction was low and the rheological properties were poor.

Independent evaluation of the deposit for paper coating markets was sought, and an experienced German geologist, Dr Gerhart Stadler was engaged to direct field operations and supervise the mineralogical studies. Erbslöh and Co of West Germany were commissioned for the industrial assessment which included beneficiation methods and product testing.

The initial work was frustrated by contamination of some of the original drillhole samples by overlying carbonate units. Consequently, the majority of the test work was done on a 40 tonne bulk sample taken from a 21m deep shaft sunk for the purpose.

* SLIDE 5 (Shaft site Plate 1)

The shaft is still accessible today, down to about 17m, and provides the only exposure of kaolinized bedrock on the site.

Some excellent work was done by Stadler and Erbslöh and a paper coating product with acceptable rheological properties was produced after extensive tests using samples from the shaft. However, the yield of fine-grained particles remained low. In laboratory tests, recoveries of about 11% < 2 μ m fraction were obtained but in small scale production tests, results were as low as 3 - 4% (Abaleen Minerals NL, 1974).

Further test work was recommended by Erbslöh but this never eventuated. Abaleen Minerals went into provisional liquidation in December 1973. Erbslöh never recovered the monies owing for the laboratory test work and did not submit a final report of their investigations.

* SLIDE 6 (Map of deposit, Fig.4)

The deposit changed hands in 1975 and again in 1977 when it was acquired by the present leaseholders. They attracted the interest of the Caledon Resources Group who, after a detailed assessment of the background to the earlier test work, drilled a further 19 reverse circulation holes to confirm the size of the deposit and to obtain further samples for testing.

The test results were disappointing in that they confirmed an overall low yield of < 2µm fraction which varied from 5 to 26%, and averaged 11%. The results also recorded poor rheological properties. Samples varied from thixotropic to dilatant and were fluid at solids contents ranging from 42 - 66%, generally well below the required 70% solids. Attempts to upgrade the rheology of selected samples based on incomplete data of the Erbslöh process were largely unsuccessful.

Recent Studies

Our involvement with Mount Hope started in late 1988 and formed the beginnings of a collaborative research project on South Australian kaolin deposits by the South Australian Department of Mines and Energy and CSIRO - Division of Soils. Several staff at CSIRO have had input into the project and I take this opportunity to acknowledge particularly contributions from Tony Milnes, Stuart McClure, Peter Self and Adrian Beech.

Our initial work included an electron microscope (SEM & TEM) study of 2 samples from drillholes MH 59 and MH 52 which showed different rheologies (Keeling et al., 1989). We also did some petrology of samples of kaolin ore collected from the shaft. This led to a more detailed study of 36 drillhole samples spread throughout the orebody. This latter study included particle

size analysis, chemistry, soluble salt content, X-ray diffraction and electron microscopy.

The initial work showed that we were not dealing with a simple weathered granite bedrock, and that the kaolin mineralogy of different samples varied substantially. The later study was designed to assess the nature and extent of this variation and the effect that this would have on future sampling for beneficiation tests and on reserve estimates.

The outcome of that assessment, which was sponsored by Caledon Resources, is currently confidential. However the work highlighted some potential problems with assessing residual kaolin deposits which I propose to discuss briefly in the time remaining.

The fact that no core samples were taken through the orebody contributed to the assumption that the kaolin formed by alteration of an essentially homogeneous granitic bedrock.

* SLIDE 7 (Thin section 16x mag, Plate 2)

Thin sections of samples from the shaft showed complexly folded quartz lenses and areas of high mica content now mostly altered to kaolinite. In this slide, taken with crossed polars, kaolinite comprises the finer grained groundmass and appears dark blue to black. Rock texture and mica content varied down the shaft, but were consistent with a host rock composed of interlayered schist and gneiss. This correlated more closely with the highly metamorphosed Wangarry Gneiss into which the Sleaford Complex granites had been intruded. Variation in kaolin content and mineralogy might therefore be expected, which would reflect the variation in original mineralogy due to compositional banding and folding. This appears to be the case,

and a wide range of kaolin morphologies were recorded across the deposit.

In the shaft area, kaolin formed from weathering of both feldspar and mica with a relatively high contribution from the mica.

* SLIDE 8 (Thin section 200x mag., Plate 3)

Remnant mica flakes are still visible interleaved in some of the coarse-grained kaolinite booklets. This type of sample contained a high proportion of coarse-grained kaolinite and proved to have special problems when determining particle size distribution and in separating the $< 2\mu\text{m}$ fraction. The separation and determination of various size fractions was done by conventional pipette sedimentation techniques.

* SLIDE 9 (Coarse platelets, Plate 4)

However, subsequent electron microscope examination of the $< 2\mu\text{m}$ fractions showed that a significant proportion of platelets were $> 2\mu\text{m}$ diameter, and up to $10\mu\text{m}$ in size. In some samples, these coarse platelets would exceed 50% of the fraction. Their inclusion in the $< 2\mu\text{m}$ fraction appears to be a function of their high aspect ratio. During sedimentation, large, thin platelets tend to adopt a glide path which results in longer settling times and hence poor separation from the finer-grained particles.

* SLIDE 10 (SEM shaft sample bulk, Plate 5)

In samples from the shaft, kaolinite crystals commonly form as coarse stacks of platelets 10 - $20\mu\text{m}$ in diameter and up to $50\mu\text{m}$ in length.

* SLIDE 11 (SEM detail of stack, Plate 6)

These stacks are quite open and readily break down with handling and dispersion to give thin platelets 0.1 - 0.3 μ m thick and 5 to 20 μ m across. The platelets have aspect ratios of 10:1 to 100:1 and a significant proportion of these collect along with the < 2 μ m fraction.

* SLIDE 12 (TEM kaolin flake, Plate 7)

The coarse platelets often comprise a mosaic of interlocking smaller euohedral kaolinite crystals (Area A). These appear to crystallise as small epitaxial overgrowths on a weathering mica cleavage surface. They subsequently become intergrown to form a larger platelet pseudomorphing the original mica surface.

The presence of these coarse particles in the < 2 μ m fraction adversely effects the viscosity and appears to be responsible for the dilatant behaviour shown by some samples (ie. these samples typically show an increase in viscosity during high speed mixing). Their presence also gives an over estimate of the proportion of < 2 μ m sized particles, which results in an over estimate of the yield of paper coating product.

* SLIDE 13 (SEM tubular kaolin, Plate 8)

We were surprised during our initial electron microscope study to find that one sample contained a significant proportion of tubular kaolin, which we assumed to be halloysite. The presence of halloysite had not been recorded in any of the previous test work on samples from Mount Hope. Abundant halloysite in the < 2 μ m fraction would preclude kaolin from that part of the deposit being used as feed for a paper coating product. Consequently, an important aspect of the later test work was to

determine the relative abundance of tubular forms in samples and to examine their distribution within the deposit.

A widely accepted test to determine the relative abundance of halloysite in a mixture with kaolinite is to saturate the prepared sample with formamide and to monitor any reaction using X-ray diffraction (Churchman et al, 1984).

* SLIDE 14 (Graph formamide results MH 54 14-15m, Fig.5)
Halloysite or dehydrated halloysite rapidly intercalate formamide and swell to give a characteristic 10° peak. The ratio of intensity of the 10° peak to the kaolinite basal 7° peak gives an estimate of the abundance of halloysite relative to kaolinite. These graphs record the results of formamide treatment of the sample shown in the previous slide. The sample contained an estimated 80% tubes yet failed to show any 10° peak after 30 minutes, the recommended maximum time for the test. There was a decrease in the intensity of 7° peak recorded at 45 minutes, and there was some swelling recorded after 2 hours which is shown in the lower trace. The swelling continued to a maximum reached after about 6 hours but unfortunately, this long term swelling is not diagnostic and was also recorded for samples which contained only kaolinite platelets. The reaction with formamide recorded for this sample was typical of that shown by other samples tested from the deposit which also contained a significant proportion of tubular kaolin.

The failure of the formamide treatment method to detect the presence of halloysite-like tubes in the Mount Hope deposit appears to be related to the degree of dehydration of the tubes. When examined in detail, the tubes show various stages of collapse.

* SLIDE 15 (Disrupted tube, Plate 9)

Some are completely disrupted.

* SLIDE 16 (Flattened tubes, Plate 10)

Others appear flattened or have rectangular end sections.

* SLIDE 17 (Terminated tubes, Plate 11)

Some show signs of recrystallisation with regular terminations on tube ends.

In order to determine the presence and proportion of tubes, we resorted to systematic point counting using representative scanning electron micrographs of the $< 2\mu\text{m}$ size fractions.

* SLIDE 19 (X-ray traces, Fig.6)

We also looked at the broader pattern of X-ray diffraction traces and did some preliminary work on comparison of traces and relating this to the electron microscope results. As this slide illustrates, there are differences in the pattern of reflections particularly in the $22-28^\circ 2\theta$ region. In some samples this correlated well with the proportion of tubes determined from electron micrographs. In other samples showing a high degree of preferred orientation, or poorly crystalline platelets, the results were more difficult to interpret.

Insufficient samples were tested to make definitive comments on the distribution of tubular kaolin within the deposit. Some drillholes, with very high concentrations of tubular kaolin at depth, showed a decrease in the tube content up the hole with a corresponding increase in the proportion of degraded tubes and the proportion of fine-grained, less well-crystalline kaolinite. There were however, examples from other drillholes which suggested a more complex relationship.

Concluding Remarks

In conclusion, we make the observation that the generally accepted methods of evaluation of a kaolin deposit (ie. using brightness and viscosity testing, together with X-ray diffraction for mineralogy, and particle size distribution by sedimentation) while essential to the assessment, in this case failed to give a true picture of the deposit. Our work has convinced us of the need to undertake sufficiently detailed investigations to ensure that the results obtained from standard methods are being correctly interpreted.

As for the Mount Hope deposit, we still have the same problems identified in the earliest test work, ie. a low yield of $< 2\mu\text{m}$ fraction and poor rheological properties. However we do have a much better understanding of the causes of these problems and can identify possible solutions.

J.L. KEELING

SENIOR GEOLOGIST

M.D. RAVEN

EXPERIMENTAL SCIENTIST

REFERENCES

- Abaleen Minerals NL, 1974. Report on kaolin project, Mount Hope Deposit. Exploration Licence No. 58, covering the period February 1972 - August 1974. *South Australia. Department of Mines and Energy. Open file Envelope, 2298* (unpublished).
- Churchman, G.J., Whitton, J.S., Claridge, G.G.C. and Theng, B.K.G., 1984. Intercalation method using formamide for differentiating halloysite from kaolinite. *Clays and Clay Minerals*, Vol.32, No.4, 241-248.
- Keeling, J.L., Self, P.G., McClure, S., Raven, M.D. and Milnes, A.R., 1989. Characterisation of kaolin samples from the Mount Hope deposit, Eyre Peninsula, South Australia. *South Australia. Department of Mines and Energy. Report Book 90/48*.
- Parker, A.J., Fanning, C.M., Flint, R.B., Martin, A.R. and Rankin, L.R., 1988. Archaean - Early Proterozoic granitoids, metasediments and mylonites of southern Eyre Peninsula, South Australia. Specialist Group in Tectonics and Structural Geology Field Guide Series No. 2. Geological Society of Australia.

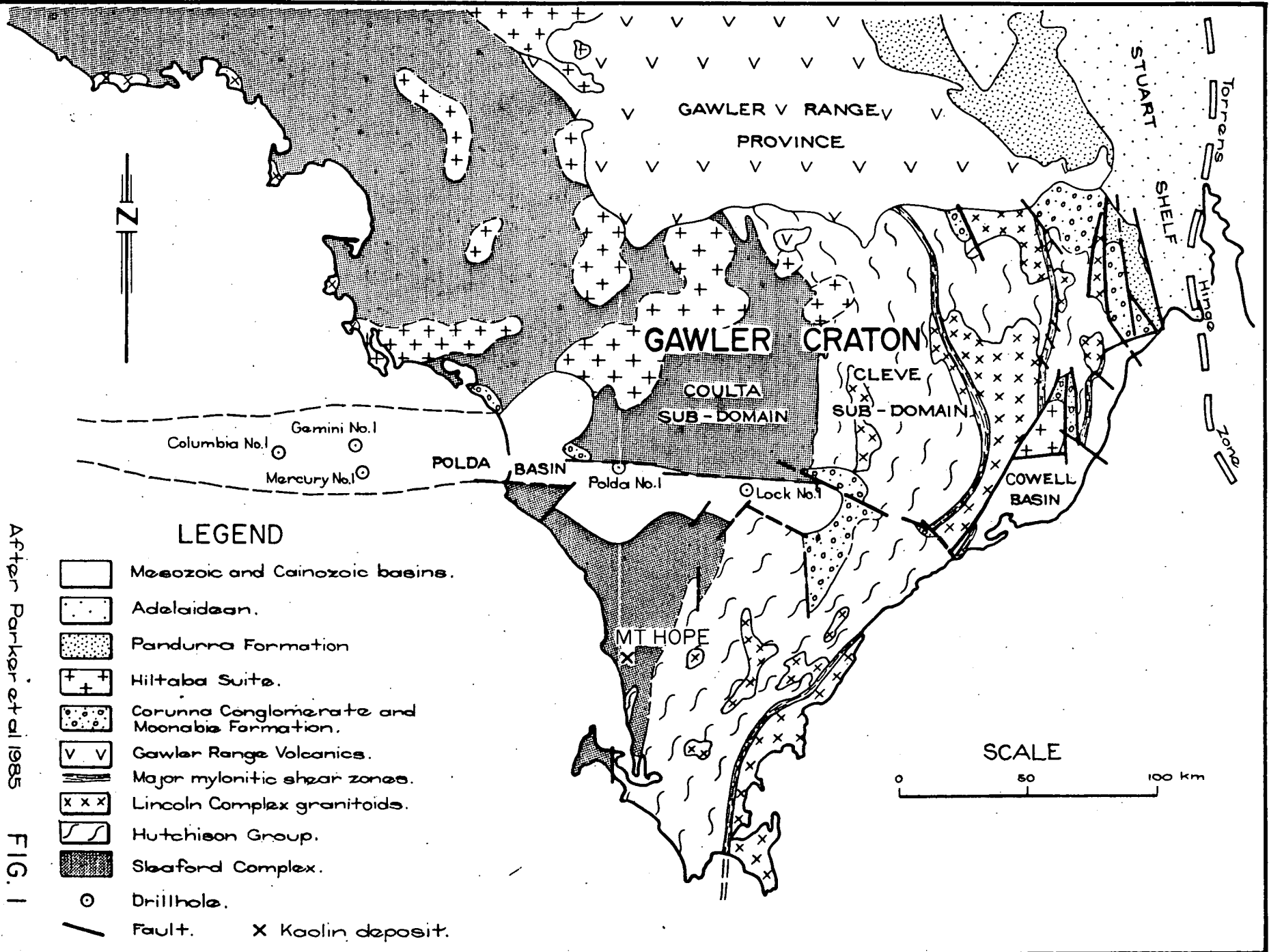
FIGURES

TECTONIC SKETCH OF EYRE PENINSULA

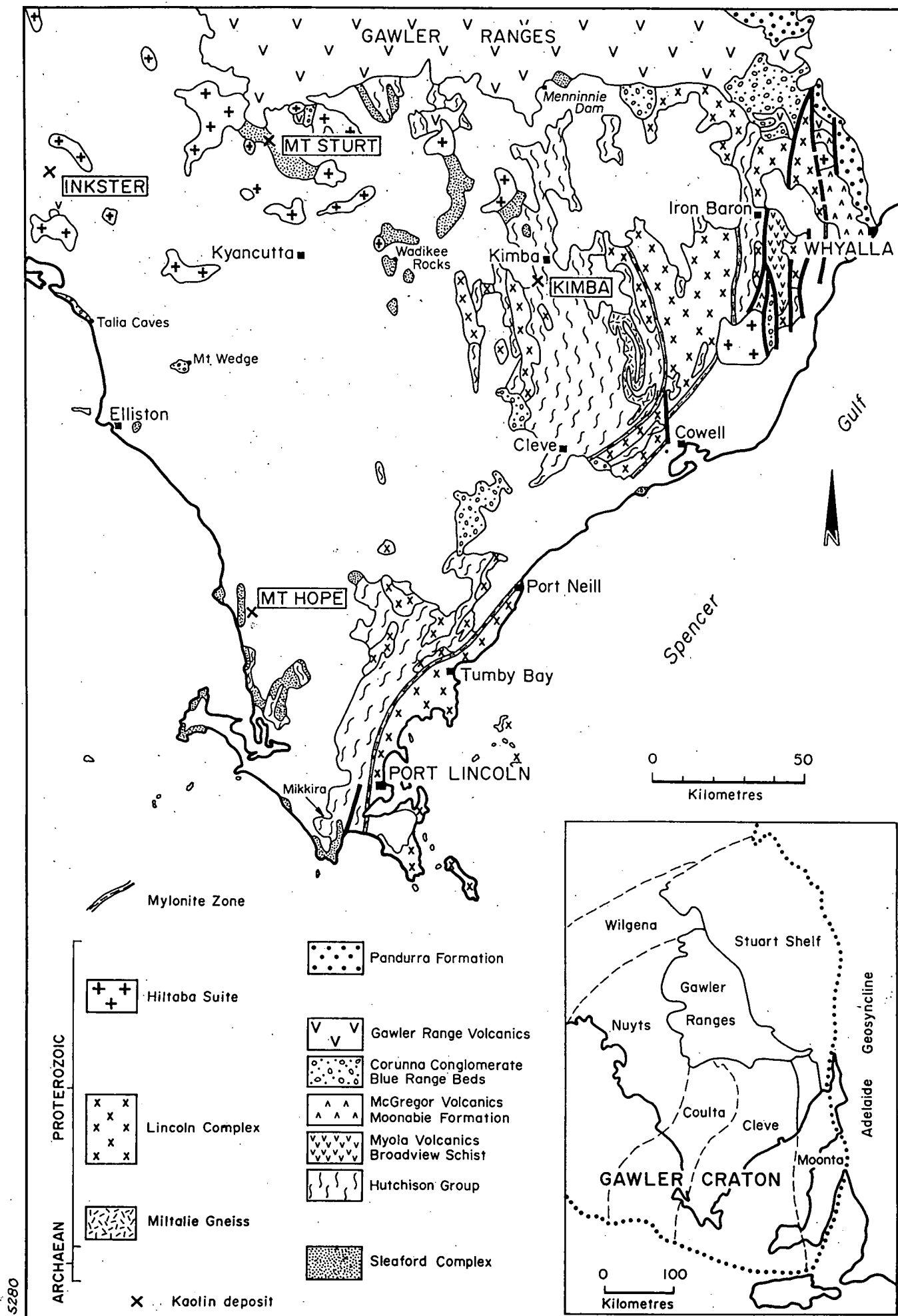
MOUNT HOPE KAOLIN DEPOSIT

DEPARTMENT OF MINES AND ENERGY
SOUTH AUSTRALIA

After Parker et al 1985 FIG. 1

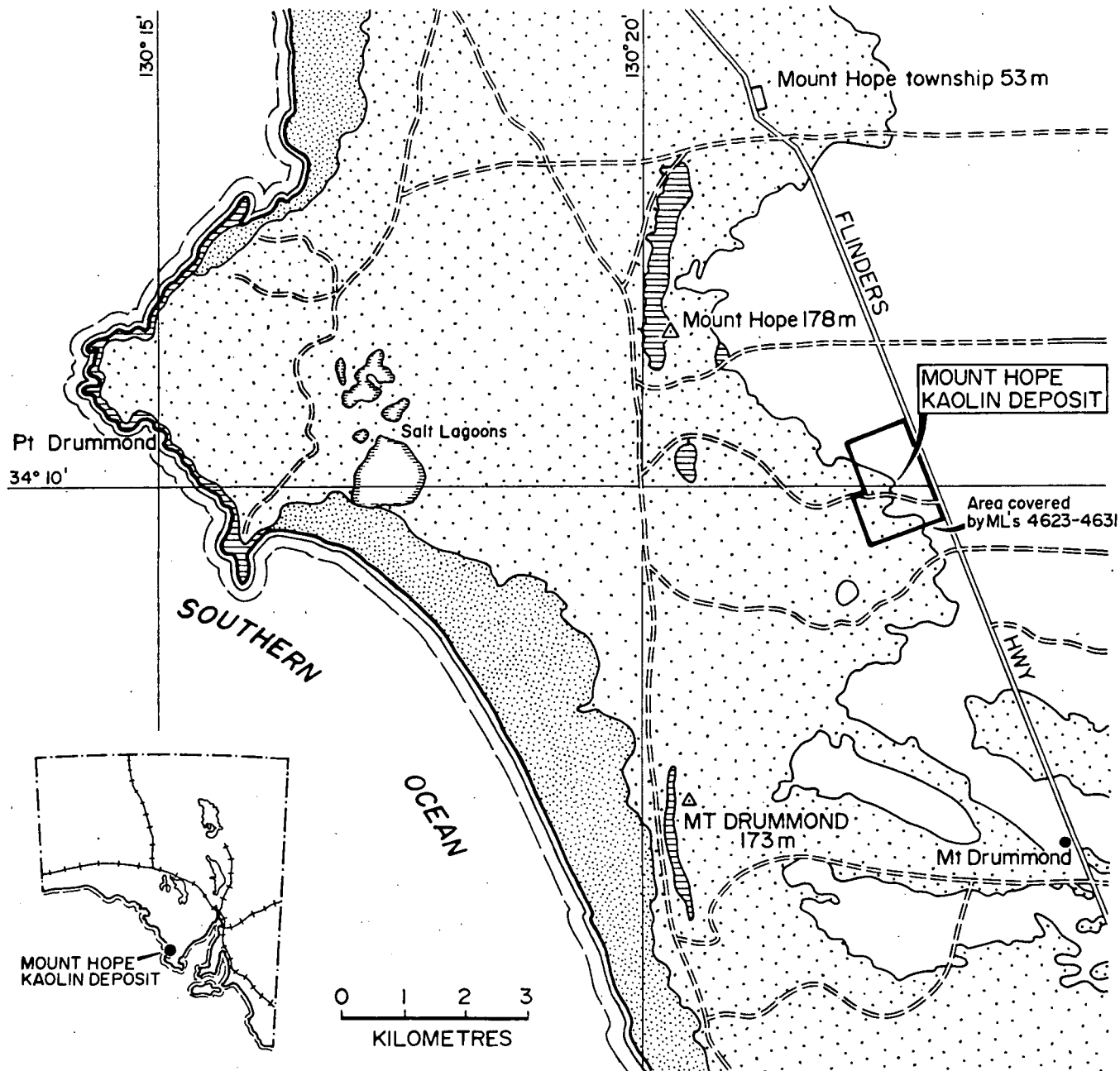


CHECKED	DATE	SCALE 1:2,000,000
	Oct '84	
DRAWN	J.W.	PLAN NUMBER
COMPILED	J. Parker	DATE
		20.3.85



**MOUNT HOPE KAOLIN DEPOSIT
LOCATION OF KAOLIN DEPOSITS - EYRE PENINSULA**

FIG. 2



Geology after Johns (1958).

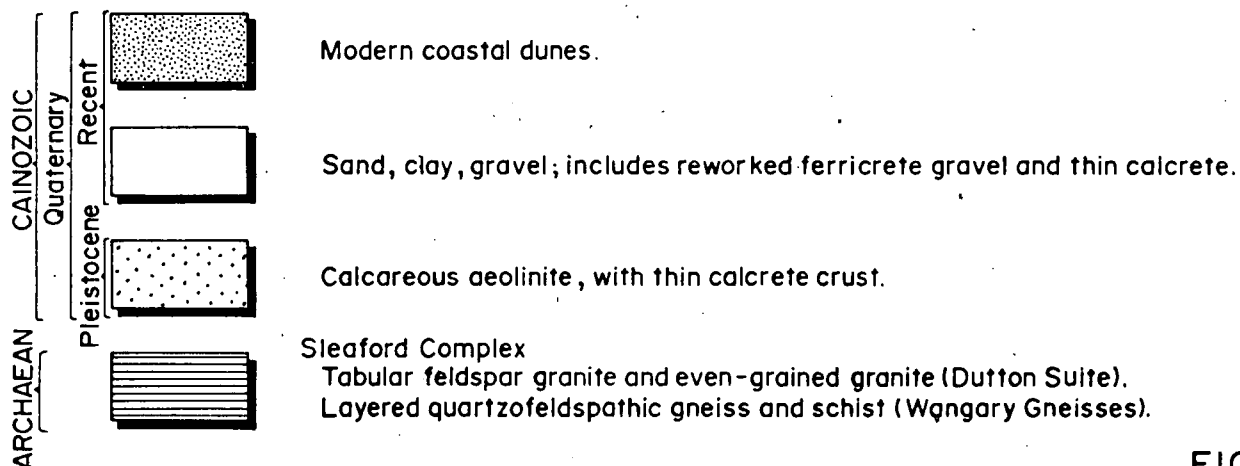
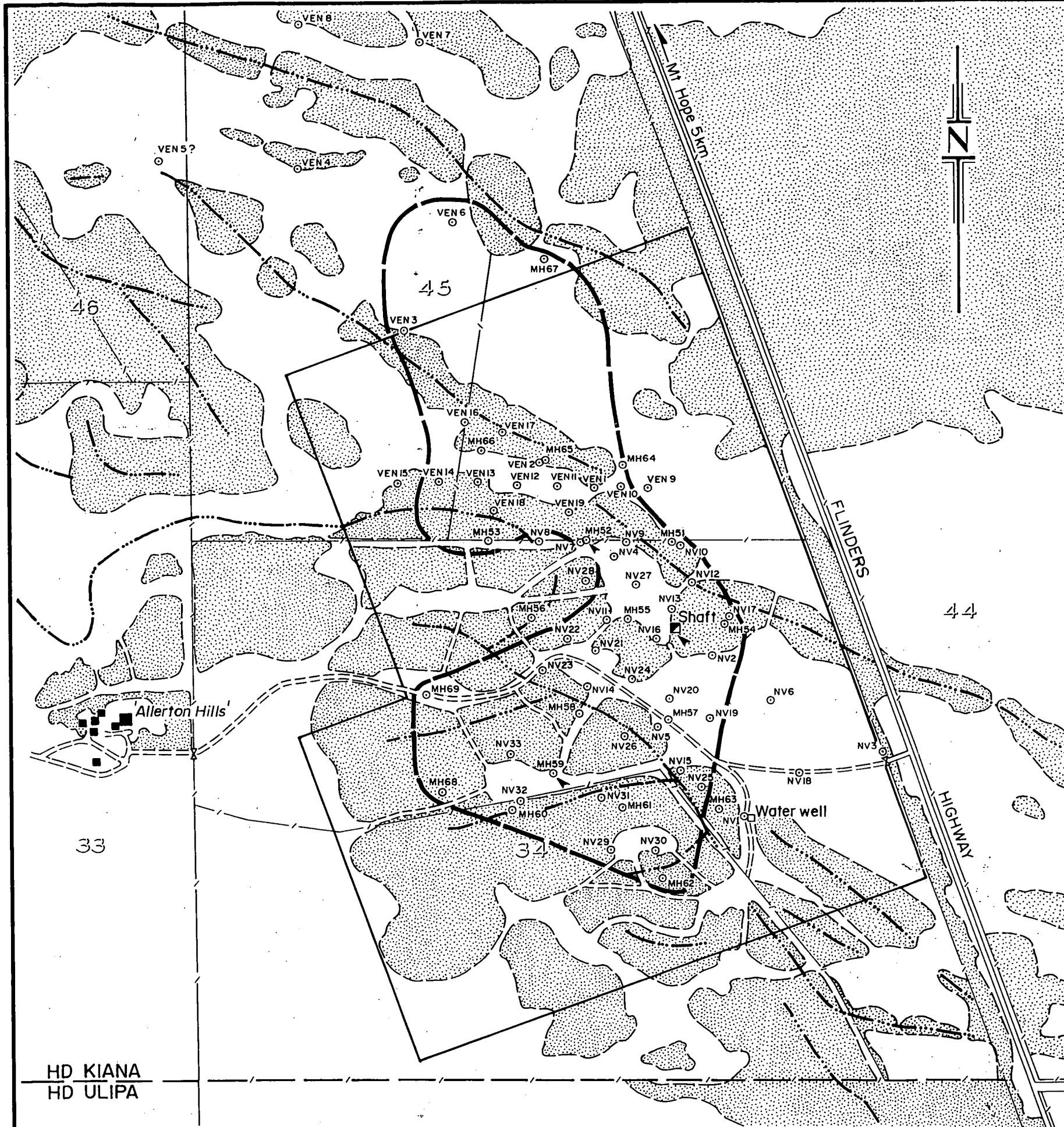


FIG. 3

DEPARTMENT OF MINES AND ENERGY
SOUTH AUSTRALIA

MOUNT HOPE KAOLIN DEPOSIT LOCATION AND REGIONAL GEOLOGY

COMPILED J. Keeling	14.11.90 C.D.O. DATE
DRAWN J.W.	SCALE 1:100,000
DATE 18-8-89	PLAN NUMBER
CHECKED X	S21044



- Drillholes
- VEN 1-19 Rotary/air holes, 1972-73.
 - NV 1-32 Rotary/air holes, 1972-73.
 - MH 51-69 Rotary/air holes, July 1986
- Possible limit of kaolin orebody as outlined by drilling.
- Prospecting shaft sunk for bulk kaolin sample.
- Track.
- Areas of remnant scrub mainly covering calcarenite dunes with calcrete surfaces. (Outline from aerial photography Jan. 1986).
- Calcarenite dune ridge line (approx).
- Outline of area covered by ML's 4623-4631.
- Buildings.
- ▲ Kaolin sample location.

FIG. 4

DEPARTMENT OF MINES AND ENERGY
SOUTH AUSTRALIA

MOUNT HOPE KAOLIN DEPOSIT
LOCATION OF DRILLHOLES

COMPILED J. Keeling	14-8-90 C.D.O. DATE
DRAWN J.W.	SCALE As shown
DATE 28-8-89	PLAN NUMBER
CHECKED X	89-383

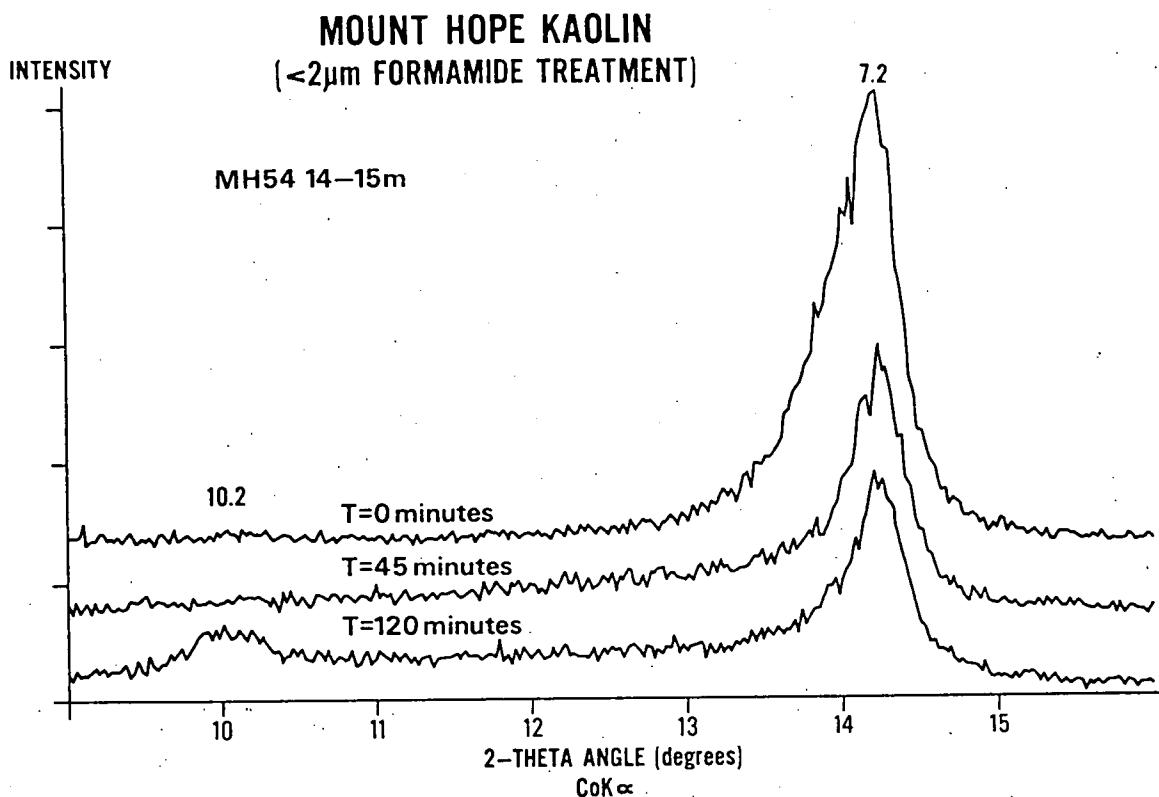


Fig. 5 X-ray diffraction traces of tubular kaolin from MH5A (14-15m) after formamide treatment.

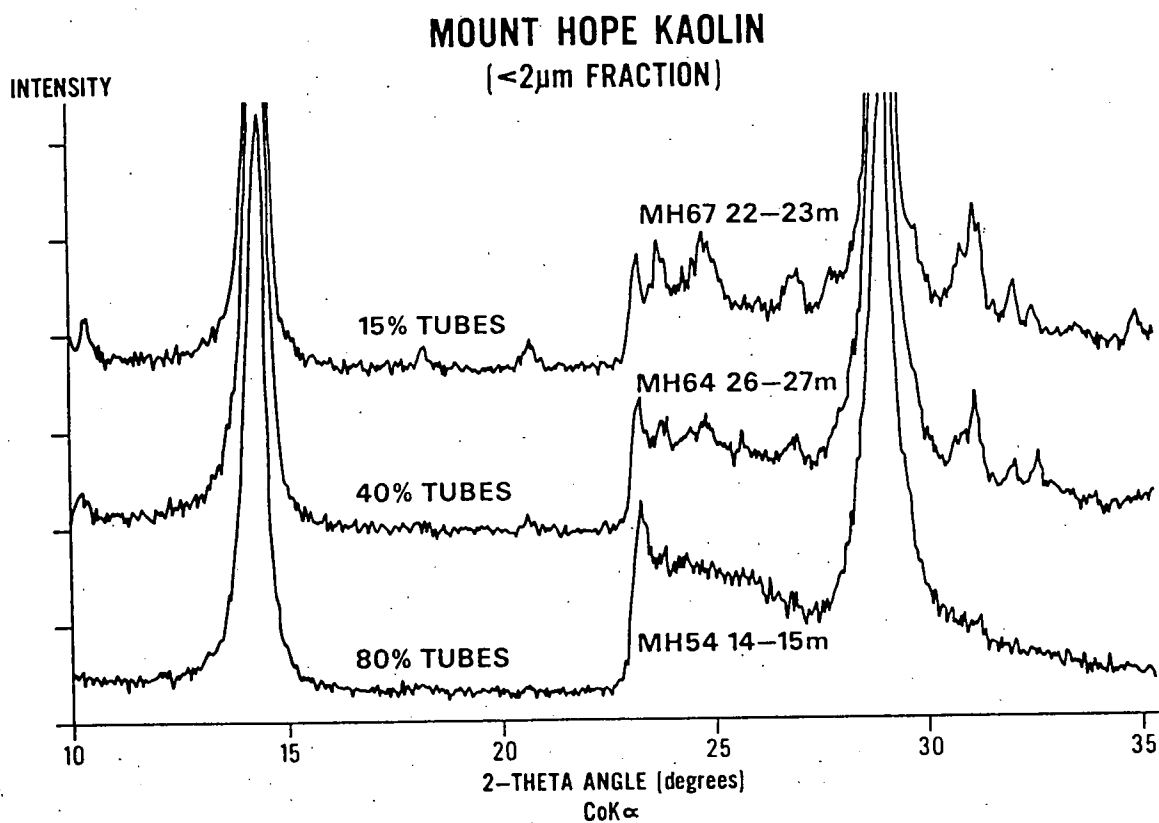


Fig. 6 X-ray diffraction traces showing a decrease in resolution of non-basal x-ray reflections with increasing content of tubular kaolin.

PLATES



Plate 1 Mount Hope Kaolin Deposit - Site of shaft sunk to 21m in 1973 to obtain a 40 tonne bulk sample.

Slide No. 39494

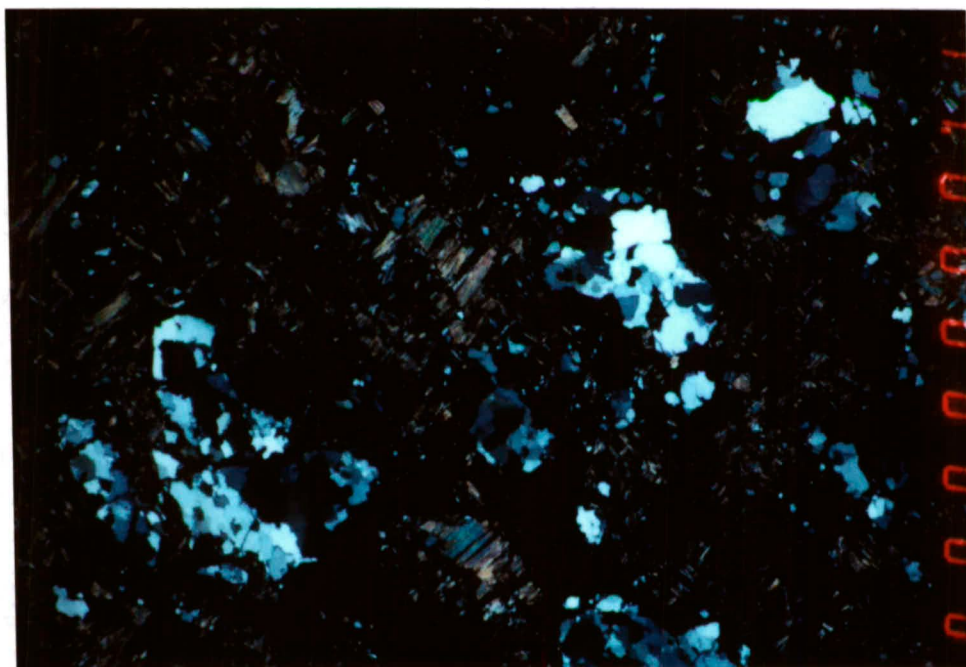


Plate 2. Thin section of kaolin ore from the shaft site (x polars) showing coarse quartz and remnant mica in a matrix of kaolinite (black). Slide width 9.5mm.

Slide No. 39495

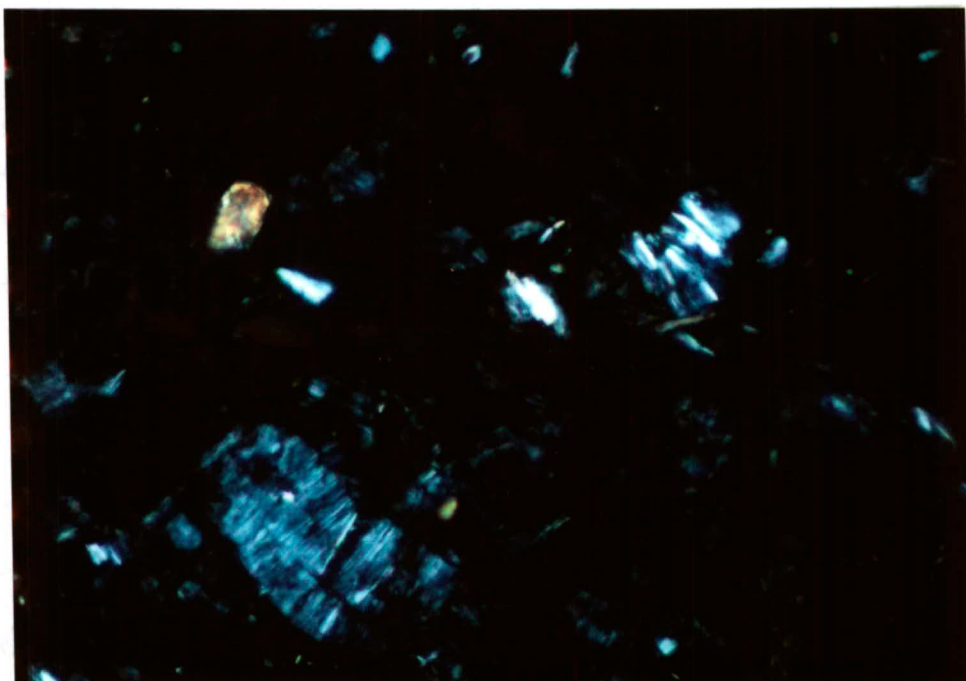


Plate 3. Shaft sample, thin section (x polars) showing remnant mica flakes interleaved in coarse crystal stacks of kaolinite. Slide width 0.9mm.

Slide No. 39496

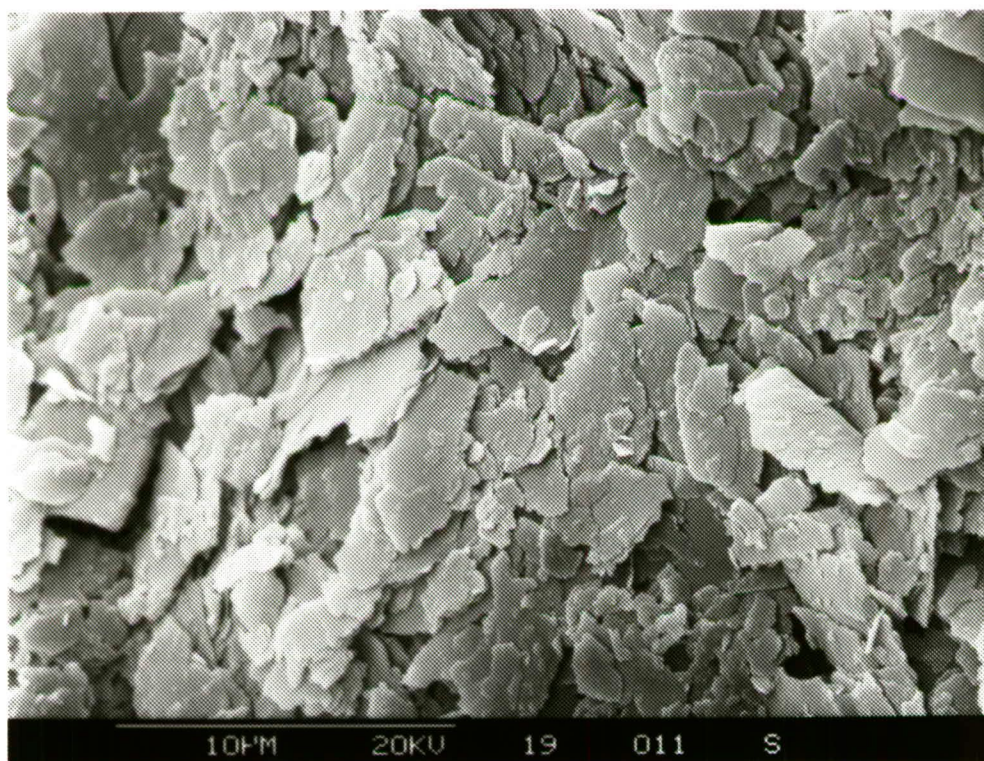


Plate 4. Scanning electron micrograph of coarse kaolinite platelets in the sedimented $<2\mu\text{m}$ fraction of a sample from hole MH 59.

Photo No. 38894



Plate 5. Scanning electron micrograph of coarse stacks of kaolinite crystals from the shaft sample.
Photo No. 38898

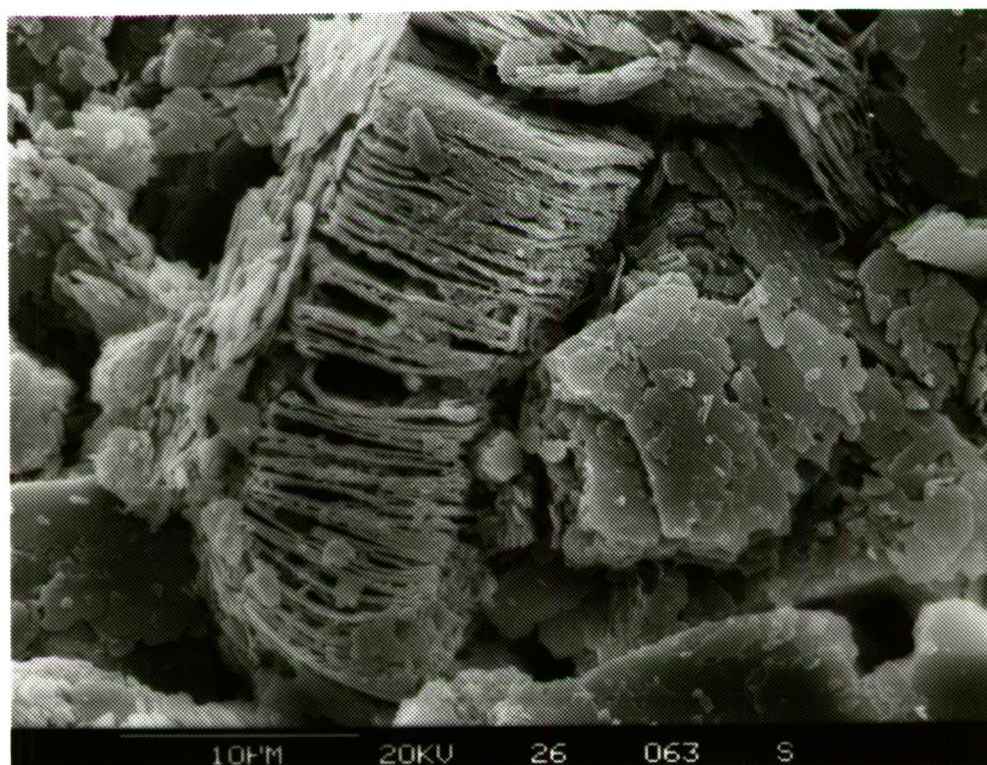


Plate 6. Detail of a coarse kaolinite stack showing open structure which is readily broken down to give a high proportion of large thin platelets.
Photo No. 38899

Plate 7. Transmission electron micrograph of a coarse kaolinite platelet which is in part made up of a mosaic of interlocking euohedral crystals (Area A).

Photo No. 38906

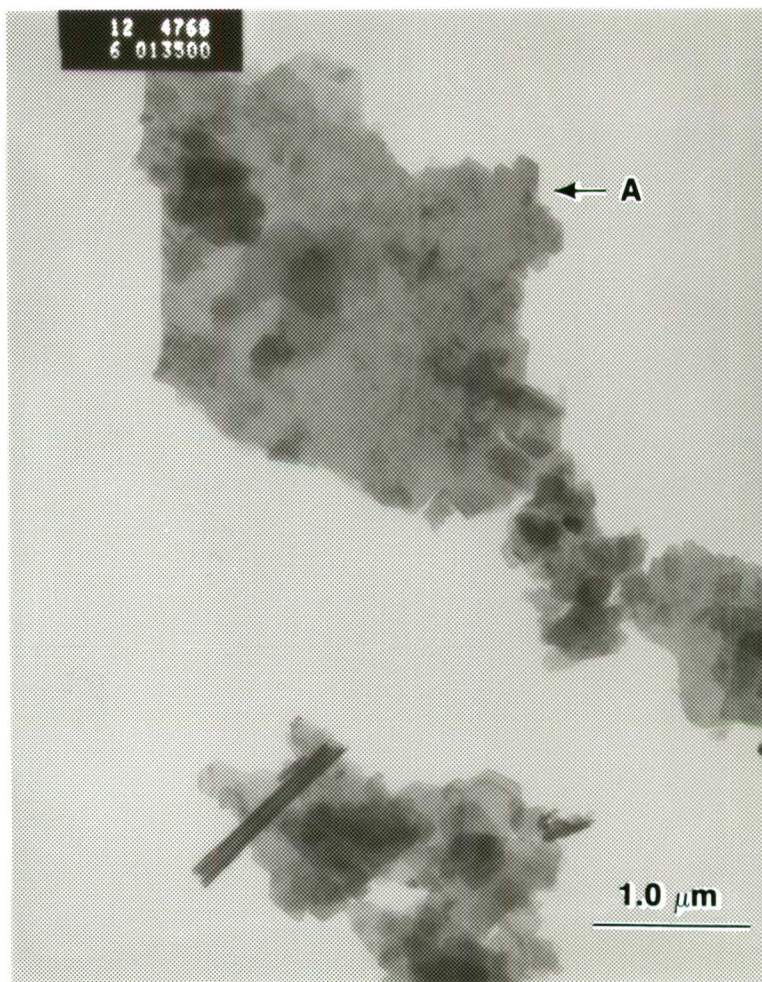


Plate 8. Dehydrated tubular halloysite in the $<2\mu\text{m}$ fraction of a kaolin sample from hole MH 54.

Photo No. 39497

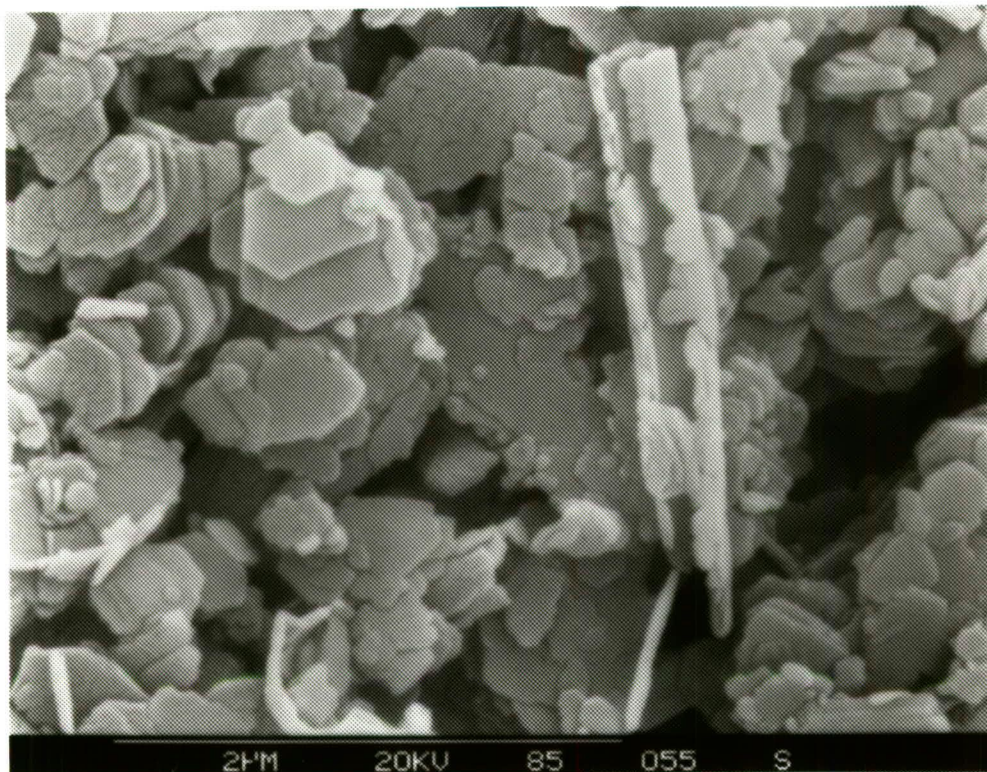


Plate 9. Disrupted halloysite tube together with well crystalline, fine-grained kaolinite.

Photo No. 38903

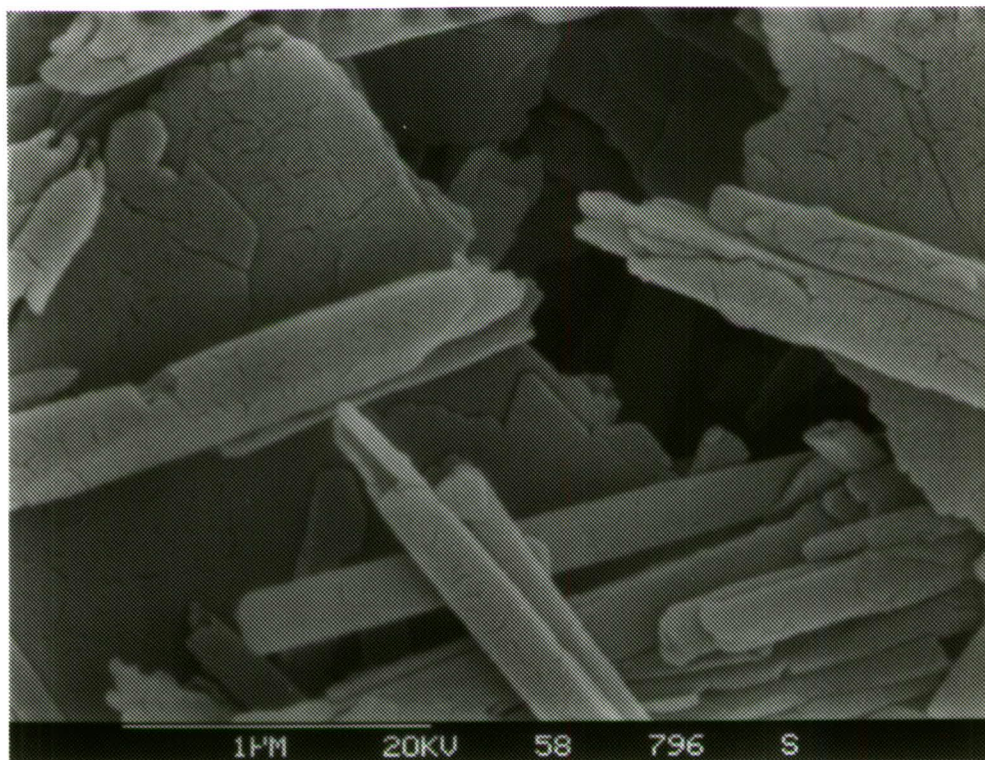


Plate 10. Detail of tubes showing flattened ends due to collapse as a result of dehydration.

Photo No. 39498



Plate 11. Detail of a rolled tube showing regular terminations on the tube end (top of photo).

Photo No. 38908

APPENDIX A

List of Conference Delegates



LIST OF REGISTRANTS

Mr M. Aspandiar	Geology Dept., Australian National University, GPO Box 4, Canberra ACT 2601
Dr R.R. Anand	CSIRO Division of Exploration Geoscience, Floreat Park WA 6014
Prof L.A.G. Aylmore	Department of Soil Science, The University of W. Australia, Nedlands WA 6009
Dr A.T. Bailey	Kaolin Australia Pty Ltd, RMB L303, Ballarat VIC 3352
Dr J. Baker	Electron Microscope Centre, University of Queensland, St Lucia QLD 4072
Lew Barnes	Commercial Minerals Limited, 100 Eastern Parade, Gillman SA 5013
Dr M. Bird	Research School of Earth Sciences, Australian National University, GPO Box 4, Canberra ACT 2601
Dr Bob Boesen	Geology Department Bendigo CAE, PO Box 199, Bendigo VIC 3550
Dr R. Bourman	Geography Department South Australian CAE, Holbrooks Road, Underdale SA 5032
David Carmichael	Department of Resource Industries, GPO Box 194, Brisbane QLD 4001
Dr A. Chivas	RSES, Australian National University, GPO Box 4, Canberra ACT 2601
Dr J. Churchman	CSIRO Division of Soils, Private Mail Bag No 2, Glen Osmond SA 5064
Mark Coghill	COMALCO Research & Technology, PO Box 316, Thomastown VIC 3074
Dr Penny Corrigan	CSIRO Division of Materials Science & Technology, Locked Bag 33, Clayton VIC 3168
Peter Dahlhaus	School of Mining Geology & Materials, Ballarat University College, PO Box 663, Ballarat VIC 3353
Aert Driessen	Bureau of Mineral Resources, GPO Box 378, Canberra ACT 2601
Dr R. Eggleton	Geology Dept., Australian National University, GPO Box 4, Canberra ACT 2601
Dr W. Emerson	CSIRO Division of Soils, Private Bag No 2, Glen Osmond SA 5064
Mr B. Faraj	Electron Microscope Centre, University of Queensland, St Lucia QLD 4072
Dr J.A. Ferguson	5 Mossman Drive, Eaglemont, VIC 3084
Dr R. Fitzpatrick	CSIRO Division of Soils, Private Bag No 2, Glen Osmond SA 5064
Dr R. Frost	Department of Chemistry, Qld University of Technology, GPO Box 2434, Brisbane QLD 4001
Assoc. Prof. R. Gilkes	Soil Science and Plant Nutrition, School of Agriculture, University of WA, Nedlands WA 6009
Mr Bill Goldfinch	Selkirk Brick Pty Ltd, 630 Howitt St., Ballarat VIC 3350
Dr Chris Goodes	COMALCO Research & Technology, PO Box 316, Thomastown VIC 3074
Prof. S. Guggenheim	Department of Geological Sciences, University of Illinois at Chicago, Box 4348, Chicago, Illinois 60680 USA
Ian Hackett	Commercial Minerals Limited, Industrial Minerals Division, PO Box 173, Granville NSW 2142



Dr P.J. Hamilton	CSIRO Division of Exploration Geoscience, PO Box 136, N. Ryde NSW 2113
Mr Simon Hardin	CSIRO Division of Materials Science & Technology, Locked Bag 33, Clayton VIC 3168
Dr J.C. Hughes	Faculty of Agriculture, University of Natal, PO Box 375, Pietermaritzburg 3200 South Africa
Mr K. Inan	Dept of Manufacturing Industry & Development, Geological Survey, PO Box 173, East Melbourne VIC 3002
Dr O. G. Ingles	RDE, 240 Foreshore Road, Swan Point TAS 7275
Mrs A. Isahak	Department of Geology, Universiti Kebangsaan Malaysia 43600 UKM Bangi, Malaysia
Dr D. Jacquet	COMALCO Mineral Products, Post Office Weipa, QLD 4874
Mr L.J. Janik	CSIRO Division of Soils, Private Bag No 2, Glen Osmond SA 5064
Dr K. Jurkschat	C/- Dr Dakternieks, Dept. of Chemical & Analytical Sciences Deakin University, Geelong VIC 3217
Mrs J. Kamprad	Bureau of Mineral Resources, GPO Box 378, Canberra ACT 2601
Roger Keane	RMB 3971, Debenham Road, Somersby NSW 2250
John Keeling	C/- S.A. Department of Mines & Energy, Box 151 P.O., Eastwood SA 5063
Lore Kiefert	Division of AES, Griffith University, Nathan QLD 4111
Dr Maite Le Gleuher	Geology Department, Australian National University, GPO Box 4, Canberra ACT 2601
Mr M.G. Lines	Commercial Minerals Ltd, 549-551 Burke Road Camberwell VIC 3124
Dr F.C. Loughnan	4 Pindari Ave, Castle Cove NSW 2069
Glen Lynagh	COMALCO Mineral Products, P.O. Weipa, QLD 4874
Dr Ian MacKinnon	Electron Microscope Centre, University of Queensland, St Lucia QLD 4072
Greg MacRae	Geological Survey of NSW, GPO Box 5288, Sydney NSW 2001
S. G. McClure	CSIRO Division of Soils, Private Bag 2, Glen Osmond SA 5064
Iain McHaffie	36 Hawke Street, Parkdale Vic 3195
Dr N. McKenzie	CSIRO Division of Soils, Private Bag No 2, Glen Osmond SA 5064
Mr M. Morgan	COMALCO Mineral Products, PO Weipa QLD 4874
Dr R.S. Murray	Waite Agricultural Research Institute, Department of Soil Science, Private Bag No 1, Glen Osmond SA 5064
Vincent O'Brien	COMALCO Research & Technology, PO Box 316, Thomastown VIC 3074
Iain Paterson	Geological Survey of NSW, GPO Box 5288, Sydney NSW 2001
Mr G. Quick	CSIRO, DBCEPO, Box 56, Highett VIC 3190
Mr Peter Pritchard	60 Morrah Street, Parkville VIC 3052

Mr Ross Ramsay	School of Mining Geology & Materials, Ballarat University College, PO Box 663, Ballarat VIC 3353
Mr Mark Raven	CSIRO Division of Soils, Private Bag No 2, Glen Osmond SA 5064
David Reid	COMALCO Mineral Products, PO Weipa QLD 4874
Dr Ivor Roberts	Dept of Mineral Exploration & Mining Geology, Western Australian School of Mines, PO Box 597, Kalgoorlie WA 6430
Huada Ruan	Soil Science and Plant Nutrition, School of Agriculture, University of WA, Nedlands WA 6009
Dr P. Self	CSIRO Division of Soils, Private Bag No 2, Glen Osmond SA 5064
Dr Ray Shaw	COMALCO Research & Technology, PO Box 316, Thomastown VIC 3074
Dr A. Shayan	CSIRO, DBCEPO, Box 56, Highett VIC 3190
Mr Balbir Singh	Soil Science and Plant Nutrition, School of Agriculture, University of WA, Nedlands WA 6009
Mr Balwant Singh	Soil Science and Plant Nutrition, School of Agriculture, University of WA, Nedlands WA 6009
Mr Sirjit Singh	COMALCO Mineral Products, GPO Box 153, Brisbane QLD 4001
Andreas Stache	11 Mackay Terrace, Bardon QLD 4065
Ms Dianne Stewart	Geology Department, Bendigo CAE, PO Box 199, Bendigo VIC 3550
Dr Reg Taylor	CSIRO Division of Soils, Private Bag No 2, Glen Osmond SA 5064
Dr Terry Turney	CSIRO Division of Materials Science & Technology, Locked Bag 33, Clayton VIC 3168
Dr Nick Uren	School of Agriculture, La Trobe University, Bundoora VIC 3083
Dr Phillipa Uwins	Electron Microscope Centre, University of Queensland, St Lucia QLD 4072
Dr N. Vagias	COMALCO Research & Technology, PO Box 316, Thomastown VIC 3074
Dr P. Walker	CSIRO Division of Soils, GPO Box 639, Canberra ACT 2601
Martin Wells	Soil Science and Plant Nutrition, School of Agriculture, University of WA, Nedlands WA 6009
Mr Don Williams	Sietronics Pty Limited, PO Box 3066, Belconnen ACT 2617
M.J. Wright	CSIRO Division of Soils, Private Bag No 2, Glen Osmond SA 5064

APPENDIX B

Conference Programme and
Abstracts of Papers

AUSTRALIAN CLAY MINERALS SOCIETY
(Incorporated)

12TH BIENNIAL CONFERENCE PROGRAM

Sunday February 3 1991

2:00 p.m.: REGISTRATION

6:30 - 9:00 p.m. WELCOME AND DINNER

Monday February 4 1991

8:00 REGISTRATION

900 OPENING: ROSS RAMSAY, BALLARAT UNIVERSITY COLLEGE
JACK BARKER, BALLARAT REGIONAL BOARD

SESSION 1: TECHNIQUES AND APPLICATIONS
CHAIR: DR ALAN CHIVAS

9:30 Low temperature thin-film elemental analysis of kaolinites.
Ian D.R. Mackinnon, Stacy A. Kaser & Philippa J.R. Uwins

10:50 FT-Raman and infra-red analysis of clay minerals.
Ray L. Frost & Peter M. Fredericks

10:10 The origin and significance of clay microstructures
R.S. Murray and J. P Quirk

10:30 Three-dimensional imaging of clay mineral cores using
computer assisted tomography applied to gamma-ray attenuation
L. A. G. Aylmore

MORNING TEA

SESSION 2: KAOLINS
CHAIR: PROF FRED LOUGHNAN

11:20 Micropores in halloysites.
G.J. Churchman, T.J. Davy, L.A.G. Aylmore & R.J. Gilkes

11:40 Morphology and formation of halloysite.
P.G. Self, G.J. Churchman and J.L. Keeling

12:00 Particle size, shape, and crystallinity relationships in size
fractionated kaolinites.
Phillipa J.R. Uwins & Ian D.R. Mackinnon

12:20 Alteration of platy kaolinite to tubular halloysite.
Balbir Singh & R.J. Gilkes

12:40 High cation exchange capacity kaolinite revisited
Tony Eggleton, Graham Taylor and Pat Walker

1:00 LUNCH

Monday February 4 (cont)

SESSION 3: SOILS

CHAIR: DR PAT WALKER

- 2:00** Properties of kaolinite from lateritic soils of Western Australia.
Balwant Singh & R.J. Gilkes
- 2:20** Some mineralogical and chemical features of soils derived from serpentinite in a humid sub-tropical environment and the role of chromium in their formation.
J.C. Hughes
- 2:40** The clay mineralogy of some soils from Johore, Malaysia
Anizan Isahak
- 3:00** The physical, chemical, and mineralogical properties of andosols from western Indonesia.
S. Sjarif and R. J. Gilkes
- 3:20** Distribution and origin of red soils in part of the Yilgarn Block of Western Australia.
R. R. Anand, R. E. Smith & H. M. Churchward
- 3:40** AFTERNOON TEA

SESSION 4: FE OXYHYDROXIDES

CHAIR: DR REG TAYLOR

- 4:10** Poorly crystalline iron oxyhydroxides and oxyhydroxysulphates in weathering environments in south Australia: observations on occurrence, genesis, properties and biomineralization
R.W. Fitzpatrick, P. G. Self and R. Naidu
- 4:30** An X-ray powder diffraction study of heated synthetic aluminium-substituted goethite.
H.D. Ruan & R.J. Gilkes
- 4:50** An X-ray diffraction study of synthetic metal-substituted goethite and hematite.
M.A. Wells, R.J. Gilkes & R.W. Fitzpatrick
- 5:10** POSTER SESSION AND PHILIPS S&E MIXER
- 5:45** COMMITTEE MEETING, 10th ICC
- 7:30** ANNUAL GENERAL MEETING PART 1
Society rules and 10th ICC report

Tuesday February 5th

FIELD TRIP

9:00 Vitclay Pipes Pty Ltd, Selkirk Brick Pty Ltd, Enfield Clay Pit,
Buninyong Clay Pit
Leaders: Peter Dahlhaus, Lex Ferguson, Bill Goldfinch

7:00 CONFERENCE DINNER

Wednesday February 6th

SESSION 5: GEOLOGY AND CLAY DEPOSITS

CHAIR: MR AERT DRIESSEN

- 8:50** Weathering and alteration at the Panglo gold deposit, Western
Australia.
F. Ivor Roberts
- 9:10** Secondary clay minerals of some Victorian basalts and their
influence on some aggregate properties.
G.W. Quick & A. Shayan
- 9:30** Hisingerite: a weathering product of olivine
Maité Le Gleuher & Tony Eggleton
- 9:50** Ballarat industrial clay resources.
Peter Dahlhaus
- 10:10** The Mount Hope kaolin deposit, Eyre Peninsula, South
Australia.
J.L. Keeling & M.D. Raven
- 10:30** Alumino-silicate minerals suitable for high grade refractories
M. G. Lines
- 10:50** MORNING TEA
- 11:20** Thermal histories and illite growth in sedimentary basins.
P.J. Hamilton, M. Giles & P. Ainsworth
- 11:40** Palaeohydrological significance of authigenic kaolinite in the
Aldebaran Sandstone, Denison trough, east-central Queensland.
Julian C. Baker & Suzanne D. Golding

SESSION 6: CLAYS IN THE ENVIRONMENT
CHAIR: DR TONY EGGLETON

- 12:00 Applications of oxygen isotope geochronology to the Australian regolith
A.R. Chivas & M.I. Bird
- 12:20 Clays and Toxic Waste Disposal
O.G. Ingles
- 12:40 Bauxitization: temperate and intemperate
Bird, M.I., Chivas, A.R., & Longstaffe, F.J.

1:00 LUNCH

SESSION 7: INTERCALATES AND PROCESSING
CHAIR: DR IAN MACKINNON

- 2:10 Viscosity and settlement of tailings.
W.W. Emerson & D. Weissmann
- 2:30 Phenomenological distinction between pillared clays and related structures.
T.W. Turney
- 2:50 Formation of β' -sialon ceramic from a montmorillonite-carbon nanocomposite by carbo-thermal reduction.
T. Bastow, S.G. Hardin & T.W. Turney
- 3:10 The role of sodium ions in the ion exchange of montmorillonite gel with partly hydrolysed solutions of aluminium chloride.
P.A. Corrigan & T.W. Turney
- 3:30 Afternoon tea
- 3:40 *Glimpses of Caimozoic weathering around Melbourne.*
J.A. Ferguson
- 4:00 AGM part 2: Confirmation of rules, biennial reports, 10th ICC discussion, award of Sietronics Prize, AOB

Following: Poster session

8:00 COMMITTEE MEETING, 10th ICC

POSTERS

1. **Illite-smectite rims in the early Permian Aldebaran sandstone, Denison Trough, East-Central Queensland-composition, Palaeohydrological significance and influence on reservoir quality.**
Julian C. Baker, Suzanne D. Golding & Ian D.R. Mackinnon.
2. **Hydrocracking and isomerization of n-octane and 2,2,4-trimethylpentane over a Pt/alumina-pillared clay.**
C. Doblin, J.F. Mathews & T.W. Turney
3. **Size fractionation to aid characterisation of kaolinite-smectites in soils.**
R. Boesen, G.J. Churchman, P.G. Self & P.G. Slade
4. **The application of clay minerals to organic geochemical studies.**
D.C. Carmichael & P.J. Hawkins.
5. **Mineralogical and magnetic susceptibility changes caused by long-term farming at six sites in South Australia.**
R. W. Fitzpatrick, R. Naidu, and N. J. McKenzie.
6. **Pedogenic barite in Australian duripans (red-brown hardpans)**
M. J. Wright and A. R. Milnes.
7. **Weathering in the South Island high country: Key factors. A clay mineralogical approach**
G. J. Churchman
8. **Kaolinite-polymer intercalates: a micro-structural study.**
John G. Thompson, Ian D.R. Mackinnon & Philippa J.R. Uwins

Thursday February 7th

9:00 **FIELD TRIP: LAL-LAL AND REGION**
Leaders Peter Dahlhaus and Phil Kinghorn

LOW TEMPERATURE THIN-FILM ELEMENTAL ANALYSES OF KAOLINITES

Ian D.R. Mackinnon, Stacy A. Kaser* and Philippa J.R. Uwins,

Electron Microscope Centre, The University of Queensland, St. Lucia QLD 4072

*Department of Geology, University of New Mexico, Albuquerque NM 87131 USA.

The Analytical Electron Microscope (AEM) is a powerful tool for the precise structural and chemical identification of fine-grained phases and has proven effective in the study of clays from a variety of environments¹. Quantitative chemical data can be obtained on many materials from regions as small as 20nm diameter with a relative precision of between 3% and 5% using well-established thin-film techniques^{1,2}. However, clays present specific problems for quantitative analysis due primarily to electron-beam induced radiation damage and/or element loss. Two other important experimental parameters for quantitative analysis include: (i) the intensity of the X-ray signal or counting statistics and (ii) absorption of lower energy X-rays in the sample due to contamination or thickness effects. For X-ray counting times greater than 50s, it has been shown that low atomic number elements can be lost from the point of analysis using typical beam currents in a 200kV AEM². Use of a low temperature cold stage during AEM analysis can significantly reduce diffusion of elements for most minerals and is shown to be effective for some clays³.

Ultramicrotomed sections of kaolinite from three different localities have been investigated using a low background, liquid nitrogen cold stage attached to a 200kV AEM. Ultramicrotomed sections of clays have been shown to provide higher statistical precision for elemental analyses compared to dispersed grains due primarily to a higher degree of consistency in sample thickness. Individual grains of Georgia kaolinite (KGa-1) and a kaolinite from the Amazon basin were selected for analysis under standardised conditions¹ at 150°C for collection times of 200s with a beam diameter ~20nm. A third kaolinite from the Weipa deposit was also prepared for preliminary analysis using the same techniques.

Averaged elemental ratios for the KGa-1 sample showed significant differences between grains and suggests that a bi-modal distribution of Al:Si may be present in the Georgia kaolinite. In the Amazon kaolinite, a total of fourteen grains were multiply analysed and the general orientation of each grain was also documented. Significant variations in Al:Si ratios were also observed for this kaolinite, although crystal orientation appeared not to be a cause of the variation. Within grains, elemental ratios ranged from highly consistent (*e.g.* Al/Si = 0.76(3) for 10 separate analyses) to quite variable (*e.g.* Al/Si = 0.56(14) for 11 analyses). All samples contained minor amounts of impurity grains such as TiO₂ and Fe-oxide. AEM analyses of both the KGa-1 and Amazon samples showed minor amounts of Fe were also contained within individual kaolinite crystals.

References: 1. IDR Mackinnon (1989) *In Spectroscopic Characterisation of Minerals and Their Surfaces*, 32-53, ACS Books, Washington DC; 2. IDR Mackinnon *et al.*, (1986) *Microbeam Analysis - 1986*, 451-455, San Francisco Press; 3. IDR Mackinnon and SA Kaser (1987) *Microbeam Analysis - 1987*, 332-334, San Francisco Press.

FT-RAMAN AND INFRARED ANALYSIS OF CLAY MINERALS

Ray L. Frost and Peter M Fredericks

Chemistry Department, Queensland University of Technology
George Street, Brisbane 4001
AUSTRALIA

The novel technique of Fourier transform (or Near infrared) Raman spectroscopy¹ is being assessed as a technique for the characterisation of clays, clay mixtures and processed clay material obtained from thermal treatment or from deuteration reactions. While clays have been studied previously by conventional Raman spectroscopy, problems have been encountered due to fluorescence and thermal degradation of the sample². The longer excitation wavelength used in the FT-Raman method leads to a significant reduction in these problems.

Quantitative methods for the analysis of clay mixtures, particularly those of commercial significance such as bentonite/kaolin/halloysite, are being investigated with a view to developing quality control procedures. Both FT-Raman and FTIR are being studied for this purpose.

References

1. Chase, D.B., J. Amer. Chem. Soc., 1986, 108, 7485.
2. Johnston, C.T., Garrison, S., Birge, R.R., Clays and Clay Minerals, 1985, 33, 483.

THE ORIGIN AND SIGNIFICANCE OF CLAY MICROSTRUCTURE

R. S. Murray and J. P. Quirk

The University of Adelaide

Waite Agricultural Research Institute

The surface area of porous materials can be obtained from nitrogen sorption isotherms in two independent ways. The first of these applies the B.E.T equation to a portion of the adsorption isotherm. The second method applies the Kelvin equation, via a model of pore shape, to the desorption isotherm to give a pore-size distribution from which the surface area can be obtained by numerical integration. For a range of clays and clay soils there is a remarkable accord between these two estimates of surface area which suggests the existence of two important microstructural features of clay matrices.

The first of these is that the geometry of micropores ($<2\text{nm}$) in clays seems to be largely cuneiform rather than slit-shaped. The presence of cuneiform voids and regions of virtual contact between particles is important in terms of the operation of inter-particle potential energy minima; without these the behaviour of clays would be different indeed.

The other microstructural feature suggested by this observation is an extremely extensive system of cracks in the clay mass which delineates *domains* or regions of common particle orientation. We have called this phenomenon *intrinsic failure* since it seems to pervade many clay systems regardless of their history. These voids are wider than those within domains so that their walls are predominantly beyond the reach of interparticle forces. In this regard they are important since they are thought to determine the strength and dispersibility of clays.

When the lamellar particle shape of the common clay minerals is taken into account both of these features should not, perhaps, be unexpected. The traditional view of clay microstructure as being dominated by slit-shaped voids requires an unrealistic degree of order. The overall isotropic behaviour of clay masses coupled with the extreme anisotropy of clay domains leads naturally to the concept of *intrinsic failure*.

THREE DIMENSIONAL IMAGING OF CLAY MINERAL CORES USING COMPUTER ASSISTED TOMOGRAPHY APPLIED TO GAMMA RAY ATTENUATION

L.A.G. Aylmore

Soil Science and Plant Nutrition
The University of Western Australia
Nedlands, Western Australia, 6009.

Abstract

In many fields of scientific and industrial research there is a wide range of applications for experimental techniques which allow the non-destructive continuous imaging of the internal structure and the processes occurring, within solid objects. The technique known as CAT scanning, involving the application of computer assisted tomography to X- and gamma ray attenuation measurements, provides an exciting and powerful method for determining the spatial distribution of bulk density, macroporosity and mineral and fluid components in cores. In CAT scanning a slice of the object under examination is modelled as an $n \times n$ matrix of small squares called pixels (Fig. 1). The purpose of the CAT technique is to determine the linear attenuation coefficient and hence the density of each pixel. This is achieved by scanning across the object linearly at $1-10^\circ$ intervals for 180° using a collimated radiation source and detector. The linear profiles at various angles are back-projected and filtered. The summation of these back projections provides an accurate measurement of the attenuation in each pixel.

Commercially available X-ray CAT scanners are extremely expensive, are unlikely to be generally available for non-medical studies and are not generally of convenient design for other studies. At the University of Western Australia's Soil Science laboratories, a conventional gamma scanner has been modified to enable the system to carry out CAT scanning. The modified scanner utilizes a 2 mm collimated gamma radiation source (e.g. ^{137}Cs , ^{241}Am or ^{169}Yb) and a similarly collimated detector. An enhanced XT compatible personal computer is used to control the scanning motion, to acquire and process the data from the radiation measurement system and finally to present the results in graphics and hardcopy forms. Appropriate software has been developed to convert multiple horizontal scans to provide a three dimensional representation of the internal structure of the object which can be sectioned, sliced or stripped away and viewed from any angle and distance using 32 colours to represent variable attenuation ranges (Fig. 2). Most recent work has been directed to the application of CAT to dual source gamma scanning to allow the simultaneous measurements of the spatial distributions of bulk density and fluid contents, e.g. water in swelling clay soils, displacement fluids in oil recovery studies etc.

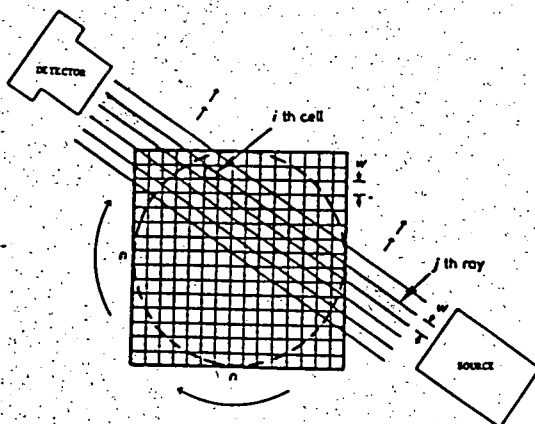


Fig. 1.

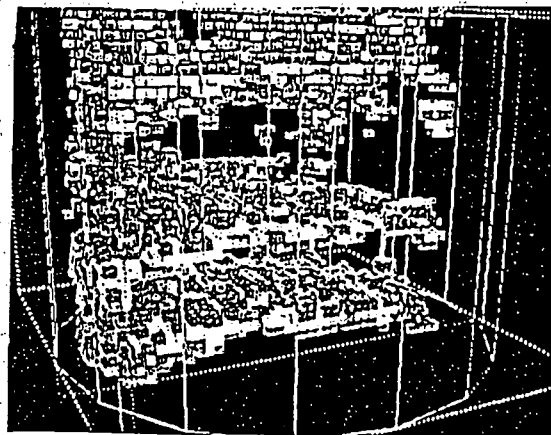


Fig. 2.

MICROPORES IN HALLOYSITES

G. J. Churchman¹, T. J. Davy, L. A. G. Aylmore
and R. J. Gilkes

¹CSIRO Division of Soils, Adelaide and Soil Science and Plant Nutrition, University of Western Australia.

Halloysites, unlike kaolinites, typically have fine pores concentrated into a very narrow size range. The characteristic pore size distribution for halloysites has been attributed to their distinctive particle shapes. Central holes in tubes have been thought to contribute to the preponderance of fine pores. Not all halloysites are tubular, however, and the pore size distribution pattern has also been ascribed to voids created by the stacking of particles.

We have examined the pore size distributions for 7 halloysites from both New Zealand and Western Australia. These included tubular, spheroidal and blocky particles of various sizes. Pore size distributions and indications of pore shapes were obtained from isotherms for the adsorption of nitrogen.

While all size distributions were narrow, both the shapes and sizes of pores were related to particle sizes, but not to particle shapes. Most pores in halloysites with mainly large particles ($>c.0.1 \mu\text{m}$ in width) were slit-shaped and small ($c.25\text{--}30 \text{ \AA}$ plate separation). Most pores in halloysites with mainly small particles ($<c.0.09 \mu\text{m}$ in width) were cylindrical and large ($>c.60 \text{ \AA}$ in radius). However, all samples contained some cylindrical pores.

Slit-shaped pores probably result from shrinkage on dehydration of blocks of layers of halloysites. Voids from particle stacking cannot explain the characteristic pores in halloysites. Cylindrical pores are probably mostly in the central holes in tubular particles.

MORPHOLOGY AND FORMATION OF HALLOYSITE.

P.G. Self¹, G.J. Churchman¹ and J.L. Keeling².¹ CSIRO, Division of Soils, PMB#2, Glen Osmond, SA5064.² SADME, PO Box 151, Eastwood, SA5063.

A suite of halloysites that have been well characterised by various analytical methods were studied by transmission electron microscopy (TEM). This study showed halloysites to have a wide variety of morphologies that could be roughly divided into 3 categories: 1) cylinders, 2) rolled tubes with varying pitch and 3) spheres. Variations within these groups could, in general, be described by the additional terms long, short or blocky.

High-resolution TEM confirmed the hypothesis of Churchman et al. (see paper in these proceedings) that pore size distributions in halloysites are not related to particle stacking but are attributable to effects of dehydration within the layers of the halloysite particles. On dehydration the curved halloysite layers straighten and presumably tend towards the ideal kaolinite structure. If the halloysite remains in a dehydrated state for long enough, sharp breaks form at the ends of the straightened layers in the halloysite tubes. When these sharp breaks occur the halloysites will no longer respond to formamide treatment. This effect is widespread in Australian kaolin deposits where it is possible to find 7Å-kaolinite with tubular morphology but which will not respond to formamide treatment (see Keeling and Raven in these proceedings).

Chemically the layers in halloysite and kaolinite are identical, yet there are obvious structural differences. These differences have been explained by forces arising from the compression of tetrahedral sheets (Bates, 1959) or from unbalanced expansions and compressions in the octahedral sheets (Radoslovich, 1963). Although these forces are also present in kaolinite plates they can only have an effect when water is present in the interlayer in which case the interlayer-water decouples the forces between the tetrahedral and octahedral sheets of successive layers. The amount of curvature caused by these forces will depend on the amount of water present during formation and the chemistry of the sheets. For example, spherical halloysite seems to form in wet, Al deficient environments where forces in both the tetrahedral and octahedral sheets have an effect.

REFERENCES.

Bates, T.F. (1959). *Am. Min.*, 44, 78-114.Radoslovich, E.W. (1963). *Am. Min.*, 48, 368-378.

PARTICLE SIZE, SHAPE AND CRYSTALLINITY RELATIONSHIPS IN SIZE FRACTIONATED KAOLINITES

Philippa J.R. Uwins and Ian D.R. Mackinnon

Electron Microscope Centre, The University of Queensland, St. Lucia QLD 4072.

Kaolinites from different geological environments have nominally different properties, such as size, shape, degree of crystallinity and impurities. These properties influence the quality of the final product used in industrial processes and determine the nature of kaolinite uses such as paper coatings and ceramics. The level of processing to which a crude ore is subjected may also play a role in determining the physical and chemical properties of the final product, and thus, in applications for laboratory intercalation experiments. In order to assess these parameters, a comprehensive study of two kaolinites has been initiated in which combined XRD, TEM, HRTEM and image analysis is used to examine properties of kaolinites before and after processing.

Transmission electron microscopy (TEM) image analysis and X-ray powder diffraction (XRD) have been used to examine the relationships between particle size, shape and crystallinity of (a) Georgia kaolinite (KGA-1), (b) Weipa kaolinite and (c) kaolinites from different stages in the Comalco processing plant. Each sample was separated into eight size fractions by repeated centrifuging, and three fractions were chosen for preliminary analysis. Particle size and shape for > 100 particles from each fraction were accurately determined using a combination of TEM micrographs and image analysis. In addition, the crystallinity index (Hinkley index) was calculated for each sample using XRD. In order to observe individual crystal parameters, such as degree of order and crystallite size in the basal dimension, ultramicrotomed thin sections were prepared for HRTEM.

Particle size analysis, using a combination of TEM micrographs and image analysis, provides a visual control of individual particles (principally lying with c^* normal to the image plane) and shows the degree of grain size fractionation during centrifugation. Although centrifuging time and revs per minute were accurately controlled, the resulting size fractions showed discrepancies to expected values calculated from Stokes' Law. In particular, the coarser size fractions showed a greater variation of grain size, and microscopy often revealed aggregates of particles with wide variation in size. On the other hand, finer sized fractions were usually homogeneous.

Preliminary assessment of Hinkley index values shows that there is a correlation between decreasing crystallinity with a decrease in particle size for crude ore samples. This relationship has been noted in other XRD and/or SEM studies of Georgia kaolinite¹. A second trend shows a decrease in crystallinity for processed kaolinite from Weipa, with the final product having the lowest crystallinity value. Crystallinity was the highest in the coarser ($< 1.5 \mu\text{m}$) size range. The $d(001)$ values increase with decreasing particle size supporting earlier theoretical predictions². HRTEM of Weipa kaolinite indicates that crystallite size in the basal direction is, on average, $< 35\text{nm}$.

References: 1. G Lombardi *et al.*, (1987) *Clays & Clay Minerals*, 35, 321-335 2. V Trunz, (1976) *Clays & Clay Minerals*, 24, 84-87.

ALTERATION OF PLATY KAOLINITE TO TUBULAR HALLOYSITE

Balbir Singh and R. J. Gilkes

Soil Science and Plant Nutrition, School of Agriculture,
The University of Western Australia, Nedlands, W.A., 6009

Halloysite is generally considered the primary form of crystallization rather than a form derived from kaolinite by solid-state alteration. In saprolite, it usually occurs as a random felted mass or radiating aggregates of crystals. Halloysite tubes of about 5 μm length are considered long, 1 to 2 μm being the most commonly observed length.

We observed parallel oriented and exceptionally long ($>10\mu\text{m}$) tubes of halloysite in the SEM image of an undisturbed sample of an *in situ* saprolite from a deeply weathered profile. An oriented lath-like morphology was evident and several laths joined together gave a plate-like appearance. The origin of this halloysite was investigated by TEM in conjunction with X-ray analysis and electron diffraction of the dispersed sample and ultrathin sections of pseudomorphs after primary minerals.

TEM and electron diffraction of the ultrathin sections showed that kaolinite plates constituting the pseudomorphs were fractured at irregular intervals along the *a* crystallographic axis to produce oriented laths elongated along the *b* axis. The fracture made an angle of approximately 55° with the *c* axis. The laths at the edges of the pseudomorphs in a relatively advanced stage of transformation were rolled to produce halloysite tubes. The cross-sections of tubes varied in diameter and degree of roundness. Some cross-sections showed planar outer faces rather than being cylindrical in cross-section. The length and number of planar faces and the angle between tube faces varied, exhibiting no consistent pattern.

The TEM investigation of the dispersed samples showed two types of twinning of the tubes. In the first type of twinning, tubes/laths were joined together side by side. In the second type, single tubes bifurcated into two individual tubes. It is considered that first type of twinning occurred by folding of adjacent laths that remained joined together while the second type occurred due to exfoliation of a thicker lath and then folding of the individual laths into tubes. Many remnant plates exhibited zig-zag boundaries where fragments had broken away. The chemical composition and cation exchange capacity (determined by AEM) of the halloysite tubes, laths and zig-zag kaolinite plates were identical and typical of kaolin minerals.

It is concluded that halloysite in this material has developed from a platy kaolinite by systematic fracture and folding. Such a transformation of kaolinite to halloysite has been proposed by several workers, but this is the first report where such convincing evidence has been provided. The transformation of kaolinite to halloysite explains the observed properties of tubular halloysites, such as splitting, twinning, planar faces and parallel orientation of the tubes.

HIGH CATION EXCHANGE CAPACITY KAOLINITE REVISITED

Tony. EGGLETON*, Graham TAYLOR**, and Pat WALKER**

Centre for Australian Regolith Studies

*Australian National University, GPO Box 4, Canberra, ACT 2601, Australia

**University of Canberra, PO Box 1 Belconnen, ACT 2601, Australia

Coarse-grained kaolinite, such as 1-2 μm Georgia or St Austell material, typically has a cation exchange capacity of 2-4 cEq/kg. After prolonged grinding, the cation exchange capacity of kaolinite increases to 10 cEq/kg, and some soil kaolinites have cation exchange capacities as high as 30 cEq/kg.

There are four interpretations generally given for high c.e.c. kaolinite:

- i) the sample contains discrete smectite, possibly in such thin packets that its presence is not detected by XRD.
- ii) the kaolinite contains interstratified smectite.
- iii) the kaolinite has coupled atomic substitution; e.g. $(\text{Al} + \text{Ca}) \leftrightarrow (\text{Si} + \text{A})$, where A represents a site normally vacant in kaolinite.
- iv) the kaolinite is fine-grained, and the exchange capacity arises from edge sites.

These four factors are considered in relation to a high cation exchange capacity Tertiary lake sediment composed predominantly of kaolinite.

Size distribution graphs for 1000 samples show that over much of the lake deposit's 100m depth, more than 90% of the sediment is clay size, with up to half the clay $<0.1 \mu\text{m}$. Direct measure of dispersed kaolinites on a TEM grid, and of ion-milled thin sections, shows that the size estimated by sedimentation is the grain diameter; the crystals' thickness is about 1/10th their diameter.

XRD analysis of 250 samples shows that the deposit is dominated by kaolinite, with significant quartz, and minor smectite, anatase, and siderite. Normative compositions calculated from 12 bulk chemical analyses can be interpreted in terms of the known mineralogy, and are consistent with quantitative XRD estimates of kaolinite:smectite ratios. Cation exchange capacities of 30 samples are all >20 cmole/kg, and a good correlation exists between CEC, and XRD detected smectite. Samples of clay which are $>98\%$ kaolinite, by XRD estimate still have a CEC of about 20 cmole/kg, of which 6 cmole/kg is charge dependent.

TEM images of clay with 6% smectite (estimated by XRD) show a small quantity of discrete smectite (>3 layers per packet) and some 1-2 layer smectites on kaolinite surfaces. Smectite volume estimate from images is 15%. TEM images of clay with no XRD detectable smectite show rare smectite packets, internal single smectite layers and more common single and double 10-Å to 12-Å layers forming the outer layer of a kaolinite crystal. Smectite volume measured from images is 7%. These kaolinite crystals also have internal defects (terminating layers), which may give rise to CEC.

The total CEC at pH8 for Lake Bunyan kaolinite with no XRD detectable smectite results from surface smectite layers (12 cmole/kg), edge exchange sites (6 cmole/kg) and possibly internal defects (2 cmole/kg).

Properties of kaolinite from lateritic soils of Western Australia.

Balwant Singh and R. J. Gilkes

Department of Soil Science and Plant Nutrition

University of Western Australia

NEDLANDS, WA 6009

Kaolinite is the most abundant clay mineral in the highly weathered soils of W.A. and it greatly influences the physical and chemical properties of the soils. In lateritic soils kaolinite crystals are often small in size, their shape is undefined and they may contain some Fe in the structure. All these properties may contribute to the poor crystallinity of kaolinite. In the present study iron oxides were removed from the clay fraction of kaolinitic soils by a dithionite treatment. Accurate measurements of basal spacings (using octacosane as an internal standard), width at half maximum height (WHH) and the formamide intercalation test were done on basally oriented specimens on ceramic plates. Random powder diffraction patterns were obtained using CaF_2 as an internal standard for the measurement of the crystallinity of kaolinites. Differential thermogravimetric analyses and cation exchange capacity measurements were obtained for the soil kaolinites and some standard kaolinites. Cation exchange capacity was measured by equilibrating the clays in 1×10^{-3} M KNO_3 at pH = 7.0 and extracting the exchangeable cations with 0.1 M BaCl_2 (pH = 3.0).

Basal spacings and WHH were generally higher and dehydroxylation temperatures were lower for the soil kaolinites compared to standard kaolinites. The formamide test did not indicate the presence of halloysite except for a sample from the pallid zone of a lateritic profile. Cation exchange capacity (CEC) of the soil kaolinites varied between 2.4 to 8.1 meq/100g (Mean = 5.5 meq/100g) including the value of Al in the BaCl_2 extract the range of CEC values increased to between 7.0 to 16.8 meq/100g (Mean = 9.8 meq/100g). The mean CEC value for standard kaolinites was 0.47 meq/100g and increased to 1.26 meq/100g on including the extractable Al analysis. All the soil kaolinites were very poorly crystalline with a mean value of 5.6 for a crystallinity index (Hughes and Brown, 1979) compared with 43.7 for well crystalline Georgia kaolinite. The crystallinity index was significantly positively correlated with dehydroxylation temperature and negatively correlated with WHH and CEC. Width at half height of the 001 reflection increased with increasing d-spacing of the same reflection.

Further work on surface area, analytical electron microscopy and chemical analysis on pure selective samples will be reported.

SOME MINERALOGICAL AND CHEMICAL FEATURES OF SOILS DERIVED FROM SERPENTINITE IN A HUMID SUB-TROPICAL ENVIRONMENT AND THE ROLE OF CHROMIUM IN THEIR FORMATION

J. C. HUGHES

Department of Crop Science, Soil Science and Agrometeorology,
University of Natal, Pietermaritzburg, Natal, South Africa

Knowledge of serpentinite-derived soils is not extensive and hence the present study was conducted to investigate the mineralogy and chemistry of nine soils from near Barberton (25°40'S, 31°10'E) in the Eastern Transvaal of South Africa. Three of the soils were sampled from near the Star Asbestos Mine which was last worked in 1982. Two of these were from an area of the most recent mine tailings and one from a more vegetated slope on older mine debris. The remaining six soils were sampled from an undisturbed area nearby. All the soils are shallow (<30cm deep) especially those on the recent mine tailings which are <10cm deep; they have been tentatively classified as lithic ustorthents. The soils, however, support in most places a relatively species-rich vegetation cover. The samples were air-dried and ground to pass a 2mm mesh sieve. Exchangeable bases, cation exchange capacity, pH, organic carbon, Kjeldahl nitrogen and particle size were determined. The <2µm clay fraction was examined by X-ray diffraction, using both random and oriented specimens, and by transmission electron microscopy. Both the <2mm and the <2µm fractions were analyzed for total elemental composition by X-ray fluorescence spectrometry.

Two of the Star Mine samples are distinct from the other seven soils sampled. Their clay fractions are dominated by chrysotile and they contain stichtite ($\text{Mg}_6\text{Cr}_2\text{CO}_3(\text{OH})_{12} \cdot 4\text{H}_2\text{O}$) which is absent in the other samples. They have low clay contents of <20%, the lowest CECs of about 6cmol/kg and the highest pHs of close to neutrality. Their organic carbon contents are also low at <1%.

Six of the remaining samples have clay contents of >30% (three are >40%), CEC values up to 33cmol/kg and extremely high organic carbon values from 7-9%. Although these soils appear similar chemically their clay mineralogy reveals differences. Three of the soil clays are dominated by talc, with some amphibole and small amounts of serpentine. The other three clays contain two serpentine minerals, one tubular and one platy, and some expanding interstratified 2:1 layer silicates. This mineralogical subdivision of the soils is supported by variations in the XRF data for the clays. The ninth soil's clay fraction consists of two serpentines and some talc and the soil has a CEC of 16.43cmol/kg and an organic carbon content of almost 3%. It thus appears to represent an intermediate stage in formation from the young Star Mine soils to the older soils on the undisturbed area.

In common with serpentinite-derived soils reported from elsewhere the present soils contain quite high concentrations of chromium (up to 3.77% Cr_2O_3) which is apparently concentrated in the mineral fraction. However, it is possible that the chromium released by weathering combines to form chromium-organic matter complexes and thus the organic matter builds up in these soils. It appears therefore that chromium is behaving analogously to aluminium in more highly weathered soils and protects the organic matter from decomposition.

The clay mineralogy of some soils from Johore, Malaysia

Anizan Isahak
Geology Department
Universiti Kebangsaan Malaysia

Abstract

The clay mineralogy of surficial materials from major geomorphic units in southeast Johore, peninsular Malaysia has been investigated. These geomorphic units consist of residual terrains probably Tertiary in age, a mid-Pleistocene alluvial complex, a Holocene alluvial complex and an ancient coastal mud deposit complex. The mineralogy of the residual terrains tends to be similar. Kaolinite, aluminous goethite and gibbsite are the dominant minerals in the weathered zones of these terrains. The mineralogy of the Holocene alluvial complex tends to be similar to that of the residual terrains due to the alluvium being derived from the residual terrains. The mineralogy of the weathered zones of the mid-Pleistocene alluvial complex is predominantly kaolinite with a minor amount of goethite. The kaolinite may have been derived from the weathering of the highly smectitic alluvial material occurring at depth or may be a separate stratigraphic unit. The mineralogy of the weathered zone of the mud deposit complex is predominantly illite. These results show that there is a major influence of sedimentary environment and/or age on the clay mineralogy of these geomorphic units.

Kaolinite crystallinity was measured according to the index of Hughes and Brown (1969). The values for the mid-Pleistocene alluvial complex are relatively low. Size and shape of kaolinite crystals has been investigated by TEM and SEM. Kaolinite crystals in the residual terrain are small and uniform whereas in the mid-Pleistocene alluvial complex, the range of size is greater. Relatively more halloysite tubes are present in clays of the mid-Pleistocene alluvial complex. Goethite and hematite were investigated for their Al-substitution and mean crystallite dimensions by XRD and crystal sizes and shapes by TEM. Both goethite and hematite tend to have rather high aluminium substitution levels ranging from 16 - 35 mole % Al in goethite and 8 - 15 mole % Al in hematite for all samples investigated. Mean crystallite dimensions determined by XRD for iron oxides are very small (~ 20-30nm) and are consistent with sizes observed by TEM.

THE PHYSICAL, CHEMICAL AND MINERALOGICAL PROPERTIES OF ANDOSOLS
FROM WESTERN INDONESIA

S. Sjarif* and R. J. Gilkes**

* Bogor Agricultural University, Bogor, Indonesia

** The University of Western Australia, Perth, Western Australia

Physical, chemical and mineralogical properties have been determined for andosols from Java and Sumatra, Western Indonesia which have been formed from various rock types and at different altitudes. Indonesian andosols are generally similar to andosols in other countries, having properties such as low bulk density, high water retention, high phosphorus sorption capacity and clay minerals dominated by allophane plus imogolite. Some Indonesian andosols containing allophane and imogolite have low pH in water (<5.0) whereas elsewhere such soils generally have higher pH (>5.0). The soil characteristics are not systematically different for soils formed from different parent materials, although soils formed on basaltic parent material tend to have higher values of allophane plus imogolite content, clay content, and soil pH. There were significant relationships between some of the soil characteristics; soils with a high allophane plus imogolite content had a high phosphorus capacity, and water retention, but low bulk density values.

DISTRIBUTION AND ORIGIN OF RED SOILS IN PART OF THE YILGARN BLOCK OF WESTERN AUSTRALIA

R.R. Anand, R.E. Smith and H.M. Churchward

CSIRO Division of Exploration Geoscience

Floreat Park, Western Australia, 6014

Red soils mantle the gently, undulating terrain of the Yilgarn Block of Western Australia. They have been studied at Mount Gibson, some 350 km north-east of Perth. The area has a semi-arid to arid climate with a 250-mm average annual rainfall, most of which falls during the cooler months of May to August. The gently undulating terrain of this area is part of the Great Plateau, a major physiographic feature in the western quarter of the continent. Deep lateritic weathering profiles are common and there has been widespread modification by stripping. Detritus derived from partial erosion of the lateritic mantle is widely distributed.

At Mount Gibson, two types of red soils are associated with the greenstone sequence, namely, calcareous red earths associated with an occasional mafic outcrop and acid red earths overlying hardpanized colluvium. The distribution of these contrasting types of soil is related to the complex physiographic history, including deep weathering, and processes of erosion and deposition. Calcareous red earths occur on broadly-concave erosional tracts set below areas of acid red earths separated by change of slope. Here, on concave tracts there are sporadic exposures of mafic weathered rocks and these areas are seen as being erosional tracts. The calcareous red earths show a close association with weathered or subcropping mafic rocks and appear to result from *in situ* weathering of rocks. By contrast, acid red earths associated with the long gentle slopes flanking these erosional tracts have formed in colluvium, derived from the erosion of the weathering profiles from the upland erosional areas. The acid red earths are underlain by gravelly-hardpanized colluvium which in turn overlies lateritic duricrust. The most common substrate to the calcareous red earths is non-calcareous dark, red-brown plastic clays which merge with mafic saprolite at a depth of 3 to 4 metres.

The clay fraction of calcareous red earths is dominated by smectite, kaolinite, and mixed, layer minerals with small amounts of hematite and Al-goethite. In contrast, the clay fractions of acid red earths are dominated by kaolinite; smectite is typically absent. Calcite is the dominant carbonate mineral in calcareous red earths. The gravel fraction of acid red earths consists of lateritic nodules/pisoliths and is dominated by hematite and Al-goethite. Calcareous red earths contain only a minor gravel fraction. Lateritic nodules and pisoliths are typically absent; the gravel fraction being dominated by 1 to 5-mm shiny, black, ferruginous granules and lithorelics.

POORLY CRYSTALLINE IRON OXYHYDROXIDES AND OXYHYDROXYSULFATES IN WEATHERING ENVIRONMENTS IN SOUTH AUSTRALIA: OBSERVATIONS ON OCCURRENCE, GENESIS, PROPERTIES AND BIOMINERALIZATION

R.W. FITZPATRICK, P.G. SELF AND R. NAIDU

CSIRO DIVISION OF SOILS, PRIVATE BAG NO 2, GLEN OSMOND, SOUTH AUSTRALIA 5064

This paper reports on the occurrence, genesis and properties of ferrihydrites with two to six broad X-ray diffraction peaks and associated poorly crystalline hydrous iron oxyhydroxides (lepidocrocite and goethite) and oxyhydroxysulfates formed during the weathering of pyrite under various earth surface environments in the Mount Lofty Ranges, South Australia. The weathering of pyrite in these landscapes occurs either because of exposure by mining or from the seepage of ground water through naturally occurring pyrite lenses. In presenting and discussing new information on these minerals it is convenient to describe the following two distinct but related landscape processes:

(1) Iron precipitates associated with mine waste waters in retention ponds.

Bigham *et al.* (1990) have recently established the properties and occurrence of a poorly crystalline oxyhydroxysulfate mineral which precipitates as a red-brown sludge in acid mine waters by both bacterial and chemical oxidation of ferrous solutions. A similar poorly crystalline oxyhydroxysulfate mineral in association with varying amounts of jarosite was identified in reddish-brown precipitates that form around margins of retention ponds and streams at abandoned mines containing pyritic waste-rock near Nairne in the Mt. Lofty Ranges.

(2) Natural iron precipitates associated with groundwater discharge into soils.

Ferrihydrites with either two, four or six broad X-ray diffraction lines and which contain appreciable silica are found in: (i) brown gel-like precipitates floating in water, (ii) dark reddish-brown, rusty friable thin crusts "caked" on the banks of water courses and (iii) dark reddish-brown, rusty friable thin crusts on soil surfaces with various iron mineral accumulations coating and weakly cementing sand grains.

TEM and SEM examination of several occurrences indicates that the ferrihydrites are minute particles and are often embedded or encrusted in sheath-like structures of Fe-oxidizing bacteria; mainly of *Sphaerotilus*, *Gallionella* and *Leptothrix*. Very thin lath-shaped, poorly crystalline crystals of lepidocrocite and goethite are often found embedded in these essentially ferrihydrite-rich deposits. The proportion of these iron oxyhydroxides is critically dependant on solution pH, Eh and ionic concentrations. The presence of these minerals can be attributed to the geochemical processes associated with the influence of high ground water-tables (following tree clearing) containing high levels of sulfur, iron and other salts. The thin surface crusts are usually developed on Typic Sulfaquents with ferrihydrite and goethite occurring as coatings on surfaces of primary grains in the form of clusters and fluffy aggregates. These minerals have crystallized in interstitial matrices of the primary grains from oxidation of mobile Fe(II) containing solutions derived from the underlying bleached horizon. Energy dispersive X-ray analyses, selective chemical dissolution, and X-ray powder diffraction data show that the iron oxyhydroxide clusters contain Si, Ca and Al. The increased acidity and the goethite and jarosite accumulations in pores of the underlying sporadically bleached and mottled horizon (E horizon) indicates repeated oxidation and reduction under seasonally fluctuating water-table conditions (dissolution and/or transformation of pyrite). The dense black sulfidic horizon (B2 horizon) at greater depth (20-50 cms) contains poorly crystalline iron pyritic minerals. These sulfide minerals are formed initially by bacterial reduction of sulfate when the groundwater is discharged at the soil surface through macropores (mainly old tree root channels) connected to semi-confined aquifers.

The processes occurring in mine waste water and ground water discharges in these landscapes are related. However, during mine weathering the oxidation of Fe(II) is more rapid and occurs under more acidic conditions than in the soil matrices of the natural landscape.

REFERENCES

Bigham, J.M., U. Schwertmann, L. Carlson and E. Murad (1990) A poorly crystallized oxyhydroxysulfate of iron formed by bacterial oxidation of iron(II) in acid mine waters. *Geochimica et Cosmochimica Acta* 54, 2743-2758.

**An X-ray powder diffraction study of heated synthetic
aluminium-substituted goethite**

H. D. Ruñ and R. J. Gilkes

Department of Soil Science and Plant Nutrition

University of Western Australia, Nedlands, 6009

Aluminium substituted goethite was synthesized by oxidation of mixed FeCl_2 - AlCl_3 solutions at a pH of 6.5-8.2 buffered by bicarbonate. Samples were extracted with 0.2 M ammonium oxalate to remove poorly crystalline compounds. Aluminium substituted goethite partly or completely changed to hematite when heated for one hour at temperatures between 200°C and 270°C. Goethite started to change to hematite at 210°C for 0 mole%, 220°C for 9.7 mole% and 19.7 mole%, and 230°C for 30.1 mole% aluminium substitution. Goethite completely changed to hematite in one hour at 230°C for 0 mole%, 240°C for 9.7 mole%, 250°C for 19.7 mole% and 260°C for 30.1 mole% aluminium substitution. An X-ray powder diffraction study of the heated samples indicated that d-spacings decreased and the width at half height of reflections increased as aluminium substitution increased. Heating also decreased d-spacings of goethite but to a lesser extent than was due to aluminium substitution. The width at half height of goethite reflections increased as the heating temperature increased. In contrast, the width at half height of hematite reflections decreased gradually as temperature increased. Aluminium substitution in goethite and hematite linearly decreased unit cell dimensions and increased the dehydroxylation temperature of goethite and the surface area of both minerals.

AN X-RAY DIFFRACTION STUDY OF SYNTHETIC METAL-SUBSTITUTED GOETHITE AND HEMATITE

M.A. Wells, R.J. Gilkes and R.W. Fitzpatrick*
Soil Science and Plant Nutrition
School of Agriculture
University of Western Australia
Nedlands, W.A. 6009

*CSIRO Division of Soils, Glen Osmond
South Australia

Synthetic goethite (α -FeO.OH) was produced from mixed metal-/ferric (Fe^{3+})-nitrate and metal-/ferrous (Fe^{2+})-chloride systems incorporating Al, Cr, Mn, Ni and Ti as isomorphous substituents. Al, Mn and Ni hematites (α - Fe_2O_3) were produced from mixed metal- and ferric-nitrate solutions. Elements were added each at five nominal levels of substitution.

Atomic absorption spectroscopic analysis (A.A.S.) of acid (pH 3), 0.2M ammonium oxalate treated samples showed an incorporation range of 0 to 20 mole% for substituent elements within the goethite and hematite structures.

Unit-cell parameters, b_0 and c_0 , of Al-substituted goethites (Fe^{3+} and Fe^{2+} systems), for levels of Al incorporation of 0-4.6 and 0-19.6 mole% respectively, decreased linearly towards the pure Al end-member, diaspore (α -AlO.OH). The a_0 dimension of Al-goethites (both systems) exhibited no trend with Al substitution. Unit-cell volumes of goethite (both series) exhibited a linear decrease with Al content.

a_0 and c_0 unit-cell dimensions of Mn- and Cr-goethites (both series) decreased with increasing metal content for substitution levels of 0-9 mole% Cr (Fe^{3+} and Fe^{2+} systems) and 0-5.3 and 0-15.3 mole% Mn for goethites derived from the ferrous and ferric systems respectively. The b_0 unit-cell dimension for Mn-substituted goethite (Fe^{3+} and Fe^{2+} systems) and Cr-goethite (Fe^{3+} system) increased linearly with Mn and Cr content shifting towards the Mn and Cr isostructural end-members, groutite (α -MnO.OH) and bracewellite (α -CrO.OH) respectively. The b_0 dimension of Cr-goethite (Fe^{2+}) decreased with increasing Cr content. Unit-cell dimensions of Mn- and Cr-goethites (both systems) followed the trend of the Vegard line for their respective pure Mn and Cr end members. Unit-cell volumes of Mn- and Cr-goethites (both systems) decreased linearly with increasing metal content with the trend for cell volume for Mn-goethite (both systems) opposing the trend of the Vegard relationship between the isostructural Fe and Mn analogues, goethite and groutite.

The a_0 , c_0 and a_0 , b_0 unit-cell parameters of Ni- and Ti-goethites (Fe^{3+} and Fe^{2+} systems) respectively, exhibited no trend with metal content for levels of incorporation of 0-10.0 and 0-5.0 mole% Ni and 0-18.7 and 0-12.2 mole% Ti (Fe^{2+} and Fe^{3+} respectively). The b_0 dimension and unit-cell volume of Ni-goethites (both systems) showed a linear increase with Ni content. The c_0 dimension and unit-cell volume decreased linearly for Ti-substituted goethites produced from both systems.

Substitution of Al (4.6-15.0 mole%), within hematite was associated with a linear decrease in a_0 and c_0 unit-cell parameters and unit-cell volume. The shift was towards the pure Al analogue corundum (α - Al_2O_3), but deviated from the Vegard line for the pure Fe and Al end-members. Unit-cell dimensions a_0 and c_0 and unit-cell volume of Ni-hematite increased linearly with Ni contents from 1.1 to 6.0 mole%. The a_0 dimension and unit-cell volume of Mn-substituted hematite increased in a linear fashion with Mn content from 3.3 to 6.0 mole% Mn.

Crystal size and morphology of goethite and hematite crystals were modified by metal substitution as determined by transmission electron microscopy (TEM). The incorporation of Cr, Mn and Ti changed unsubstituted, goethite (Fe^{2+} system) from cigar-shaped laths (260 x 920nm) to more rounded, lath-like crystals (35 x 145nm) for the highest levels of metal substitution. With incorporation of Al and Ni spherical particles 3-5 and 26nm in diameter respectively, are formed. For substitutions of Al, Cr, Ni and Ti the raft/lath-like morphology of crystals of unsubstituted goethite (Fe^{3+}) (115 x 600nm) was retained. Laths for the highest levels of Al, Cr, Mn, Ni and Ti substitution had sizes of 92 x 250, 190 x 420, 110 x 385 and 260 x 800nm respectively. Mn at the highest level of substitution (15.3 mole%) induced an acicular (42 x 650nm) morphology.

Ni and Mn substituted hematites exhibited an equant particle morphology. Crystal size increased from 76 to 132nm for 1.1 and 6.0 mole% Ni-hematite respectively. Mn-hematite particles increased in size from 39 to 97nm over the substitution range of 3.3 to 6.3 mole%Mn respectively. Al hematite crystals varied from pseudo-hexagonal crystals (112nm) for 4.6 mole% Al to platy particles (430nm) for 15.0 mole% Al.

Ratios of crystal size determined by TEM and XRD line broadening for Al-, Cr-, Mn-, Ni- and Ti-substituted goethites (Fe^{3+} system) and Cr, Mn and Ti goethites (Fe^{2+} system) indicate the presence of a sub-structure of coherently diffracting crystallite domains predominantly developed parallel to the c dimension (i.e. length) of the goethite crystals. TEM to XRD crystal size ratios for Al-, Ni-goethites (Fe^{2+} system) and Al-, Ni- and Mn-substituted hematites ranged from 0.3 to 2.3 and approached unity with increasing substituent metal content. This indicates that some goethite and hematite crystals consist of a sub-structure of several coherently diffracting domains.

WEATHERING AND ALTERATION AT THE PANGLO GOLD DEPOSIT, WESTERN AUSTRALIA

F Ivor Roberts

WESTERN AUSTRALIAN SCHOOL OF MINES

The Panglo gold deposit, located about 30 km north of Kalgoorlie within the Archaean Yilgarn Block of Western Australia, is a shallow, low grade, bulk tonnage lode located beneath a salt lake. At the Panglo gold deposit, as is typical for much of Western Australia, the regolith has developed over a long period of time. Possibly since the Permian, much of the Yilgarn Block has represented a stable and emergent craton, and has been exposed to various climatic conditions. From the Cretaceous to mid-Miocene the Yilgarn Block was subjected to extensive deep lateritic weathering by a humid, warm to tropical climate. From the Miocene, however, the climate has been much drier and as a consequence there has been a lowering of water-tables, a slowing of chemical weathering reactions and the presentation of the pre-existing regolith.

The rock types at the Panglo gold deposit consist of a sequence of undifferentiated sedimentary rocks, as well as mafic and ultramafic volcanic rocks. The mafic volcanic rocks represent the host rock for the gold mineralisation and is accompanied by wall rock alteration. Hydrothermal alteration at Panglo typify propylitic mineral assemblages of the Kalgoorlie region and comprise of varying quantities of iron-sulphides, chlorite, sericite and carbonate minerals.

To determine the consequences of weathering of the phyllosilicate minerals in the propylitised zones, mineralogical analyses was undertaken on material collected from two drill holes. These holes contained a representative sequence of the mineralisation, in addition to a sequence from the highly weathered rock at the surface of the salt lake to fresh rock at depth. Results of this study will be presented, together with comments regarding the presence of smectite and interstratified clay minerals on the stability of the slopes in the open cut pit.

Secondary clay minerals of some Victorian Basalts and their influence on some aggregate properties

G.W. Quick and A. Shayan

CSIRO Division of Building, Construction and Engineering
P.O. Box 56, Highett, Vic. 3190

Abstract

Several basalts were collected from three operating quarries in the Melbourne supply region. Various properties of the aggregates such as clay content, methylene-blue adsorption, water absorption, drying shrinkage and porosity have been determined, and the textural features examined by optical and scanning electron microscopy. Attempts have been made to relate the properties to the extent of alterations experienced by the rock, and from this deduce service performance. For the so-called "green basalts" containing secondary clay minerals, the properties of the rock are directly influenced by the extent of alteration and the quantity of swelling clay minerals formed in the rock. A number of samples of grey basalt from one source showed very high dimensional changes under conditions of cyclic wetting and drying, although deleterious swelling clays of the smectite group were not evident. These latter basalts contained iddingsite instead of swelling clay minerals, and had high porosities as measured by mercury intrusion and water absorption. The iddingsitised olivine crystals showed considerable microcracking which would have an influence on the magnitude of measured porosity and water absorption. The unacceptable dimensional stability of these grey basalts that have no obvious swelling clay components, may have been caused by the high porosities. However, further work using more sensitive refined techniques such as transmission electron microscopy of ultra thin sections would need to be done before drawing a final conclusion.

HISINGERITE: A WEATHERING PRODUCT OF OLIVINE

Maïté Le Gleuher and Tony Eggleton

Centre for Australian Regolith Studies
Australian National University
Canberra, ACT

Introduction The terms "green products" and "bowlingite", used during the last decades for the products formed during the early stage of the alteration of olivine in volcanics, refer to phases consisting mainly of chlorite and Fe-rich saponite (Baker and Haggerty, 1967; Delvigne et al, 1979; Ildefonse, 1983; Eggleton et al., 1987; among others). In the basalts of the Monaro Region, olivine phenocrysts are replaced by chlorite, Fe-rich saponite and hisingerite. In the literature concerning the alteration of basalts, hisingerite is found in cooling joints and in cracks, very often in association with siderite or pyrite (Shayan, 1984). "Green products" and hisingerite have been related to a low temperature deuteric alteration, under non-oxidative conditions. In the Monaro basalts, smectites and hisingerite seem to have been formed under weathering conditions. The study has been carried out with methods allowing a strictly in situ investigation: optical microscopy, microprobe analyses, XRD of material removed from the thin sections, and T.E.M.

Three stages have been recognized based on textural, mineralogical and chemical changes in the alteration products: (1) chlorite; (2) Fe- saponites; (3) hisingerite. Alteration of olivine into iddingsite and more advanced weathering of these products into Al-Fe-Mg smectites, and halloysite (Eggleton et al., 1987; Le Gleuher, 1990) will not be reported here.

Result and Interpretation The freshest basalt consists of phenocrysts of olivine Fo₈₀, Ti-Augite, labradorite, ilmenite and of palagonized glass. Samples were collected from a drilling core, from the freshest rock and from hard corestones included in more weathered material and located in the upper 1.5 meters.

The first episode is characterized by the development of chlorite oriented perpendicular to the intracrystalline clasts of the olivine grains. The chlorite is a ferroan-clinocllore with a Fe^{2+}/Mg of 1.5 and is similar in composition to the chlorite which rims the palagonized glass. Calcite has been also observed along cracks in few grains and in the central part of the altered glass. The chlorite formation requires an external Al supply which cannot be provided by the plagioclases, as it is still unaffected. Chlorite formation is seen to be contemporaneous with the glass palagonization.

The second step is represented by the Fe-rich saponites. Two smectites have identical composition with a Fe^{2+}/Mg ratio of 0.3 but present very distinct micromorphologies: randomly oriented microcrystallites along the chlorite rims, and a "chevron" pattern composed of smectites with a high birefringence and a coarse cleavage parallel to the base or to the edges of the chevrons.

These smectites may be outlined by a narrow band of smectites with a higher iron content and a Fe^{2+}/Mg ratio of 0.9. The three types of smectites have less than 0.6 Al per unit cell [All the structural formulae are calculated on the basis of 20(O) and 4 (OH)].

The third episode has been observed in the corestones surrounded by a material where the olivines are totally pseudomorphosed and the plagioclases partially converted. Microcrystalline smectites and "chevron-like" smectites also develop along the cracks. The Al content is higher, ranging from 1.3 to 2.7 Al per unit-cell and the iron content slightly higher, $\text{Fe}^{2+}/\text{Mg} = 0.5$. The olivine relicts are almost completely replaced by a honey-yellow, isotropic material, glassy in appearance. This product contains more iron than the smectites, Fe^{2+}/Mg ranging from 4 to 5, and slightly lower Al concentrations (1.1 to 1.5 Al per unit-cell). X-ray diffraction of this material show very broad and diffuse lines of smectites. With T.E.M, this product has a very distinct morphology and cannot be confused with the tangled strands characteristic of smectites. It consists of circular structures 100-200 Å in diameter similar to those observed by Shayan (1984) and Eggleton (1987), and Shayan et al. (1988). Narrow bands of smectites along microcracks might be responsible for the diffuse lines in XRD.

The diagnostic for the determination of hisingerite is still controversial, depending mainly on the observation scale and on the samples which have been investigated. In a diagram of total Fe in octahedral position vs Mg in octahedral position, (Brigatti's, 1982), the compositions of more than half of the glassy products of this study not included in the hisingerite area. However, T.E.M shows that they are non-crystalline phases and not nontronite. The octahedral:tetrahedral cation ratio is close to 1:2. Hisingerite studied by Eggleton et al (1983) and Eggleton (1987) present a ratio close to 1:1.

This study shows that the hisingerite composition is not as restricted as reported in the literature. It is a non crystalline phase with a Fe-smectite composition.

When formed in an environment where Al is released in solutions by the weathering of plagioclases, the Al-content of the Fe-rich saponite is much higher than in the smectites observed in the freshest samples. The Al concentrations of hisingerite also seems to be related to the degree of alteration of the plagioclases surrounding the olivines phenocrysts. Fe-rich saponites and hisingerite are likely to be weathering products of olivine, under non oxidative conditions.

References

- Brigatti M.F., (1982). Hisingerite: a review of its crystal chemistry: in Proc. Int. Clay. Conf. Bologna and Pavia, 1981, H. van Olphen and F. Veniale Eds, 97-110 Elsevier, Amsterdam.
- Shayan A., Sanders J.V., Lancucki C.J., 1988 — Hydrothermal alteration of hisingerite material from a basalt quarry near Geelong, Victoria, Australia. Clays & Clay Min., 36, No 4, 327-336.
- Ildefonse P., 1983. Alterations primétoiriques et météorique des olivines du basalte de Belbys (Contal, France). Soc. Géol. Mem. 72, 69-78.

BALLARAT INDUSTRIAL CLAY RESOURCES

Peter Dahlhaus
Geology Department
Ballarat University College

The geological history of the Ballarat Region has produced a variety of industrial clay resources which are currently exploited to sustain important local industries. On the basis of their geological setting, these clay resources have been grouped into three major categories.

The deeply weathered Lower Palaeozoic sediments provide the low-plasticity component in brickmaking. These clay deposits, which are up to 30 metres thick, result from intense weathering during the Cainozoic and comprise mainly illitic clay minerals. The industrial clay deposits of this type are exploited at North Ballarat and Creswick.

The plastic component of the clay mixes used in brick, pipe and tile making is being extracted from the Napoleons-Enfield area. These clays are post-basaltic, probably deposited in a lacustrine environment formed by the damming of the ancient Leigh River by Plio-Pleistocene volcanic flows. The more plastic component of the pipe making clay mix is extracted from the Tertiary clays at Buninyong. These clay deposits occur within the alluvial deep leads.

The kaolin clay deposits of the Ballarat region are currently being mined at Pittong and Lal Lal. Both these deposits are derived from the residual weathered profile of the Devonian granodiorite, which was deeply weathered during the Tertiary. Until recently, a source of very pure kaolin has been deeply weathered Devonian dyke rocks. Discovered during gold mining last century, these dykes have been recorded to depths of 590m and kaolinised to a depth of 100m.

A study of the Ballarat clay resources conducted for the Ballarat Regional Board for Planning and Development Inc. concluded that while exploration potential is good, the current planning constraints may limit the future utilisation of the clay reserves. Low value clays are particularly vulnerable to the planning and environmental requirements, since the significant cost of gaining permission for extraction makes good deposits marginal.

The greatest potential for industrial clay exists in the kaolin clay deposits of the Lal Lal area. The area has a history of producing high quality (and therefore, high value) clays and has not yet been fully explored. The area is subject to severe environmental constraints, but the value of the resource may outweigh the high establishment costs.

THE MOUNT HOPE KAOLIN DEPOSIT, EYRE PENINSULA,
SOUTH AUSTRALIA

J L KEELING and M D RAVEN*

S A Department of Mines and Energy

*CSIRO Division of Soils (Adelaide)

During 1972-73, Abaleen Minerals NL drilled 52 rotary/air holes to outline a large primary kaolin deposit 6km south-southeast of Mount Hope township on southwestern Eyre Peninsula. Preliminary investigations by Robertson Research (Australia) Pty Ltd and Amdel Ltd showed that the samples comprised well-crystallised kaolinite of moderate to good brightness, but gave a low yield of $<2\mu\text{m}$ size particles with poor rheological properties. Bulk samples from a shaft sunk in the central portion of the deposit were dispatched to Erbslöh & Co in West Germany who after extensive test work, reported that they had produced a sample fraction with improved viscosity which met paper-coating specifications (Abaleen Minerals NL, 1974). In December 1973, while test work was in progress, Abaleen Minerals went into provisional liquidation. Attempts to independently repeat the West German results were unsuccessful (to date).

The deposit was re-examined in 1986 by S A Kaolin Pty Ltd and a further 19 reverse circulation holes were drilled. This exploration confirmed and extended the area of known kaolinization but laboratory tests again were disappointing with samples showing a low yield of $<2\mu\text{m}$ fraction (5-26%, average 11%) and poor rheological properties (thixotropic or dilatant at solids content ranging from 41-60%).

Investigations by the authors have shown that the deposit is in deeply weathered granite gneiss and schist of probable Sleaford Complex of Archean age which is overlain by 5 to 12m of Bridgewater Fm. calcarenite. Kaolin was formed by alteration of feldspar and mica and throughout the deposit shows a variety of morphologies. These include broad ragged-edged sheets, coarse open crystal stacks, thin platelets comprising a mosaic of smaller crystals, individual euhedral crystals, and rolled sheets or tubes. Non-kaolin

minerals present are predominantly quartz, with minor mica and rutile/anatase, and trace amounts of iron oxides and a rare earth phosphate, probably monazite.

For some samples, dispersion in water results in a high proportion of coarse thin platelets of kaolinite which may comprise the bulk of, or be difficult to separate from, the $<2\mu\text{m}$ fraction. These particles appear to be responsible for the dilatant effects observed. The $<2\mu\text{m}$ fraction of some samples comprises predominantly tubular forms. The tubes do not respond to the formamide treatment method used to identify halloysite (Churchman et al, 1984) and are therefore identified as kaolinite. They are often collapsed and may show splitting along the tube axis. In detail, some tubes show pseudo-hexagonal growth edges. Samples from the deposit with a high proportion of tubes do however show characteristic XRD traces which could assist with identification to outline the distribution of tubes within the deposit.

Production of a coating-grade kaolin will require beneficiation which improves the yield and effective separation of the $<2\mu\text{m}$ size particles. Areas with a high content of tubular kaolinite may only be suited to production of filler-grade kaolin.

REFERENCES

- Abaleen Minerals NL, 1974. Report on kaolin project, Mount Hope Deposit. Exploration Licence No. 58, covering the period February 1972 - August 1974. *South Australia. Department of Mines and Energy. Open file Envelope, 2298* (unpublished).
- Churchman, G.J., Whitton, J.S., Claridge, G.G.C. and Theng, B.K.G., 1984. Intercalation method using formamide for differentiating halloysite from kaolinite. *Clays and Clay Minerals, Vol.32, No.4*, 241-248.

ALUMINO-SILICATE MINERALS SUITABLE FOR HIGH GRADE REFRACTORIES

M. G. Lines

Commercial Minerals Ltd
549-551 Burke Road, Camberwell VIC 3124

ABSTRACT

During 1989 Commercial Minerals Ltd acquired the operating assets of Australian Industrial Minerals including the Williamstown sillimanite, kyanite, and mica mine which has been in operation since the turn of the century. Located some 40km north of Adelaide the deposit is opencast and selectively mined to produce roughly 10,000 tpa of ore. There are four main products from the orebody - a white kaolinised sillimanite marketed as kaosil, sillimanite, mica and kyanite. At the mine site kaosil and mica are crushed and screened to - 75mm before transportation to the processing plant at Gillman, Adelaide. At Gillman the sillimanite is calcined prior to crushing and screening.

Kaosil accounts for over 80% of the mine's production and because of its unique crystalline structure it has good thermal shock resistance and thus is mainly used in refractories. Milled kaosil is sold to the domestic market and also exported, with the main markets being the UK, New Zealand, and South East Asia. The sillimanite contains 50-60% Al_2O_3 with the alumina content dependent on the extent of kaolinisation. Owing to its interlocking fibrous habit the minerals has to be calcined at 1,100-1,200°C before crushing. Sillimanite accounts for about 5% of the mine's output and is sold to domestic refractory manufacturers. Kyanite is found associated with the sillimanite and a small but declining production is sold domestically, again for refractories.

THERMAL HISTORIES AND ILLITE GROWTH IN SEDIMENTARY BASINS

HAMILTON, P.J., CSIRO Div of Exploration Geoscience, NSW

GILES, M., Shell UK, London, England

AINSWORTH, P., SURRC, Glasgow, Scotland

K-Ar dating is used extensively to assess timing of illite diagenesis relative to the time of hydrocarbon charge to petroleum reservoirs. The viability of such application is critically assessed by integration of age data with burial history curves and petrographic observations from Jurassic samples from the Brent oil province of the North Sea.

Illite ages from sandstones with detrital clay matrix ("dirty sandstones") are generally older than those from "clean sandstones". This probably results from contamination with detrital illite in the former. Consequently, it is found that illite ages for finest size fractions from "clean" sandstones from within oil legs generally match calculated times of oil migration and approximate the cessation of illite formation. However, illite diagenesis can persist at reduced rates in water wet portions of oil zones after oil accumulation.

It has been observed that neoformed illite first appears at *ca.* 2300m depth, corresponding to a temperature of about 80° C. The corresponding time is tens of millions of years greater than the youngest illite ages. This indicates a time span for illitisation that is significantly greater than the measured age difference between coarsest and finest fractions of an illite separate. Further, none of the K-Ar data provides evidence of recent diagenesis (<15 Ma) even though it might be expected to have occurred.

A model for illite growth is proposed that explains some of the above observations. An understanding of the importance of fluid flow rates in promoting illite forming reaction rates suggests that age data are always biased by sampling of grains formed at the maximum rate of growth.

**PALAEOHYDROLOGICAL SIGNIFICANCE OF AUTHIGENIC KAOLINITE
IN THE ALDEBARAN SANDSTONE,
DENISON TROUGH, EAST-CENTRAL QUEENSLAND**

Julian C. Baker* and Suzanne D. Golding

Department of Geology & Mineralogy, University of Queensland,
St. Lucia, 4072

Authigenic kaolinite occurring in deep subsurface sandstones of an important hydrocarbon reservoir, the Early Permian Aldebaran Sandstone, has been studied using thin section, XRD, SEM and isotopic techniques. Where the Aldebaran Sandstone is no longer an active aquifer, kaolinite is an intermediate-stage phase as shown by its, (1) textural relationships with co-existing authigenic minerals, and (2) occurrence in sandstones which are now either saturated with strongly alkaline soda brines or contain gas. The kaolinite is highly depleted in deuterium ($\delta D_{SMOW} = -115$ to -99 ‰; $N = 3$) and ^{18}O ($\delta^{18}O_{SMOW} = +7.8$ to $+8.9$ ‰; $N = 4$) indicating that acid water involved in its formation must have been meteoric. Deep penetration of this water is linked to Late Triassic structuring in the Denison Trough, an event which led to exposure of the Aldebaran Sandstone by the Early Jurassic prior to its re-burial beneath Jurassic and Cretaceous sedimentary rocks. The intimate association between kaolinite and existing carbonate dissolution porosity in the unit suggests that the formation of this porosity is related to flushing by the same unconformity-derived water. Leaching of aluminosilicate grains probably also occurred during this flushing event giving rise to volumetrically important grain dissolution porosity and the Si^{4+} and Al^{2+} required for kaolinite precipitation.

Where the Aldebaran Sandstone is presently undergoing meteoric flushing near its outcrop area, authigenic kaolinite is relatively enriched in ^{18}O ($\delta^{18}O_{SMOW} = +11.8$ ‰; $N = 1$). This reflects its precipitation largely from post-Mesozoic meteoric water which was isotopically heavier than the Mesozoic water involved in the precipitation of the intermediate-stage kaolinite. The temporal change in the isotopic composition of these waters can be related to the latitude dependence of the isotopic composition of meteoric water and the northward drift of the Australian continent to lower latitudes since the Mesozoic Era.

* *Present address:* Electron Microscope Centre, University of Queensland, St. Lucia, 4072

Clays and Toxic Waste Disposal

O.G. Ingles

Clays have a special role in toxic waste disposal: firstly because of their low permeability they can serve to contain the waste and prevent it spreading in ground waters with severely adverse environmental effects: secondly because of their ability to adsorb and hold toxic metal cations on the exchange complex, as well as to take up many toxic organic molecules, thus preventing their wider dissemination by surface and underground waters.

This paper discusses the practical requirements for containment of toxic wastes by clays by reference to actual waste disposal site experience in Tasmania, and points to the need to formulate practical rules for waste containment sites based on further research into clay soils with the specific objective of defining their behaviour over long periods of time.

The instances cited cover disposal of purely organic wastes, of mixed toxic metal and organic wastes, and wastes of unknown provenance and toxicity.

Bauxitization: Temperate and Intemperate

Michael I. Bird[†], Allan R. Chivas[†] and Frederick J. Longstaffe*

[†]Research School of Earth Sciences, Australian National University,
P.O. Box 4, Canberra, A.C.T. 2601, AUSTRALIA

*Geology Department, University of Western Ontario,
London, Ontario, N6A 5B7, CANADA

The $\delta^{18}\text{O}$ composition of gibbsite from bauxites formed at high palaeolatitudes (up to 55°S) indicate equilibrium with low- $\delta^{18}\text{O}$ meteoric waters, suggesting formation in a cool to cold environment. Recognition that the gibbsite-water oxygen-isotope fractionation curve is insensitive to temperature in the 0-30°C range enables mineral pairs such as gibbsite-kaolinite to be used to quantitatively estimate palaeotemperatures. Such an approach yields reasonable temperature estimates for young bauxite formed in non-monsoonal tropical regions ($\sim 34 \pm 6^\circ\text{C}$) and suggests much lower temperatures ($\sim 10 \pm 5^\circ\text{C}$) for bauxites formed at high palaeolatitude in the southeastern highlands of New South Wales and the southern Gippsland region of Victoria. These data are in accordance with previous $\delta^{18}\text{O}$ determinations on clay minerals and recent palaeobotanical evidence from southeastern Australia. The conclusion that bauxitization is not strictly a tropical or sub-tropical weathering phenomenon means that care should be exercised in interpreting the palaeoclimatic significance of bauxites in the geological record.

VISCOSITY AND SETTLEMENT OF TAILINGS

W.W. Emerson and D. Weissmann

CSIRO Division of Soils, Adelaide

The dominant minerals present in the clay sized fraction of acid extracted tailings from the Ranger Uranium Mine at Jabiru are chlorite and quartz. There is also a high concentration of sulphates in solution mainly magnesium, but including aluminium. Changes in the viscosity of concentrated suspensions of the tailings have been measured as the pH is raised with either lime or calcined magnesite. Comparison experiments have been run with ground, acid treated chlorites. The increase in the floc strength is greater when lime is added. The increase is sufficient to prevent settlement of the coarser particles. The result also is an increased settlement volume.

Up to now, tailings have been neutralised with lime. Settlement in the tailings dam is less than expected. Possible reasons for this will be discussed.

PHENOMENOLOGICAL DISTINCTION BETWEEN
PILLARED CLAYS AND RELATED STRUCTURES.

T.W. Turney

CSIRO, Division of Materials Science and Technology,
Locked bag 33, Clayton, Victoria, 3168

Pillared clays are of considerable current interest as new molecular sorbents or microporous catalysts. However, the term "pillared clay" is often loosely and incorrectly used to describe any material (often multiphasic) resulting from ion-exchange of a bulky cation with the interlayer cations of a clay mineral. Working definitions are given, of the various types of structure which can result from such ion-exchange processes. Three structural models may be experimentally distinguished by a combination of X-ray diffraction, electron microscopy and porosity measurements. Each model may be described in terms of a composite structure, with layered, nanometre-sized domains.

Structure	Interlayer Spacing	Layer Order	Microporosity
Pillared	increased	yes	yes
Stuffed	increased	yes	no
Delaminated	none	no	yes

Examples of pillared structures, include some preparations of alumina-montmorillonite, alumina-fluoromica and vandia-hydrotalcite nanocomposites.

Stuffed structures include the chlorite clays, alumina- $\text{Ca}_2\text{Nb}_3\text{O}_{10}$ and valleriite (FeCuS_2 -hydrotalcite).

Delaminated structures are poorly ordered and include many alumina-, Fe_2O_3 -, FeS -, Cr_2O_3 -clay nanocomposites.

FORMATION OF β' -SIALON CERAMIC FROM A MONTMORILLONITE-CARBON NANOCOMPOSITE BY CARBOTHERMAL REDUCTION.

T.Bastow, S.G.Hardin* and T.W.Turney

CSIRO Division of Materials Science and Technology

Locked Bag 33, Clayton 3168, Victoria, Australia

The carbothermal reduction in an N_2 atmosphere of a nanocomposite between dodecylammonium-exchanged montmorillonite and polyacrylonitrile (PAN) have been studied. Comparison with analogous reactions involving sodium-exchanged montmorillonite and dodecylammonium-exchanged montmorillonite (without PAN), shows that in the presence of PAN, the formation of silica, cordierite or mullite is almost completely suppressed. The only crystalline phase detected between 1000-1300°C was a β' -sialon, having a much higher Si:Al ratio (7.05:1) than that of the precursor clay (2.44:1). Reduction of the octahedral AlO_6 layer derived from the parent clay structure begins near 1200°C, forming increasing amounts of $Al(N,O)_4$ tetrahedra with temperature, so that by 1600°C, complete reduction to AlN_4 (i.e. bulk AlN) has occurred. In contrast, reduction of the tetrahedral SiO_4 layers is appreciable as low as 1100°C, and is almost complete (to SiN_4 tetrahedra in β' -sialon) by 1200°C. No intermediate $Si(N,O)_4$ environments are found. By 1600°C, complete conversion to SiC_4 tetrahedra (i.e. bulk SiC) has occurred. A mechanism is suggested involving sequential reduction of $Si(OSi)_4$ and $Si(OSi)_3(OAl)$ groups. Solid-state ^{27}Al and ^{29}Si NMR spectroscopic, X-ray diffraction, transmission electron microscopy and thermogravimetric data are given.

THE ROLE OF SODIUM IONS IN THE ION EXCHANGE OF
MONTMORILLONITE GEL WITH PARTIALLY HYDROLYSED SOLUTIONS OF
ALUMINIUM CHLORIDE

P.A. Corrigan and T.W. Turney

CSIRO Division of Materials Science and Technology
Locked Bag 33, Clayton 3168, Victoria, Australia

The reactions of Na^+ -exchanged montmorillonite gel with partially hydrolysed solutions of aluminium chloride have been studied. The sodium ion concentration appears to be an important factor in the pillaring process. The interlayer separation of the initially formed clay product, as determined by XRD spectra, indicates that only a small proportion of the clay has the large oxoaluminium " Al_{13} " cations intercalated between the clay layers. However, the aluminium must be incorporated onto the clay since a fully pillared product is obtained on washing the clay and removal of excess ions. This pillaring process appears to be readily reversible as reaction with NaCl solutions reduces the interlayer spacing back to that observed for the Na^+ -exchanged clay. Low concentrations of salt solution give a completely reversible reaction as the pillared clay can be reformed with washing. Higher concentrations of NaCl displace aluminium ions from the clay into solution so that the aluminium pillars are not reintroduced by subsequent washing. Clay products were investigated using XRD spectra, elemental analysis and surface area determination. Reactions of montmorillonite with a solution containing " Al_{13} " chloride in which there is a much lower sodium ion concentration were also studied. These show that there is a limit to the amount of aluminium that can be incorporated into the clay. Under this limit, there is a small range of incorporated aluminium where the clay remains fully pillared, presumably with a change in pillar density. As the amount of aluminium decreases even further, the pillars do not appear to be less densely packed, rather the clay is only partially pillared.

**ILLITE-SMECTITE RIMS IN THE EARLY PERMIAN ALDEBARAN SANDSTONE,
DENISON TROUGH, EAST-CENTRAL QUEENSLAND - COMPOSITION,
PALAEOHYDROLOGICAL SIGNIFICANCE AND INFLUENCE ON RESERVOIR
QUALITY**

Julian C. Baker⁺, Suzanne D. Golding and Ian D.R. Mackinnon*

Department of Geology & Mineralogy, University of Queensland, St. Lucia, 4072

*Electron Microscope Centre, University of Queensland, St. Lucia, 4072

Authigenic illite-smectite grain rims occurring in nearshore-marine sandstones of the basal Aldebaran Sandstone have been studied using thin-section, XRD, SEM, HRTEM, microprobe and isotopic techniques. The rims are up to 20 μm thick and consist of a meshwork of irregular, crinkled flakes oriented perpendicular to grain surfaces. They are a very early diagenetic phase, and probably precipitated in response to an increase in the ionic concentration of interstitial seawater due to early expulsion of cation-enriched fluids from directly underlying marine mudrocks of the Cattle Creek Formation.

The illite-smectite is an allevardite-ordered species with 20 to 25% expandability (XRD), and contains Ca, Mg and Fe in addition to Si, Al and K (microprobe). Its $\delta^{18}\text{O}_{\text{SMOW}}$ values of +8.9 to +11.3 ‰ (N = 6) reflect the involvement of ^{18}O -depleted meteoric water during illitisation of the rims at elevated burial temperatures. Since the basin was subsiding (compacting) during this time, the water is likely to have been "meteoric" connate water derived from very thick mudrocks, sandstones and coals of the *freshwater* Reids Dome beds directly underlying the Cattle Creek Formation.

HRTEM shows that crystallite size of the illite-smectite varies from 20 to 230 Å in the basal direction. Lattice fringes invariably show 10 Å periodicity reflecting an ordered arrangement of illite and collapsed smectite.

The illite-smectite rims have had a dramatic effect on subsequent diagenesis and present reservoir quality. In Christmas Creek #1, the occurrence of relatively thin, poorly developed rims has led to the obliteration of most primary intergranular porosity by promoting quartz grain-to-grain contact dissolution (pressure solution). In contrast, relatively thick, well developed rims in the Warrinilla wells have preserved volumetrically significant amounts of intergranular porosity by inhibiting grain-to-grain contact dissolution and quartz overgrowth formation. Recorded gas flows from the base of the Aldebaran Sandstone in the Warrinilla area reflect the existence of this porosity.

⁺*Present Address:* Electron Microscope Centre, University of Queensland, St. Lucia, 4072

HYDROCRACKING AND ISOMERIZATION OF n-OCTANE AND
2,2,4-TRIMETHYLPENTANE OVER A Pt/ALUMINA-PILLARED CLAY

C.Doblin^a, J.F.Mathews^a and T.W.Turney^a

CSIRO Division of Materials Science and Technology,

Locked Bag 33, Clayton Vic. 3168, Australia.

^aDepartment of Chemical Engineering, Monash University,
Clayton Vic. 3136, Australia.

The hydrocracking and isomerization of n-octane and 2,2,4-trimethylpentane over an alumina-pillared clay, containing 0.16% Pt was investigated in a microreactor operating at atmospheric pressure and varying temperatures (175-325°C) and varying WHSV (0.48-7.5h⁻¹). The structure of the catalyst changed during the first 30 hours of use before becoming stable, as shown by XRD. Hydrocracking of n-octane produced significant but diminishing quantities of methane and ethane during the first 30 h on stream. During this time the dominant classical bifunctional reaction mechanism was accompanied by a second reaction mechanism, possibly hydrogenolysis or cleavage by a non-classical penta-coordinate carbonium ion. After the initial period, the catalyst performed as an ideal hydrocracking catalyst, as characterized by high isomerization yields up to medium conversions, and showed product distributions very similar to those found in Pt loaded large pore zeolites.

GLIMPSES OF CAINOZOIC WEATHERING AROUND MELBOURNE

J.A. FERGUSON

13 geological cross-sections across typical Melbourne claypits show the time sequences of deep weathering events. These deep weathering profiles were in existence and partly stripped by erosion at the time of Older Basalt lava eruptions at Cranbourne, Campbellfield and Keilor. Similar occurrences are known from Harkaway and central Melbourne. Although several different flows and sources are involved they are regarded as being probably Oligocene in age. The weathering sequences below the basalts were formed on the nearly peneplained Nillumbik Terrain which must therefore have been eroded somewhat earlier.

Each Older Basalt occurrence is profoundly weathered either throughout its section or very deeply from its upper surface. This weathering which would have taken some time, also happened under the higher rainfall and temperature conditions of the earlier Tertiary. In some occurrences the weathering proceeded to very fine grained kaolinite as at Keilor while elsewhere as at Cranbourne and Harkaway there is residual montmorillonite in the profile. This almost certainly attests to the different drainage conditions at the two sites.

The Bulla Granodiorite developed pallid zone kaolinitic weathering profiles which progressively eroded and shed pale coloured sands into the Keilor area before and after the extrusion of Older Basalt there.

Lysterfield Granodiorite at Berwick developed a deep kaolinitic weathering profile before the Older Basalt flowed over it and exposures of pallid zone weathering of the same granodiorite at Hallam probably formed at the same time. The mid-Tertiary sediments that overlie the partly stripped weathered granodiorite consist of goethite cemented sandstones and light coloured sands in which another mottled zone is formed by a continuation of the same leaching processes.

Leaching of lesser intensity formed mottled and pallid zones on Miocene marine sediments around Toorak and Malvern, and a pallid margin developed by leaching to the Pliocene prior "Merri Creek" at Craigieburn.

Lower flows of the Newer Basalts at Craigieburn developed not a deep leached profile but a red soil which is unlike the black montmorillonite soils formed on the latest flow under the present climate.

These last two examples show the progressive diminution in intensity of leaching as the climate became cooler and drier since the end of Miocene times.

The upper zones of deep weathering are now largely stripped by erosion. Pallid zones are left as plateau and ridge top remnants in a discontinuous band from Tally Ho and Mitcham through Doncaster and Preston to Keilor and Sunbury. Southwestwards from this they can sometimes be seen descending below the edge of the Brighton Group but their subsurface extent is not well known. Northeastwards from the pallid zone band only the high ridges at Summerhill and Yambat retain pallid zone material. The further reaches of the Nillumbik Terrain extending from Arthurs Creek through St Andrews to Christmas Hills has been eroded on the hilltops to the brown reef weathering zone and in the valley bottoms to grey reef. It is clear that uplift of the Divide or downwarping of Port Phillip sunland have initiated an accelerated erosion cycle which is progressively stripping the formerly extensive deep weathering zone.

SIZE FRACTIONATION TO AID CHARACTERISATION OF
KAOLINITE-SMECTITES IN SOILS
(Poster)

R. Boesen¹, G. J. Churchman, P. G. Self and P. G. Slade

¹Geology Department, Bendigo CAE and CSIRO Division of
Soils, Adelaide

Kaolinite-smectites, although apparently common in Australian soils, are difficult to identify and characterise because they give poor XRD patterns. However, their smectitic component enable them to strongly influence soil physical properties.

Several soils were separated into different particle size ranges within the clay ($<2 \mu\text{m}$) fraction by (1) centrifugation and (2) dispersion of sodium-saturated soils in dialysis columns. Method (2) proved especially suitable for obtaining a range of the finest clay fractions. The very fine ($<0.05 \mu\text{m}$) fractions often give better-defined XRD patterns for kaolin-smectites than the complete clay ($<2 \mu\text{m}$) fractions. The diffraction patterns and the CEC values both indicated that smectitic components tend to concentrate in the finer clays and kaolinitic components in the coarser clays.

Towards the surface of soils containing kaolinite-smectites, the smectitic component usually decreases and the kaolinitic component increases. XRD patterns, particularly of the finest fractions, of samples from a well-investigated profile, show that these are best described as a mixture of a kaolinite-smectite phase and a distinct kaolinite phase. The proportion of kaolinite in the interstratified phase increases towards the surface. The proportion of distinct kaolinite is relatively uniform throughout the profile. This result is consistent with both simulated XRD patterns and electron microscopy.

THE APPLICATION OF CLAY MINERALS TO ORGANIC GEOCHEMICAL STUDIES

D.C. Carmichael and P.J. Hawkins
Queensland Department of Resource Industries
Brisbane

The application of clay minerals to investigations of the hydrocarbon potential of mudrocks is increasingly being recognised by the petroleum industry. However few investigations have examined the influence of clay minerals on results obtained from pyrolysis analysis of source rocks. These analyses are widely used to assess the petroleum source rock potential of mudrock units in sedimentary basins.

As part of a study of the hydrocarbon generation potential of the Eromanga Basin north of 24°S, clay mineralogical and organic geochemical analyses have been conducted on mudrock intervals within the Jurassic Birkhead and Westbourne Formations. Composite cuttings samples have been selected from petroleum wells for these analyses. X-ray diffraction techniques were used for clay mineral identification. Total organic carbon (TOC) and Rock-Eval pyrolysis techniques have been used as screening tools in the evaluation of the source rock potential of these mudrocks. In addition, vitrinite reflectance studies have been carried out to determine the level of organic maturation of the mudrock intervals.

To enable a valid interpretation of Rock-Eval pyrolysis data, additional information which includes the type and amount of clay minerals in the mudrocks has been required. The effects clay minerals have on Rock-Eval pyrolysis analysis have been examined by Espitalié & others (1980). They made artificial mixtures of illite, illite/smectite, or kaolinite with organic-rich rocks and found that during pyrolysis a proportion of the pyrolysate was retained by the illite and illite/smectite clays. Partial adsorption of the pyrolysate onto these clays necessitates higher temperatures for expulsion of the pyrolysate. This creates anomalously high Tmax values, which in turn makes the interpretation of organic matter types from a van Krevelen-derived diagram (hydrogen index/Tmax crossplot) less reliable.

Accordingly, a study was initiated to assess the validity of Departmental pyrolysis results from samples taken from petroleum wells. This involved the correlation of the clay mineral composition of the mudrocks with the following pyrolysis parameters: S_2 (residual hydrocarbon potential yield), hydrogen index (mg hydrocarbon/g TOC) and T_{max} ($^{\circ}C$). Preliminary results indicate that different relative percentages of the clay minerals in the mudrocks do not appear to have affected the pyrolysis values. This may be due to the lower total clay percentage in the mudrocks, typically less than 30 per cent, compared with 50 to 80 per cent clay minerals in the artificial mixtures.

A direct relationship between an inorganic maturation indicator, illite layer percentage in the illite/smectite clays, and an organic maturity indicator, vitrinite reflectance (R_v , max), has been established for the northern Eromanga Basin. Mudrocks with illite layer values of 55 per cent and greater can be correlated with R_v , max of 0.7 and greater. This is within the potential oil generation window.

References:

- ESPITALIÉ, J., MADEC, M., & TISSOT, B., 1980: Role of mineral matrix in kerogen pyrolysis: influence on petroleum generation and migration. The American Association of Petroleum Geologists, Bulletin 64, 59-66.

MINERALOGICAL AND MAGNETIC SUSCEPTIBILITY CHANGES CAUSED BY LONG-TERM
FARMING AT SIX SITES IN SOUTH AUSTRALIA

R.W. FITZPATRICK, R. NAIDU AND N.J. MCKENZIE

CSIRO DIVISION OF SOILS, PRIVATE BAG NO 2, GLEN OSMOND, SOUTH AUSTRALIA, 5064.

Although long-term farming (especially increased cultivation) affects surface soil characteristics (e.g. soil structure) few mineralogical studies provide an insight into the processes responsible for observed differences. Representative pedons from 6 paired sites (farmed/cultivated and adjacent virgin soils) in the lower mid-north of South Australia were compared by horizon, to examine the effect of farming/cultivation on mineralogical and magnetic properties. The pedons spanned a range of Vertisols (Entic Chromoxerert and Typic Chromoxerert) and Alfisols (Calcic Palexeralf, Typic Palexeralf, Natric Palexeralf and Typic Natixeralf).

Equivalent horizons of farmed and virgin pedons were compared using X-ray powder diffraction, thermal (DTA, TGA), scanning electron microscopy, selective chemical dissolution, and mass magnetic susceptibility analyses of the $< 2\text{mm}$ and $< 2\mu\text{m}$ fractions of samples. Several mineralogical differences were identified. The Ap horizons of all the farmed Alfisols displayed higher mass magnetic susceptibility values. These findings, combined with results from additional experimentation, suggest that maghemite and hematite has either formed or been concentrated in Ap horizons by one or more of the following mechanisms: (i) transformation of goethite by burning of stubble or tree litter during clearance; (ii) transformation of iron particles abraded from tillage shares and (iii) concentration of maghemitic and hematitic glauabules in sand and silt size fractions by selective removal of dispersed clay sized layer-silicates, via water erosion and/or increased illuviation.

The upper parts of the Bt horizons of farmed pedons had lower mass magnetic susceptibility values, thus indicating dissolution of maghemite and hematite via an increase in reductomorphic conditions (i.e. increased wetness). This is caused by greater infiltration (due to loss of rainfall interception by trees), reduced evapotranspiration (removal of deep rooting vegetation) and decreased hydraulic conductivity caused by micro-structure breakdown and compaction (via cultivation and trampling). Clay-sized ($< 2\mu\text{m}$) kaolinite and smectite from A horizons at several paired sites showed differences in X-ray peak intensities and line broadening for the 001 spacings.

We conclude that the effects of long-term farming have altered the mineralogical properties of both the iron oxyhydroxide and layer-silicate minerals in the soils examined. Depending on soil type, these mineralogical alterations and/or transformations are caused primarily by a change in the soil-water regime which appears to be the major factor in altering the weathering condition. Further results of the study and some possible implications with regard to mineralogical identification of induced hydromorphic conditions are discussed.

PEDOGENIC BARITE IN AUSTRALIAN DURIPANS (RED-BROWN HARDPANS)

M.J. WRIGHT AND A.R. MILNES

CSIRO DIVISION OF SOILS, PRIVATE BAG NO. 2, GLEN OSMOND

Recent work on duripans (red-brown hardpans) in Australia has revealed a number of previously unsuspected post-formational processes. The most remarkable of these is the apparent neoformation of barite.

Anomalous amounts of this mineral were revealed by XRS on whole powder samples of duripans from south-west Queensland and north-west South Australia but not in examples from Western Australia. The common factor in this pattern of occurrence is the presence of Cretaceous marine sediments in zones of duripans occurrence in the eastern half of Australia. Barite is commonly observed as small pods (< 5 cm) in such sediments at the Coober Pedy opal fields, for example. Strontium levels in the same samples were not similarly anomalous, indicating that the barite is relatively pure barium sulphate. Gypsum, originating in saline playas and distributed by aeolian activity, is common in these landscapes, providing a ready source of sulphate.

While examination of duripan samples by SEM reveals detrital barite (discrete glaeboles), it also shows the same mineral filling voids (channels) in such a way as to present clear evidence of neoformation. The name "baritans" is here formally proposed for such cutans of barite.

There is a paucity of literature on pedogenic barite but work in the USA has identified the presence of authigenic barite in aquic soils in some southern States (Lynn et al., 1971) and Stoops & Zavaleta (1978) presented micromorphological evidence for barite neoformation in an aquic soil in Peru. The occurrence in Australia of pedogenetic barite in duripans, a feature of arid landscapes, hardly lends support to a requirement of aquic conditions for its development. On the other hand, examination of climatic records, and landscape relationships of duripans here indicates that periodic waterlogging, following extreme rainfall events, may enable episodic formation and neoformation of a number of minerals including palygorskite, calcite and gypsum, as well as low temperature phases of silica, mainly involved in cementation of the duripans.

References:

Lynn, W.C., Tu, H.Y. and Franzmeier, O.P. (1971). Authigenic barite in soils. *Soil Sci. Soc. Am. Proc.*, 35:160-161.

Stoops, G.J. and Zavaleta, A. (1978). Micromorphological evidence of barite neoformation in soils. *Geoderma*, 20:63-70.

WEATHERING IN THE SOUTH ISLAND HIGH COUNTRY : KEY FACTORS.
A CLAY MINERALOGICAL APPROACH
(Poster)

G. J. Churchman
CSIRO Division of Soils, Adelaide

According to Jenny's (1941) equation, soils are a product of a number of key factors (climate, biology, topography, parent material and time).

Solution of the equation requires: 1. monosequences, over which changes in only one key factor are predominant; and 2. a quantifiable soil property that is affected by persistent changes, but not by random, short-term variations. These conditions have been met in this study of 26 soils in 5 different areas of the South Island, New Zealand. The major mineralogical change in these soils is the loss of K^+ from micas. This occurs in 2 distinct stages: 1. to give a regularly interstratified mineral (mica-vermiculite or mica-smectite) and 2. to form a separate expanded phase (vermiculite or smectite).

It was concluded that:

1. Rainfall (MAP) is the main climatic weathering factor.
2. Stage 1 requires 700 - 800 mm MAP on schist.
3. Stage 1 takes < 1000yr. under heavy rainfall (MAP >1m).
4. Granite promotes weathering, greywacke retards it.
5. Stage 2 occurs only under forest.
6. The effects of slope and vegetation are inseparable.
7. Clay minerals may provide an imprint of past environments, and could indicate where changes in e.g. climate and vegetation have occurred.

KAOLINITE-POLYMER INTERCALATES: A MICROSTRUCTURAL STUDY

John G. Thompson*, Ian D. R. Mackinnon and Philippa J.R. Uwins,
Electron Microscope Centre, The University of Queensland,
St. Lucia 4072

*Research School of Chemistry, Australian National University,
Canberra, ACT 2600.

Intercalation of kaolin group minerals is dependant on the dipolar nature of the kaolinite layer which allows the insertion of small polar molecules, such as dimethylsulphoxide (DMSO)¹. In nature, water can also be an intercalant, as in the case of halloysite. Large molecules can be introduced into the kaolinite structure by displacing a previously intercalated, intermediate molecule², or alternatively, kaolinite-pyridine intercalates can be synthesised via formation of an intermediate hydrated kaolinite³.

Samples of Georgia kaolinite (KGa-1) and Weipa kaolinite have been intercalated with polyacrylamide using a displacement reaction with the intermediate kaolinite-N-methylformamide. This method has recently been described by Sugahara *et al.*². Starting materials, as well as synthesised products, have been characterised by XRD, SEM/EDS and HRTEM. The basal spacing for the intercalated product is 11.5Å which is slightly larger than for the stable form produced by Sugahara *et al.*² (11.4Å). XRD of the intercalated product indicates that ~25% of the KGa-1 kaolinite is not intercalated. The Hinkley Index (HI) for the kaolinite fraction of the intercalated product has a value of 1.27 and is higher than that for the bulk KGa-1 starting material (0.96). However, size fractionated KGa-1 shows a variation in HI with the highest value occurring in the largest size range⁴. This variation of HI values implies that a specific size fraction of the Georgia kaolinite does not readily intercalate due to a different degree of order or crystallinity.

Kaolinite:polyacrylamide is very unstable under electron beam irradiation over a range of accelerating voltages. However, HRTEM images of intercalated grains at -160°C show that layers are consistently expanded over the basal extent of a crystal. Where lattice fringes are measureable, intercalated crystals of sizes ranging from 5nm to 22nm show an ordered arrangement of expanded layers ~10.8Å wide. The size range for intercalated kaolinite:polyacrylamide observed with HRTEM is consistent with the interpretation of HI data for kaolinite size fractions which suggests that the smaller size particles are more amenable to intercalation.

References: 1. M Raupach *et al.*, (1987) *Clays and Clay Minerals* 35, 208-219; 2. Y Sugahara *et al.*, (1990) *Clays and Clay Minerals* 38, 137-143; 3. PM Costanzo and RF Giese, (1990) *Clays and Clay Minerals* 38, 160-170; 4. G Lombardi *et al.*, (1987) *Clays and Clay Minerals* 35, 321-335.

AUTHOR INDEX

Ainsworth, P.	27	Keeling, J.L.	6, 24
Anand, R. R.	14	le Gleuher, Maïté	21
Aylmore, L. A. G.	4, 5	Lines, M. G.	26
Baker, Julian C.	28, 35	Longstaffe, F.J.	30
Bastow, T.	33	Mackinnon, Ian D.R.	1, 7, 35, 43
Bird, M.I.	30	Mathews, J.F.	36
Boesen, R.	37	McKenzie, N. J.	40
Carmichael, D.C.	38	Milnes, A. R.	41
Chivas, A.R.	30	Murray, R.S.	3
Churchman, G.J.	5, 6, 37, 42	Naidu, R.	15, 40
Churchward, H. M.	14	Quick, G.W.	20
Corrigan, P.A.	34	Quirk, J. P.	3
Dahlhaus, Peter	23	Raven, M.D.	24
Davy, T.J.	5	Roberts, F. Ivor	19
Doblin, C.	36	Ruan, H.D.	16
Eggleton, Tony	9, 21	Self, P. G.	6, 15, 37
Emerson, W.W.	31	Shayan, A.	20
Fitzpatrick, R. W.	15, 17, 40	Singh, Balbir	8
Fredericks, Peter M.	2	Singh, Balwant	10
Frost, Ray L.	2	Sjarif, S.	13
Giles, M.	27	Slade, P.G.	37
Gilkes, R. J.	5, 8, 13, 10, 16, 17	Smith, R. E.	14
Golding, Suzanne D.	28, 35	Taylor, Graham	9
Hamilton, P.J.	27	Thompson, John G.	43
Hardin, S.G.	33	Turney, T.W.	32, 33, 34, 36
Hawkins, P.J.	38	Uwins, Philippa J.R.	1, 7, 43
Hughes, J.C.	11	Walker, Pat	9
Ingles, O.G.	29	Weissmann, D.	31
Isahak, Anizan	12	Wells, M.A.	17
Kaser, Stacy A.	1	Wright, M. J.	41

APPENDIX C

Notes for Mid-Conference Excursion to Heavy Clay Industries in the Ballarat Area

**Field Trip Itinerary — ACMS Conference, Ballarat
Tuesday February 5, 1991**

9.00 am	Depart Ballarat University College
9.20 am	Arrive Vitclay Pipes (Excursion Stop 1)
10.20 am	Depart Vitclay Pipes
10.30 am	Arrive Selkirk Brick (Excursion Stop 2)
10.30 am	Morning tea
11.00 am	Inspection of plant and pit
12.00	Depart Selkirk Brick
12.20 pm	Arrive Ballarat University College
12.30 pm	Lunch
2.00 pm	Depart Ballarat University College
2.30 pm	Arrive Enfield (Excursion Stop 3)
3.00 pm	Afternoon tea
3.30 pm	Depart Enfield
4.00 pm	Arrive Buninyong (Excursion Stop 4)
4.45 pm	Depart Buninyong
5.00 pm	Arrive Ballarat University College
6.30 pm	Depart for Dinner at Sovereign Hill

GENERAL NOTES ON THE CLAY INDUSTRY AT BALLARAT

Four major clay-based industries now operate at Ballarat. Each of these is separately summarised below:

(A) Selkirk Brick Pty Ltd

Plant Location: Howitt St, Ballarat.

Company Products: Building bricks and pavers.

Production: 50 million bricks per annum.

Markets:

The main market for these bricks is in Australia, particularly Victoria. Selkirk's share of this very competitive market is approximately 15%. The main outlet is Melbourne where about 50% of output is sold. Other market areas are Geelong, western Victoria, Gippsland, South Australia, New South Wales, Queensland and the Australian Capital Territory. Selkirk also owns Bendigo's Philip Bricks, which provides an additional outlet for their product. The principal reason for the ability to sell to such a wide market is the quality of the product. It is noted that they are one of the few brick manufacturers to consistently meet Australia standards since 1971. Selkirk have recently commenced exporting pavers to Japan.

Employment:

Selkirk Bricks has approximately 130 employees at its Ballarat plant. The company contracts a local earthmoving company to mine and stockpile the clay from their pits.

Clay Types used:

Buff and red plastic clay are mined at Enfield. This clay provides the plasticity, essential in the extrusion process. A shale clay is mined on-site at their plant. This non-plastic clay gives good firing, and porosity characteristics. Shale clay is also extracted from a pit at Creswick. This non-plastic clay is used primarily for its colours. These various clays are blended to obtain the desired extrusion and firing characteristics.

Other constituents:

Basalt - used as a filler and a flux. When fired under reducing conditions an attractive colour results. As a filler the basalt reduces moisture, which reduces the energy required for drying the brick prior to firing. The basalt is currently supplied as crusher fines.

Fritz - this is a ferro-based material that is applied surficially to enhance the appearance of the brick.

Flux - used as a binding agent in the firing process.

Current mining operations:

EIL 446 Enfield - Red and buff plastic clay.

EIL 152 North Ballarat - Red and buff shale clay.

EIL 5587 Creswick - Red and buff shale clay.

Resource details:

Location: Enfield.

Mine Product: Red and buff plastic clay.

Geology: Tertiary/Quaternary fluvial sediments.

Mine Life: 20 years at current production rates.

Mining Methods: Contractors using scrapers are employed for three months per year to excavate and stockpile the annual need.

Location: Ballarat North.

Mine Product: Non-plastic red and buff coloured shale clay.

Geology: Deeply weathered Ordovician sediments.

Mine Life: 50 years.

Mining Methods: Contractors using scrapers are employed to excavate and stockpile the clay as required.

Location: Humbug Hill, Creswick.

Mine Product: Non-plastic red and buff coloured shale clay.

Geology: Deeply weathered Ordovician sediments.

Mine Life: 50 years.

Mining Methods: Contractors using scrapers are employed to excavate and stockpile the clay as required.

Future Expansion:

Selkirk has recently invested over \$1m upgrading their facilities in order to maintain their competitiveness in the industry. Selkirk has a firm commitment in the continued development of their industry at Ballarat.

(B) Vitclay Pipes Pty Ltd

Company Details:

Formerly Martin's Stoneware (1960); Vitclay Pipes Pty Ltd established in 1971. A subsidiary of Brick & Pipe Industries since 1988.

Plant Location: Gregory St. Wendouree.

Company Products:

Vitrified pipe, sewer and drainage - 99.5% of total output.

Planter, socketless pipe

Sinkstones, pressed gully traps

Gutter bricks.

VitRam

Production: 27,000 tonnes of finished products per annum.

Markets:

Australia provides the main market for pipes. Vitclay currently holds 50% of the Australian market for sewer pipes. Approximately 15% of the products are exported to New Zealand, SE Asia, and Saudi Arabia.

Employment:

Vitclay currently employs approximately 87 personnel at its Ballarat plant.

Clay Types used:

Buff and red clay from Buninyong and Enfield. The Buninyong clay is used for its strength and the Enfield clay for its extrudability.

Other constituents: Grog - rejected pipes are recycled as a filler.

Current mining locations:

EIL 485 Enfield - Red and buff plastic clay

EIL 385; EIL 802 - Red and buff plastic clay

Until 1972, the clay deposits at Lartner street, Ballarat, were the major source of raw materials for the company.

Resource details:

Location: Enfield

Mine Product: Red and buff plastic clay

Geology: Tertiary/Quaternary fluvial sediments.

Mine Life: n.a.

Mining Methods: Local earthmoving contractors are used to stockpile the clay on site. The clay is trucked to the plant as required.

Location: Buninyong

Mine Product: Red and buff plastic clay

Geology: Tertiary fluvial sediments.

Mine Life: n.a.

Mining Methods: Local earthmoving contractors stockpile the clay on site. It is trucked to the plant as required.

Future Expansion:

The company has a continued commitment to improving technology to maintain competitiveness in the industry. The pipe manufacture is now largely automated.

(C) PGH Eureka Ceramics*Company Details:*

Formerly Eureka & Terra Cotta Tiles Co.; since 1988, a wholly owned subsidiary of BTR Nylex.

Factory Location: Cnr Stawell and Charlesworth Sts.

Company Products: Ceramic floor tiles.

Production: 900,000 m /annum of ceramic quarry tiles (value - \$13,500,000)

Markets:

The main market for the tiles is within Australia. PGH holds approximately 30% of the local market, the remaining 70% being mostly imported. 15% is sold in Victoria, 5% in New Zealand, and the remaining 75% interstate.

Employment:

PGH has 108 employees at its Ballarat plant.

Clay Types used:

1. Buff and red clay are mined at Buninyong and Napoleons. These clays constitute the basic ingredient of the product and are used for their plasticity, essential in the extrusion process. The base colour is unimportant, as the tile is ultimately glazed.
2. Kaolin clay/fireclay - Rowsley, in the Parwan Valley, near Bacchus Marsh. Rowsley clay is used for its paler colour, coarseness, and higher silica. This clay also assists in the drying process.
3. Kaolin clay/plastic clay - Axedale. This clay is used to counter "black core" caused by fast firing and to give the desired level of porosity.

The main ingredient of the tile is local clay, and the other clays are added to control the product specification for customer requirements and the firing properties.

Other constituents:

Grog - used as a filler, assist in firing and to regulate porosity and shrinkage. The grog is supplied by recycling tiles, although with the use of the new fast firing technique additional grog from other sources is required. Brick grog is used but

often has unacceptable results. Crushed granite is used both as a filler and a source of flux. The granite from Hamilton and Pyramid Hill is being tried. Basalt - used as a filler and a flux. When fired under reducing conditions an attractive colour results. Basalt is suitable as a flux due to the high firing temperatures of 1080°C to 1100°C. This is currently supplied as crusher fines.

The tile is broadly constituted of between 50% and 70% clay, with the remainder being grog and basalt. The mixture of clays varies, with the local clay proportion being 50% to 60%.

Current mining locations:

EIL 1154 & EIL 749 Napoleons - red and buff plastic clay.

Unmined lease areas:

EIL 186 & EIL 1153 Buninyong - red and buff plastic clay.

Until 1972 the clay deposits at Lartner street, Ballarat, were the major source of raw materials for the company.

Resource details:

Location: Enfield

Mine Product: Red and buff clay

Geology: Tertiary/Quaternary fluvial sediments. The red clay underlies the buff clay horizon.

Mine Life: 35 years at current usage.

Mining Methods: One contractors is employed to win and deliver the clay to the plant.

Future Expansion:

The company has recently invested \$7 million in a fast firing plant to make their operation more efficient and flexible. The new plant is more efficient, reducing firing time from 1.5 days to 84 minutes. Flexability is provided in the new operation as the tiles are fired horizontally rather than the conventional method of the vertical split tile. This allows greater variety of design and glazing since there is less demand on green structural strength of the tile during firing.

In addition, the company will be relocating their Sydney operation to Ballarat during 1991. The new plant will be manufacturing whiteware (sanitaryware).

(D) Kaolin Australia Pty Ltd

Company Details: Wholly owned by English China Clays (ECC)

Plant Location: Pittong, Victoria.

Company Products:

Kaolin Australia Pty Ltd produces the following processed kaolin products:

Eckacote, Pittong Filler. - Paper coating and filler

Eckalite I, Eckalite II, Eckalite 120. - Paint filler

Eckalite I, Eckalite II, Eckalite BDF - Rubber filler

These products are essentially 99% kaolinite.

Kaolin's products are principally used in the paper industry as a filler and coating, with minor supplies as fillers and pigments for rubber, paint and plastics; refractory use; pottery use; and fibre-glass.

Production output:

Figures are not easily available, but for the year ending September 1984, 110,000t of decomposed granite was mined at Pittong from which 30,000t of refined kaolin was produced.

Markets:

The main market for the processed kaolin is Australian. Of the paper grade product, over 60% is used for filler and coating in paper manufacture at Fairfield (Melbourne) and Petrie (Brisbane). Roughly 40% of the kaolin is exported to New Zealand and Southeast Asia, esp. Indonesia. (Other sales are to Thailand, Taiwan, Philippines with minor sales to South Africa and Iraq).

Employment: not available.

Clay Types used:

The clay is solely derived from residual clay developed in deeply weathered granite. The principal source is from the Pittong/Linton region adjacent to the processing plant, which has been mined at various levels since 1920. Clay is also trucked to the plant from a pit at Lal Lal which has similar geology. The properties of both clays are utilized to extend the range of products and more efficiently use the reserves.

By Products:

Quartz - In processing the decomposed granite, inert quartz grains (of sand and gravel size) are extracted. This quartz, which is stockpiled on site as a by-product, is often used as a source of road base material.

Current mining locations:

ML 555 Pittong- Residual kaolin
ML 318 Lal Lal- Residual kaolin

Resource details:

Location: Pittong, 35 km. west of Ballarat.
Mine Product: Residual kaolin. Kaolin is being mined from private land under agreement with the landowner just south of Pittong.
Geology: Tertiary deep weathering of Devonian granite.

Location: Lal Lal
Mine Product: Residual kaolin.
Geology: Pre-basaltic Tertiary deep weathering of Devonian granite. Estimated reserves of 1.5 million tonnes.

Special extraction processes:

Initially the inert quartz and other impurities are removed by wet sieving to 53 μ m. The clay is then bleached before being refined. In brief, refining comprises sieving the bleached material to 83% < 2 μ m for the paper industry, 60% < 2 μ m for the refractories industries, and other specified ratios of aluminium and silicon for the fibre-glass industry.

EXCURSION STOP 1. - Vitclay Pipes Pty. Ltd.

The clay pipe industry began at Ballarat in 1925 when Michael Martin, a civil engineer, commenced pipe manufacture to supply pipes for Ballarat's sewerage scheme. The success of the company was immediate, and business flourished during the 1930's as the pipes were manufactured for government irrigation schemes in the Mallee. In 1960 Martin Stoneware Pipe Pty Ltd became a wholly owned subsidiary of Humes Limited.

Vitclay Pipes Pty Ltd as we know it today came about on the 1st April 1971 with the merger of Commonwealth Pottery, which operated on the site of the present Blackburn operations, the Rocla Pipe plant, located at Cambellfield, and the Humes Pipe plant, located at Ballarat. At the time this merger was seen as a means of improving the clay pipe industry in general.

The company produces vitrified pipe for both sewer and drainage applications. This comprises approximately 99.5% of total output. Minor products are planters, socketless pipes, sinkstones, pressed gully traps, gutter bricks and VitRam. Production is around 27,000 tonnes of finished products per annum.

Australia provides the main market for pipes. Vitclay currently holds 50% of the Australian market for sewer pipes. Approximately 15% of the products are exported to New Zealand, SE Asia, and Saudi Arabia.

Raw materials are buff and red clays from Buninyong and Enfield. The Buninyong clay is used for its strength and the Enfield clay for its extrudability. Rejected pipes are recycled as a filler (known as "grog").

The flow chart for manufacture is attached (Fig. 1). Essentially, the raw materials are blended, ground and then extruded. The "green" extruded pipes are then dried and inspected. The firing is carried out in a tunnel kiln, approximately 120 metres long. During the 47 hour cycle the pipes pass through the various heating zones and the salt-glazing zone, reaching a maximum of 1120°C. The burnt ware is then transferred to the loading dock, where dimensional and hydrostatic testing is carried out prior to delivery.

EXCURSION STOP 2. - Selkirk Brick Pty Ltd

See also description on page 2 of these notes, under the heading "General notes on the clay industry at Ballarat". The flow chart for the manufacture of Selkirk bricks is presented in Figure 2.

The moisture content of clays in situ ranges from 8% to 25% (wet weight bases), whereas brick production requires 15%. Material drying of the clays during summer stockpiling operations is necessary.

Clay mixes for the 50 different brick colours/types vary from 40% to 60% shale and 60% to 40% plastic clay. Manganese dioxide from BHP's mine on Groote Eylandt is added as a colourant in some products.

Production rate is 1 million bricks per week. This is one eighth of Victoria's needs. 3m³ of clay is used for 1000 bricks, ie annual consumption 150,000 m³. Overburden removed prior to clay winning approaches 100,000 m³ per annum.

VITCLAY - BALLARAT PLANT

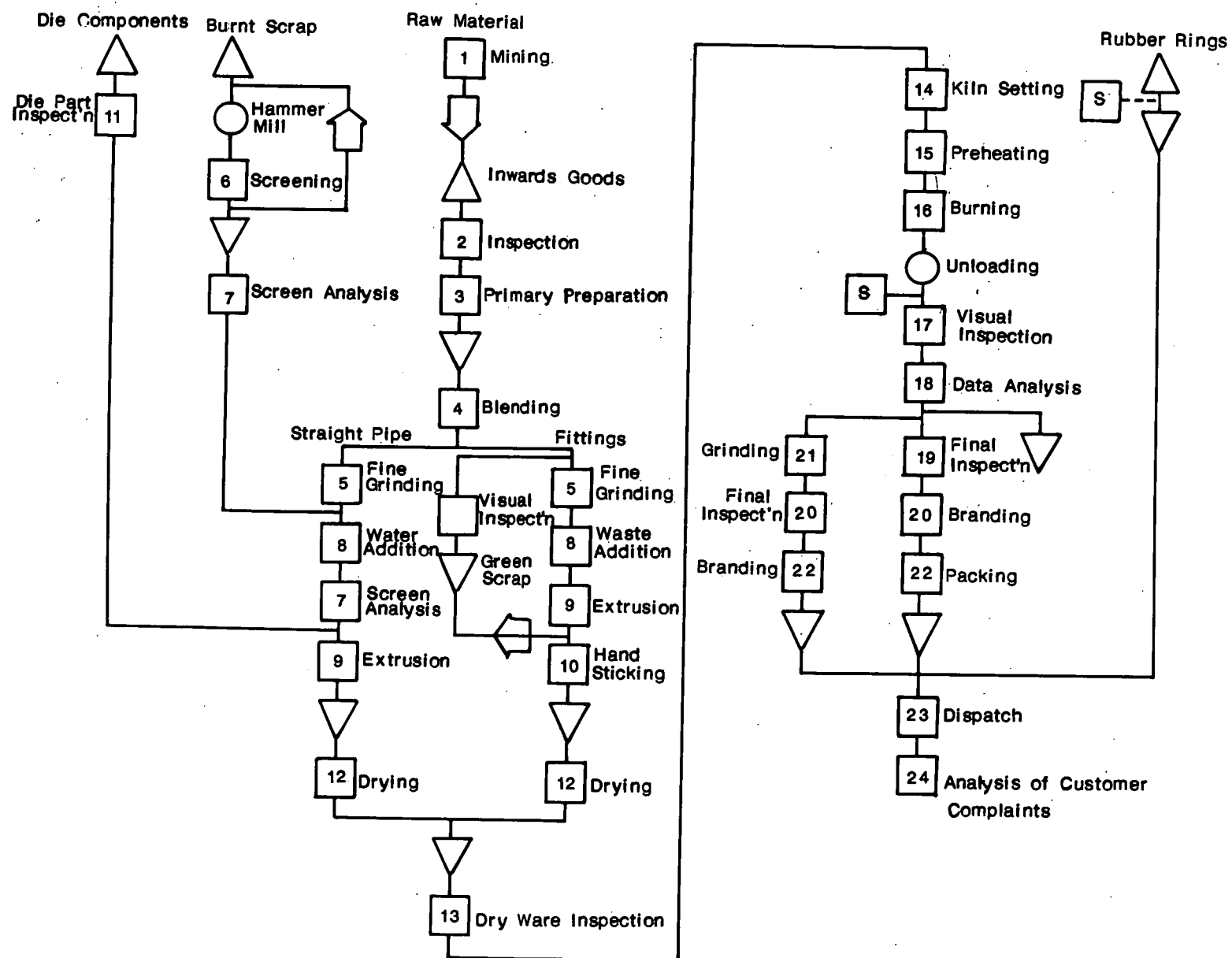
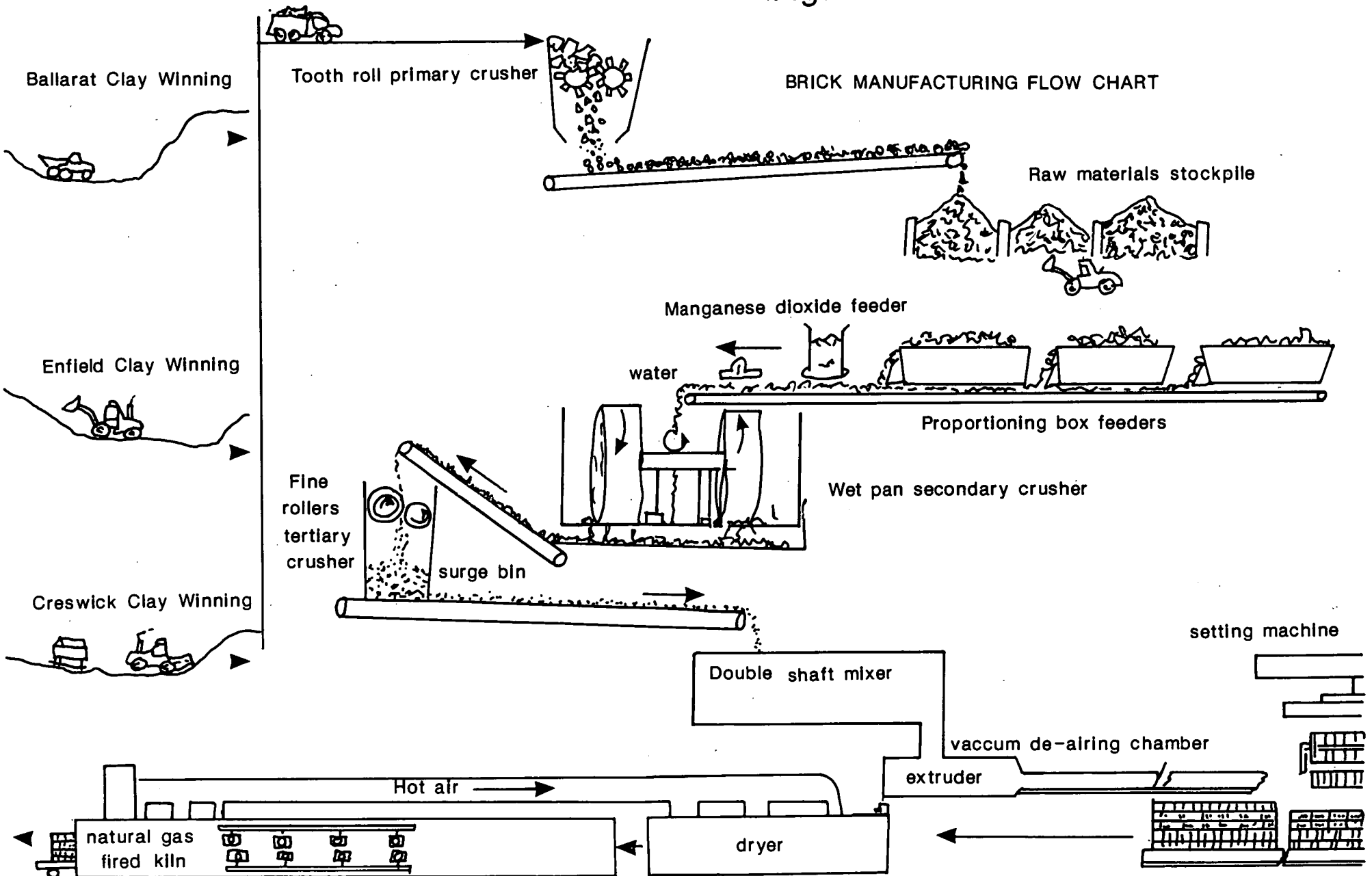


Fig. 2 SELKIRK BRICK



EXCURSION STOP 3. - Enfield Clay Pit

Notes on Clay Deposits at Enfield, Victoria

Dr J. A. Ferguson

Clay deposits are worked by three Ballarat clay industries along Dog Trap Creek, a western tributary of Yarowee River 15 - 20 km south of Ballarat. Selkirk Brick Pty Ltd uses the clays in cream, grey and pink brick mixes; Vitclay Pipes Pty Ltd makes sewer pipes using half the mix from here and PGH Ceramics uses similar clays a little further north as a component in floor tile mixes.

Dog Trap Creek has a broad valley and flows south to north. It probably originated as an upper tributary of a middle Tertiary Avoca drainage system. Subsequently it has been captured by the headward erosion of the Yarowee River and diverted southward into the Otway Basin. Mapping of the deep leads by the Geological Survey of Victoria shows that this capture occurred before the basalt eruptions from Mount Rowan and Mount Buninyong (north and southeast of Ballarat) which are held to be 2 - 3 million years old. These lavas filled large parts of the Yarowee Valley and diverted it eastward as a lateral stream. The basalts did not penetrate Dog Trap Creek where the clay deposits are now worked.

The brick and pipe clays are fluvial channel fill and lateral meander deposits only 3 km from the present headwaters of a western tributary of Dog Trap Creek. It is likely that they were supplied from a bigger drainage basin now truncated by headward erosion of Woody Yaloak River tributaries.

Surrounding and underlying the clays are Ordovician silty and sandy shales, extensively invaded by quartz veins which have been extensively explored by gold prospecting shafts. Upper parts of the Ordovician exposures have been extensively kaolinised by early Tertiary laterisation. Red and yellow shaly alteration products formed at the same time below the kaolinised zone. These are the source materials which eroded to form the downstream clay deposits over a considerable period of middle Tertiary time.

The deposits begin with a partially indurated purplish red clay and quartz pebble deposit (Fig. 3, section). Above this is a bottom grey clay, carbonaceous in part and probably formed in a peaty swamp. This is followed by a variable interval of yellow angular quartz gravel and sand with grey clay lenses. Above this is the main silty grey clay deposit. Overlying this is a sequence of red and grey plastic clays. These are the strongest and most plastic clays of the deposit and fire pink and orange-red. The red component shows subvertical ferruginous mottling and represents a considerable break in deposition and an interval of weathering and vertical leaching. Another persistent angular quartz gravel deposit overlies this zone. On the main input channel these sands and gravels are over three metres thick. Elsewhere there is evidence of gullying and backfill of the plastic clay horizon. A second red and grey clay also with vertical iron oxide concentrations overlies the gravels. Grey and orange silty soil horizons top the sequence.

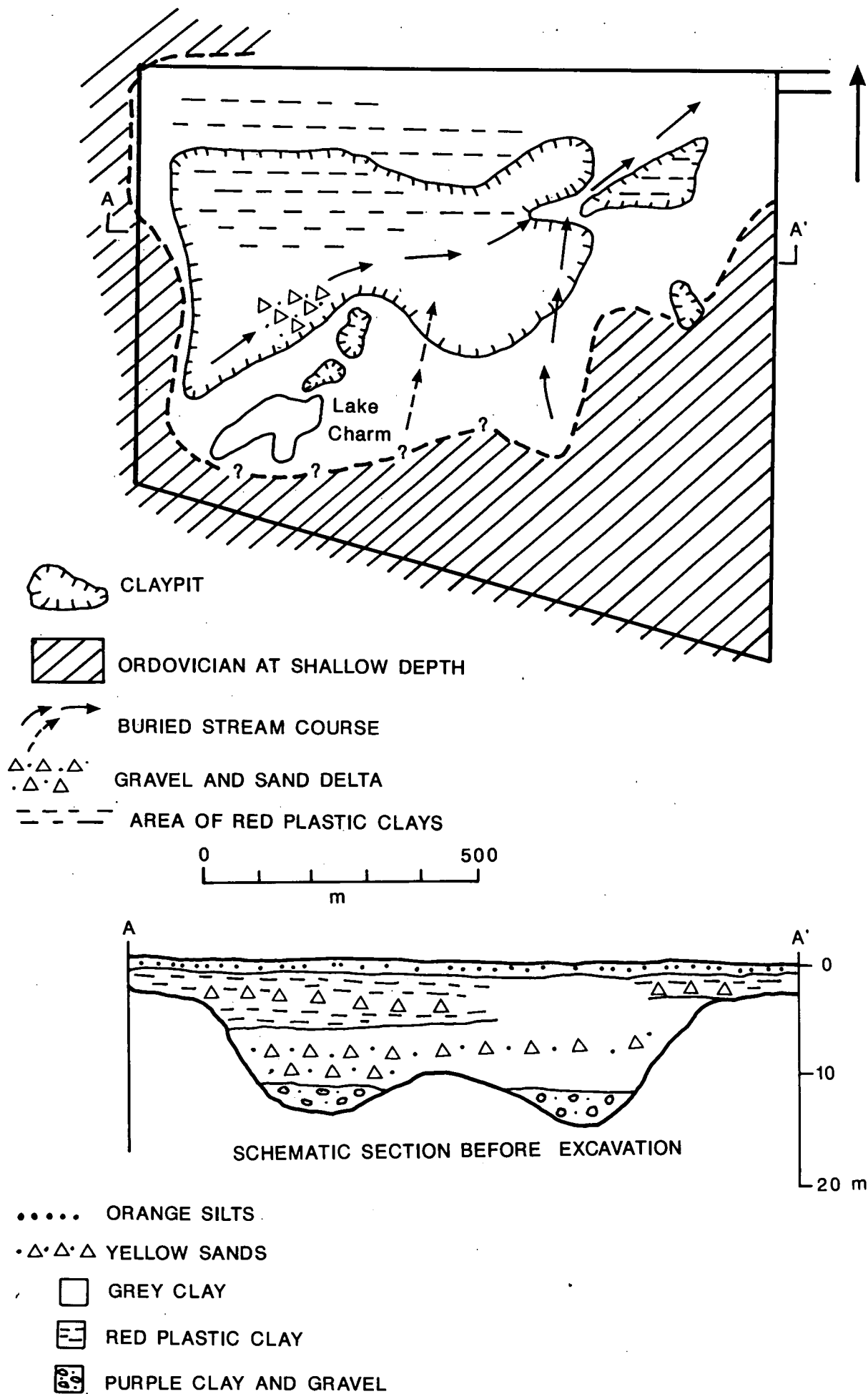


Fig. 3 ENFIELD CLAYPIT

The red plastic clays are higher in clay particles than the grey clays which are silty. Ceramic properties are listed below:

	Red plastic Selkirk	Grey Selkirk	Grey Vitclay
Dry shrinkage, linear and transverse		3.81%(L), 2.88%(T)	
Fired shrinkage	3.5% (1080°C)	6.0% (1080°C)	3.93%(L), 5.06%(T) (1120°C)
Ignition loss		2.43%	
Absorption		7.0%	
Dry Strength		1.57 MPa	
Fired Strength		15.82 MPa	
Pyroplastic Index		10.61 E-6	

X-ray diffraction results (Fig. 4 to 12) for 9 samples from the Enfield pit are available (courtesy John Stanner and Tony Eggleton; the Australian National University). For each sample, XRD traces are presented for (a) the untreated whole rock; (b) the separated clay fraction, <2 µm grain size; and (c) the glycolated clay fraction. The samples represent the stratigraphic and technological subdivisions of the clay deposit from top to bottom together with two extra samples of the main grey clays for checking lateral variability. The samples are:

- Sample 1. Red silty subsoil, west end (overburden).
- Sample 2. Top red mottled clay, west end.
- Sample 3. Upper "yellow seam" of red and grey plastic clay.
- Sample 4. Top grey clay west end.
- Sample 5. Bottom grey clay, west end.
- Sample 6. Bottom clay, west end (indurated).
- Sample 7. Kaolinised Ordovician shale, west end.
- Sample 8. Top grey clay, middle of pit.
- Sample 9. Bottom grey clay, middle of pit.

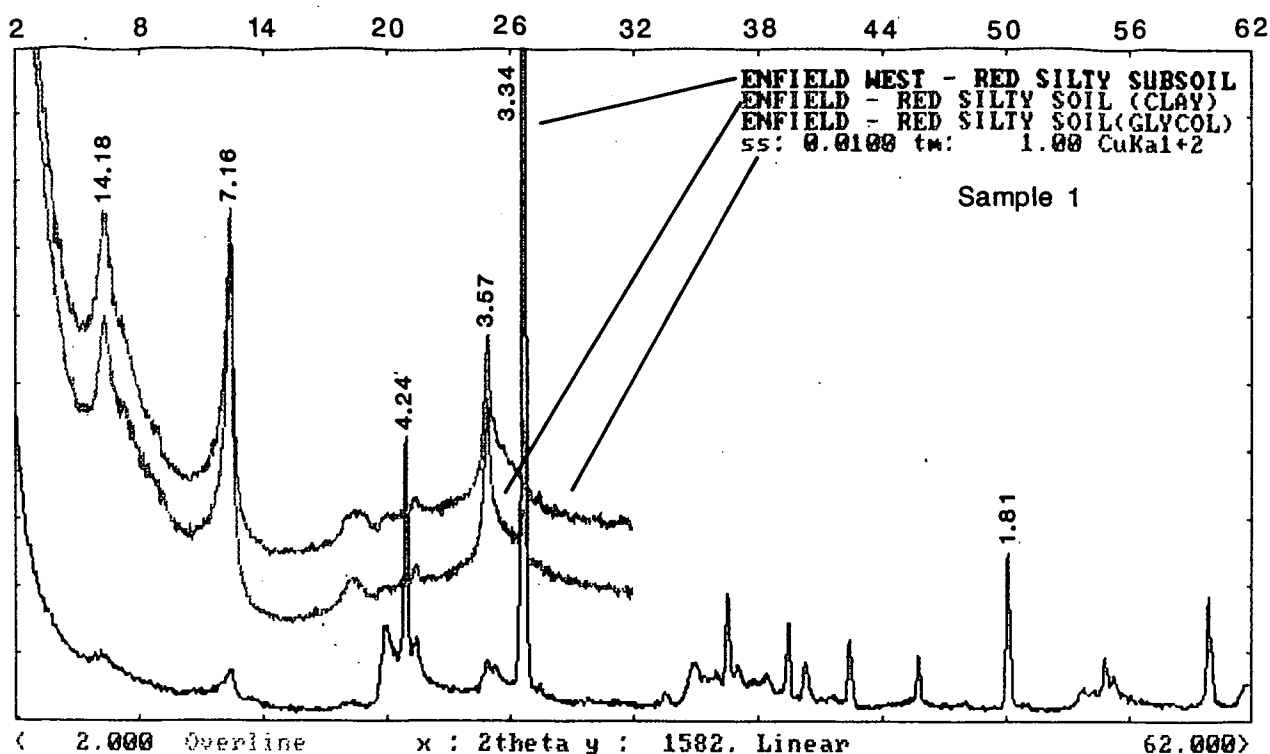


Fig. 4. XRD results, Enfield Pit. Sample 1 — red silty subsoil, west end (overburden)

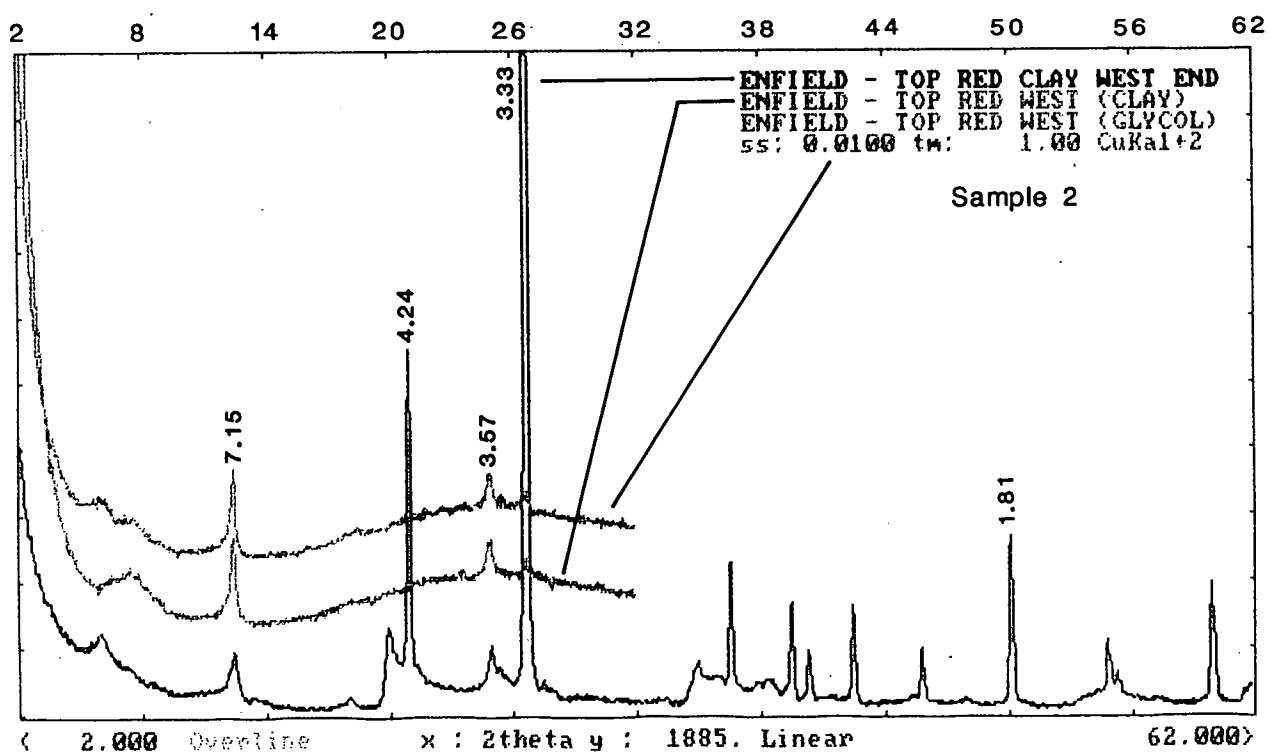


Fig. 5. XRD results, Enfield Pit. Sample 2 — top red mottled clay, west end

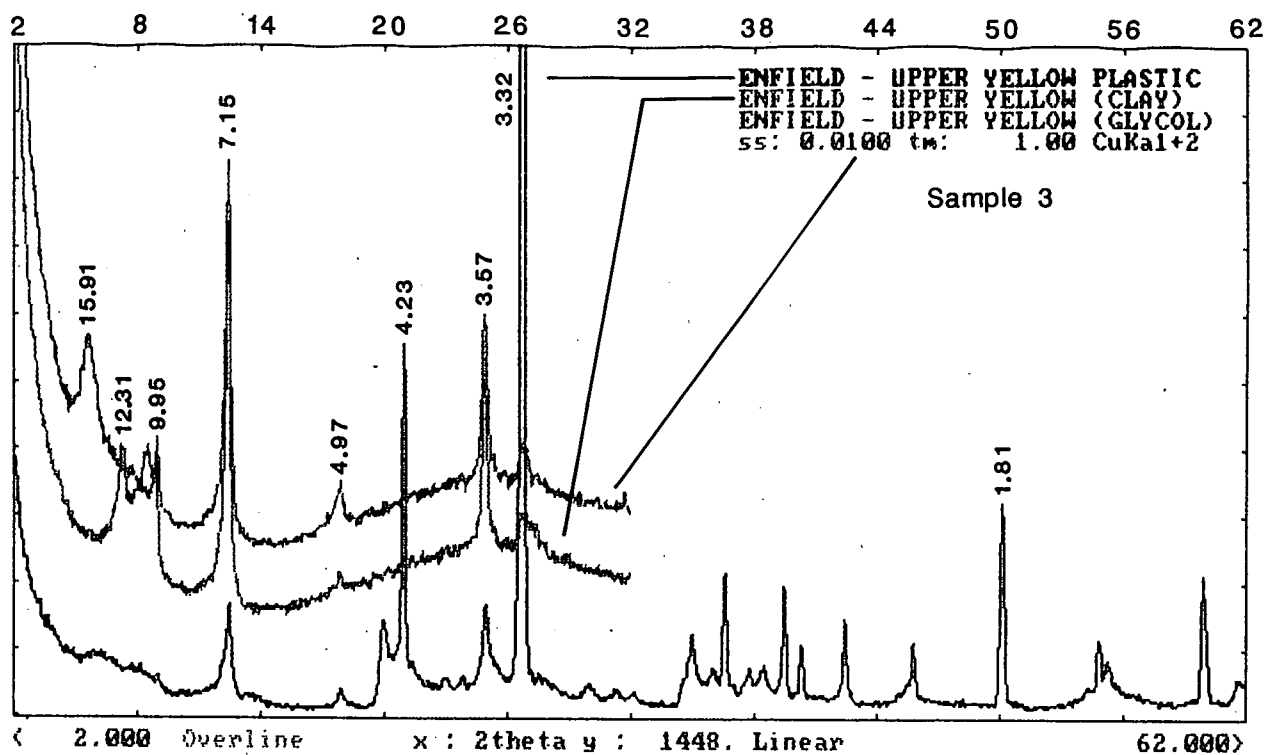


Fig. 6. XRD results, Enfield Pit. Sample 3 — upper "yellow seam" of red and grey plastic clay

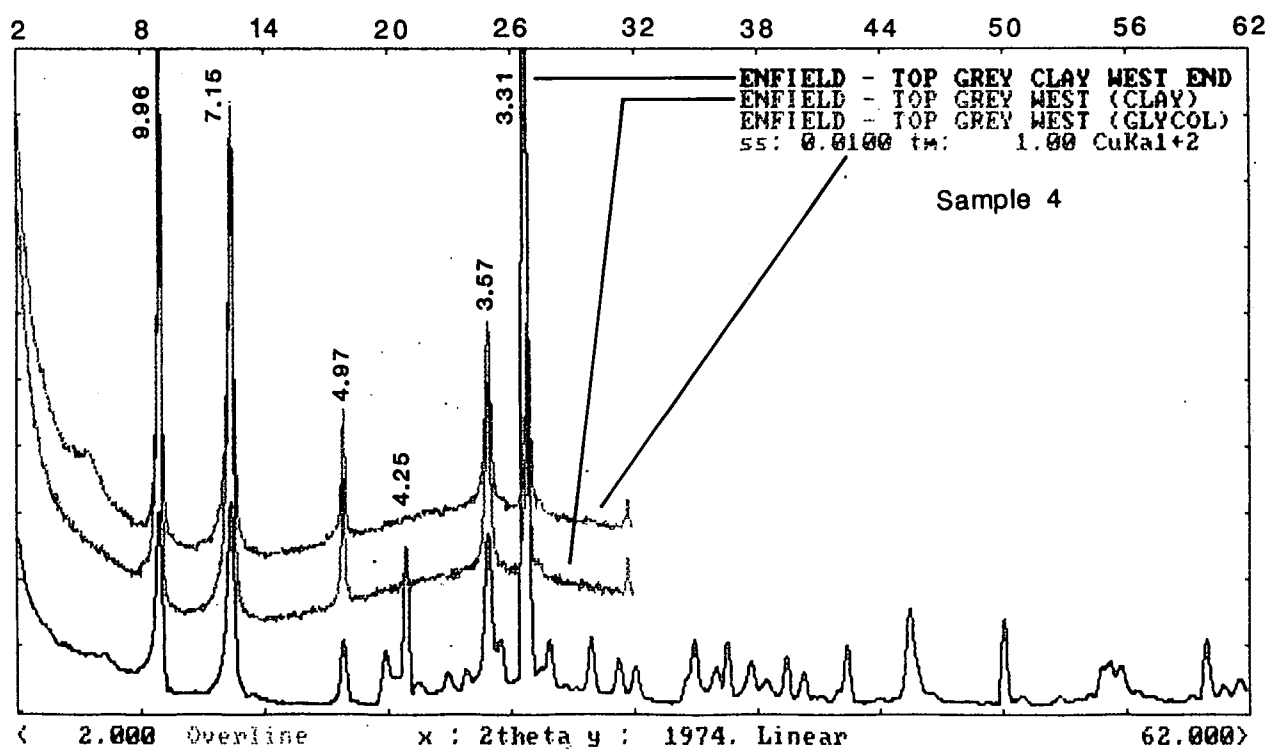


Fig. 7. XRD results, Enfield Pit. Sample 4 — top grey clay west end

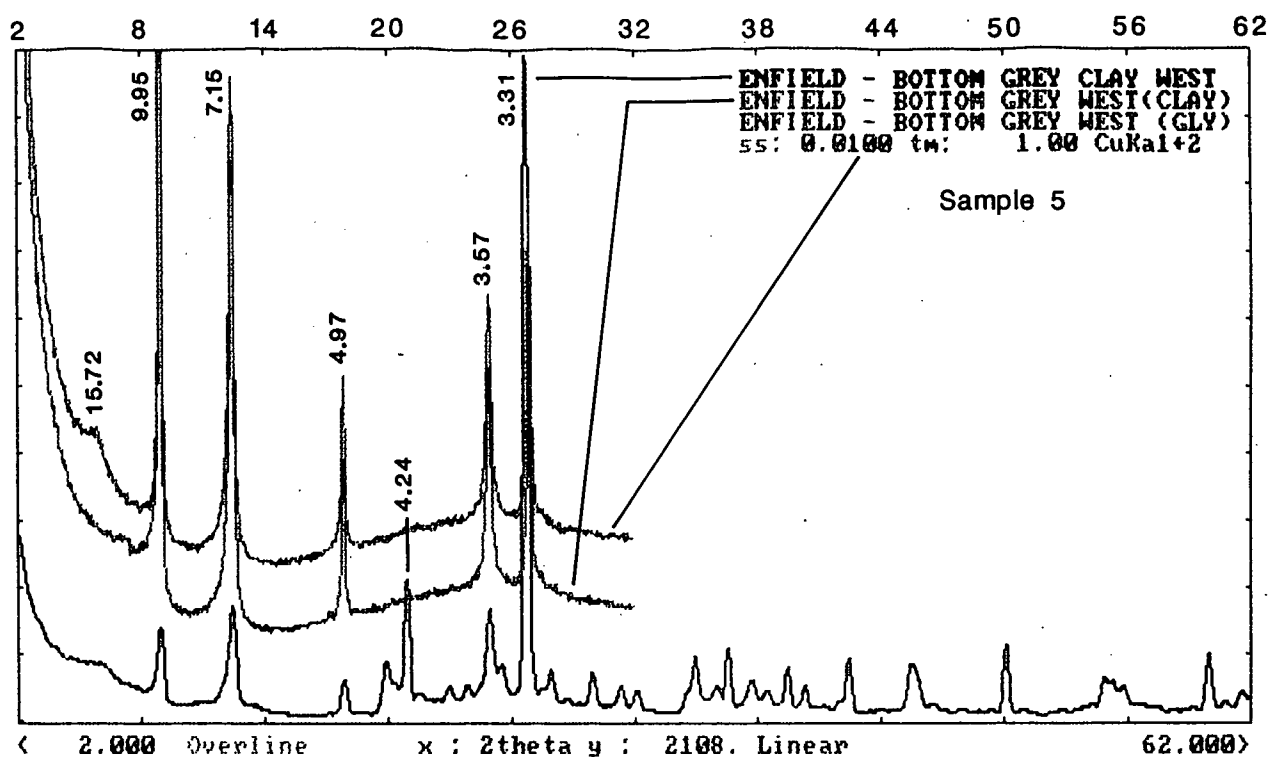


Fig. 8. XRD results, Enfield Pit. Sample 5 — bottom grey clay, west end

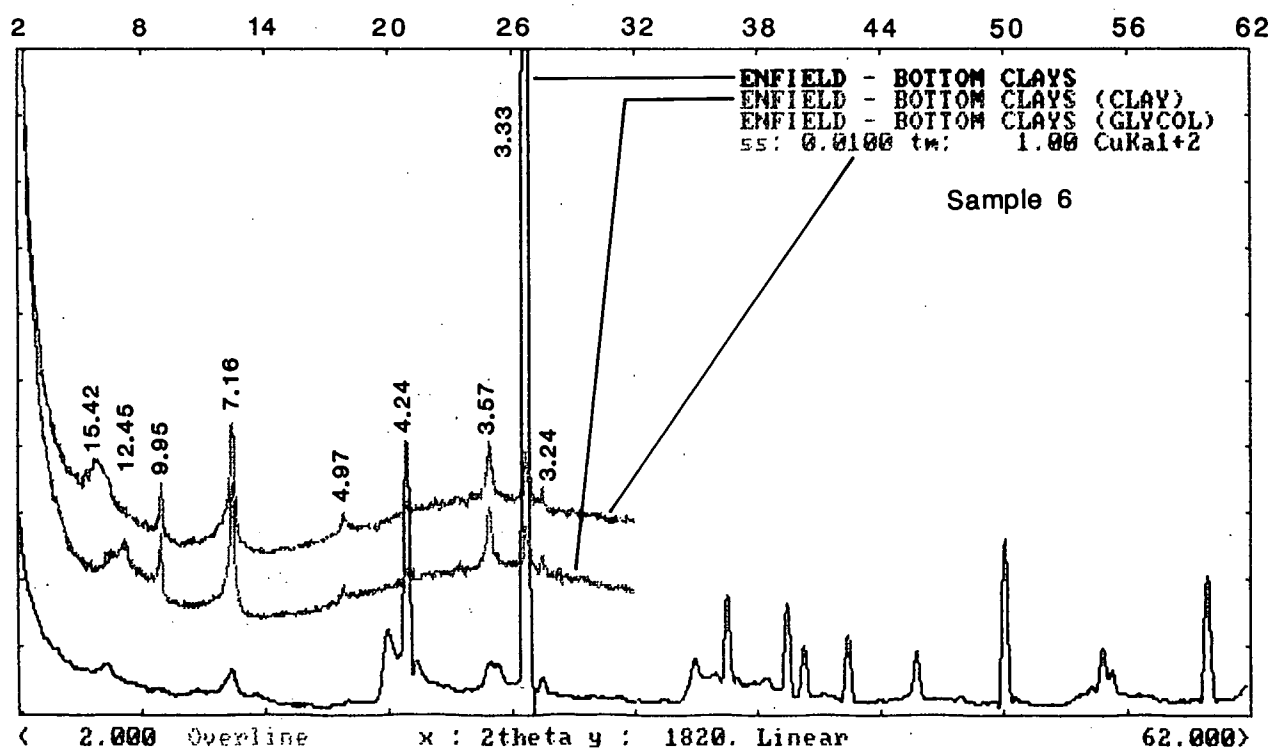


Fig. 9. XRD results, Enfield Pit. Sample 6 — bottom clay, west end (indurated)

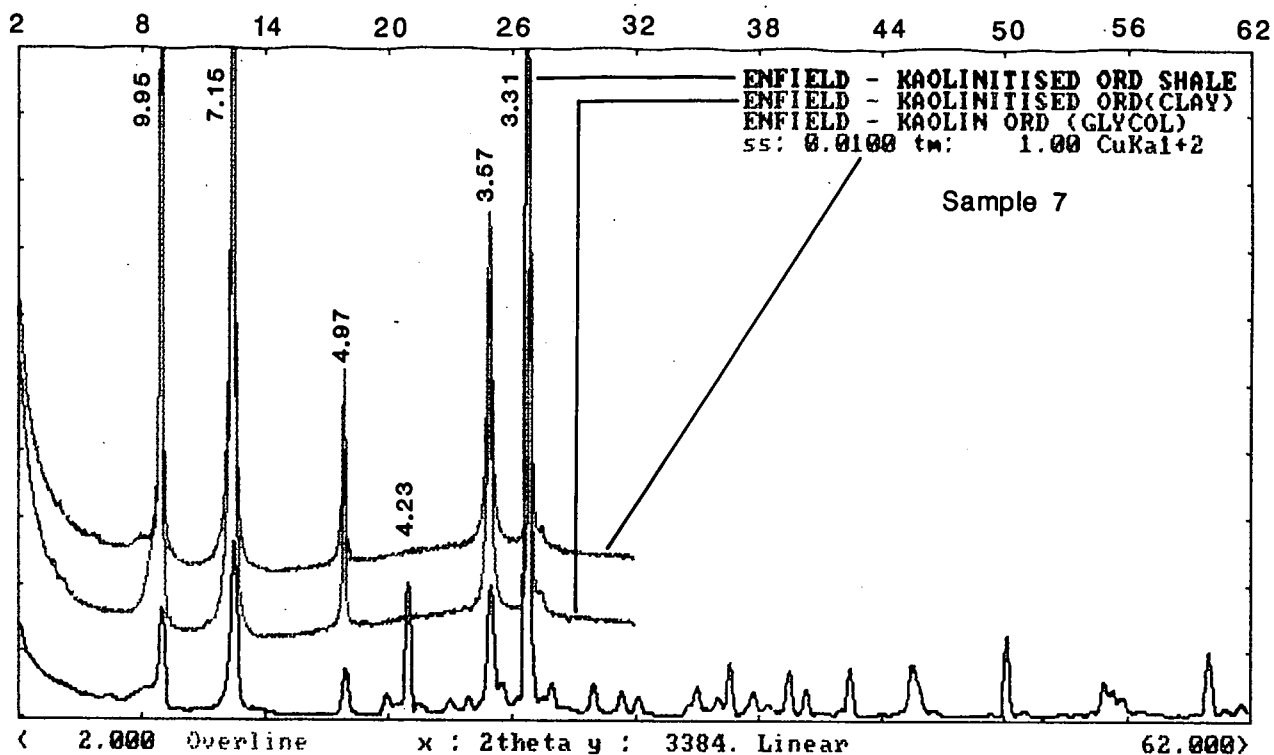


Fig. 10. XRD results, Enfield Pit. Sample 7 — kaolinised Ordovician shale, west end

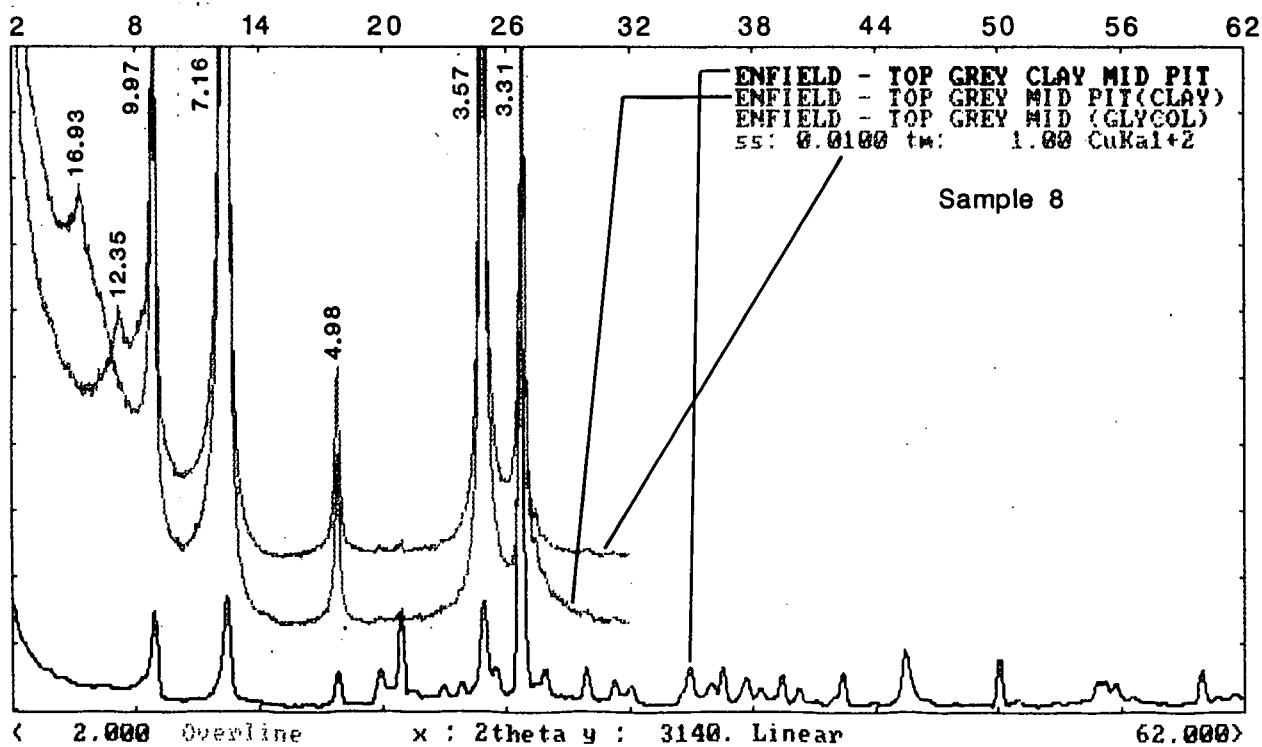


Fig. 11. XRD results, Enfield Pit. Sample 8 — top grey clay, middle of pit

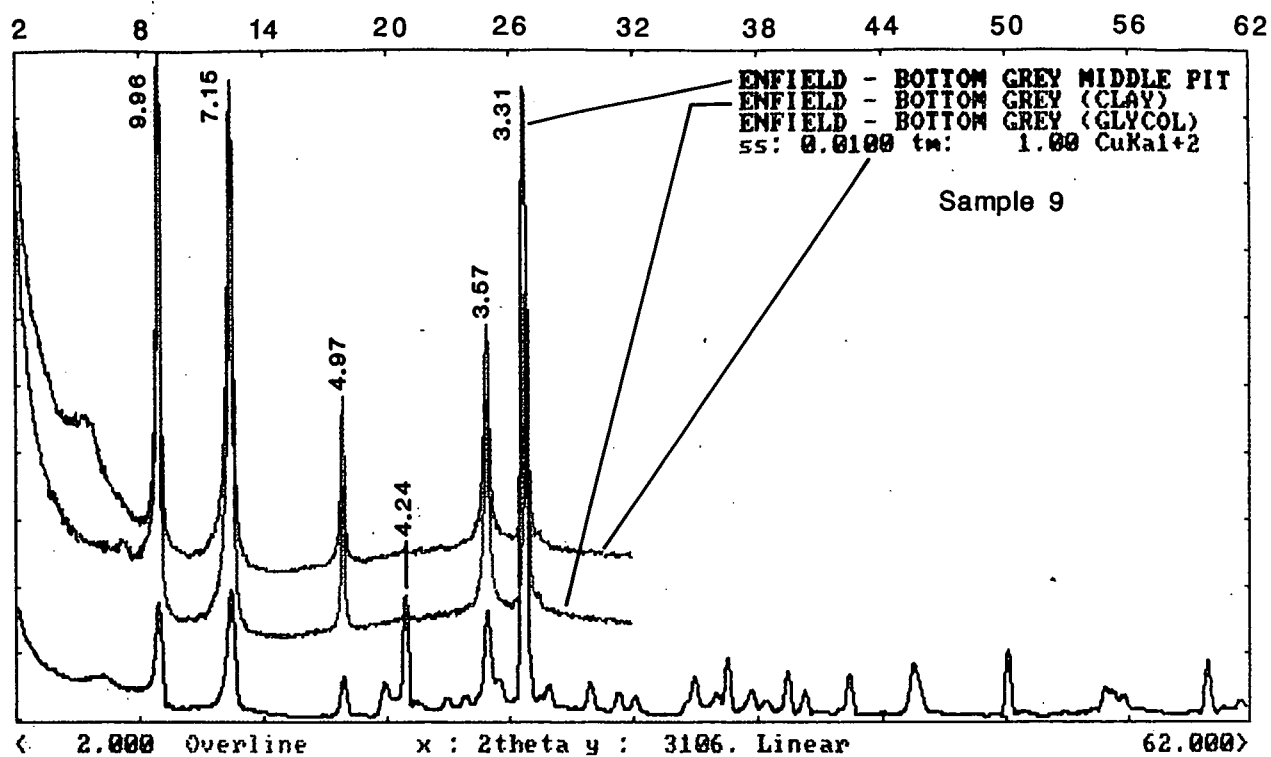


Fig. 12. XRD results, Enfield Pit. Sample 9 — bottom grey clay, middle of pit

EXCURSION STOP 4. - Buninyong Clay Pit

Notes on Clay at Buninyong, Victoria

Dr J A Ferguson

Clay has been won from a pit 3.5 km west of Buninyong for use as a 50% component in clay sewer pipes manufactured by Vitclay Pipes Pty Ltd of Ballarat.

The clay comes from a middle Tertiary deep lead deposit formed by a stream which drained an Ordovician shale provenance in the Forest Hill - Buninyong area and was a tributary of the Avoca deep lead system (now part of the Yarowee River deep lead system, following headward extension of the Yarowee River and flooding of the older landscape by 2 - 3 million year old basalt flows from north of Ballarat). Gold prospecting shafts penetrated right through the clay deposit.

The clay deposit has not been fully explored in its deepest section, but is probably over 15 metres deep. The deepest clays extracted are in a reduced grey-blue state and have a high shrinkage, but are very plastic and give high green strength. Above these there exists a modified version of the same clay, probably oxidised during a mid-Tertiary weathering phase and somewhat lower in shrinkage. The upper part of the alluvial deposit consists of sandy clays and clayey gravels 5 - 7 metres deep. An acceptable clay mix can be made by discarding the more gravelly sections and mixing part of the sandy clay with the plastic higher shrinkage clay beneath. The clay deposit thins rapidly upstream along two tributary valleys where only thin Recent alluvium covers Ordovician shale.

Ceramic tests on the composite Buninyong stockpile gave the following results:

Extrusion moisture	18%
Drying shrinkage	5.65% linear; 6.16% transverse
Fired shrinkage	2.88% linear; 3.12% transverse (1110°C)
Fired weight loss	5.85%
Fired absorption	4.37%
Dry strength	3.19 MPa
Fired strength	26.65 MPa
Pyroplastic Index	3.85 E-6

Buninyong clay is used in pipe mixes because it gives good plasticity for forming, good green and dry strength, and low pyroplastic index. The fired strength is in part due to the reduced condition of the clay, which gives a strong black core at tunnel kiln firing cycles. However, its plastic nature is likely to increase lamination and off-straight extrusion of pipes and to cause spalling at 300 - 500°C, especially if drying is incomplete.



Plate C1. Vitclay Pipes Pty Ltd (Nubrik), Ballarat plant showing stockpiles of off-white, silty, kaolin from Enfield Pit in the background and left foreground and Bunninyong smectite/kaolin clay, centre right. Neg. No. 39499



Plate C2. Vitclay Pipes, Ballarat. Green (unfired) sewer pipes (right) are stacked on kiln cars ready for firing. After firing, reject pipes (centre) are recycled as 'grog' filler in clay mixes. Neg. No. 39500



C20

Plate C3. Selkirk Brick Pty Ltd, Ballarat North pit showing deeply weathered Ordovician shale used as a non-plastic component of brick clay blends. Neg. No. 39501



Plate C4. Selkirk Brick, extrusion plant. Production, 1 million bricks per week. Neg No. 39502

G02521



Plate C5. Enfield Clay Pit, 20 km south of Ballarat. Tertiary channel and swamp deposits are mined for pale and red burning semi-plastic clay for the brick and pipe industries.

Neg. No. 39503



Plate C6. Enfield Clay Pit. Detail of pale grey silty clay over mottled yellow-brown to red-brown moderately plastic clay.

Neg. No. 39504



Plate C7. Buninyong Clay Pit, 3.5 km west of Buninyong.
Tertiary montmorillonite/kaolin clay used as a 50% component in
clay sewer pipe blends. Neg. No. 39505

APPENDIX D

Field Guide for Post-Conference
Excursion of Kaolin Mining at
Lal Lal and Pittong

**Field Trip Itinerary — ACMS Conference, Ballarat
Thursday February 7, 1991**

MORNING

9 am	Busses depart from Ballarat University College carpark C1.
9.15	Visit to English China Clay's pit at Lal Lal
10.25	Lal Lal Bog-iron Deposits and Blast Furnace. (morning tea)
11.30	Lal Lal Dyke kaolin mine
12.00	Lal Lal Falls

12.45 pm	Lunch at Ballarat University College
----------	--------------------------------------

AFTERNOON

2.00 pm	Busses depart Ballarat University College
2.40	English China Clay's pit at Pittong
4.30	Return to Ballarat University College

LAL LAL

Lal Lal, situated 20 kilometres southeast of Ballarat, has two types of kaolin deposits:

- high quality but small kaolin deposits formed by the weathering of dykes of undetermined rock type.
- larger deposits formed by the insitu weathering of granodiorite

Kaolin was discovered in the Lal Lal area during the 1850's gold prospecting. It has been mined in the Lal Lal - Mt Egerton area almost continuously since 1860's.

Regional geology and geomorphology

The regional geology of the Lal Lal area has been examined by previous workers, the most prominent being Krause (1882), Dunn (1907), Baragwanath (1948), Yates (1953), Currey & Cox (1972) and Roberts (1984). The geology is illustrated in Figure 1 (Day et al. 1988).

The geological history of the region is summarised as follows:

1. Deposition of Ordovician sediments in a marine environment. Lithification and deformation of the sediments, followed by subsequent invasion by numerous quartz veins.
2. The sediments were intruded during the Devonian by granitic magmas, which cooled to form the granite masses, now exposed. These granites have been dated at 355 ± 4 million years.
3. Following the intrusion of the granites, the area underwent regional uplift, and an extensive period of erosion began. The erosion exposed the quartz reefs and parts of the formerly deep-seated granites.
4. From the late Mesozoic to the Cainozoic times, further uplift of the Central Highlands caused renewed erosion in the drainage systems. Coarse gravels, sands and clays were deposited along the Tertiary river valleys.
5. Block faulting to the south during the Tertiary produced the small Lal Lal Graben. The graben, which is only one kilometre wide, contains at least three coal seams of Palaeocene to Eocene age.
6. The numerous lava flows of the Plio-Pleistocene Newer Volcanics covered much of the country, the lava spread beyond the valleys to flood the landscape resulting in the familiar flat volcanic plains of the present day.
7. Following the volcanic activity, the landscape has been dissected by the present-day drainage to produce the current landscapes. (Fig. 2).

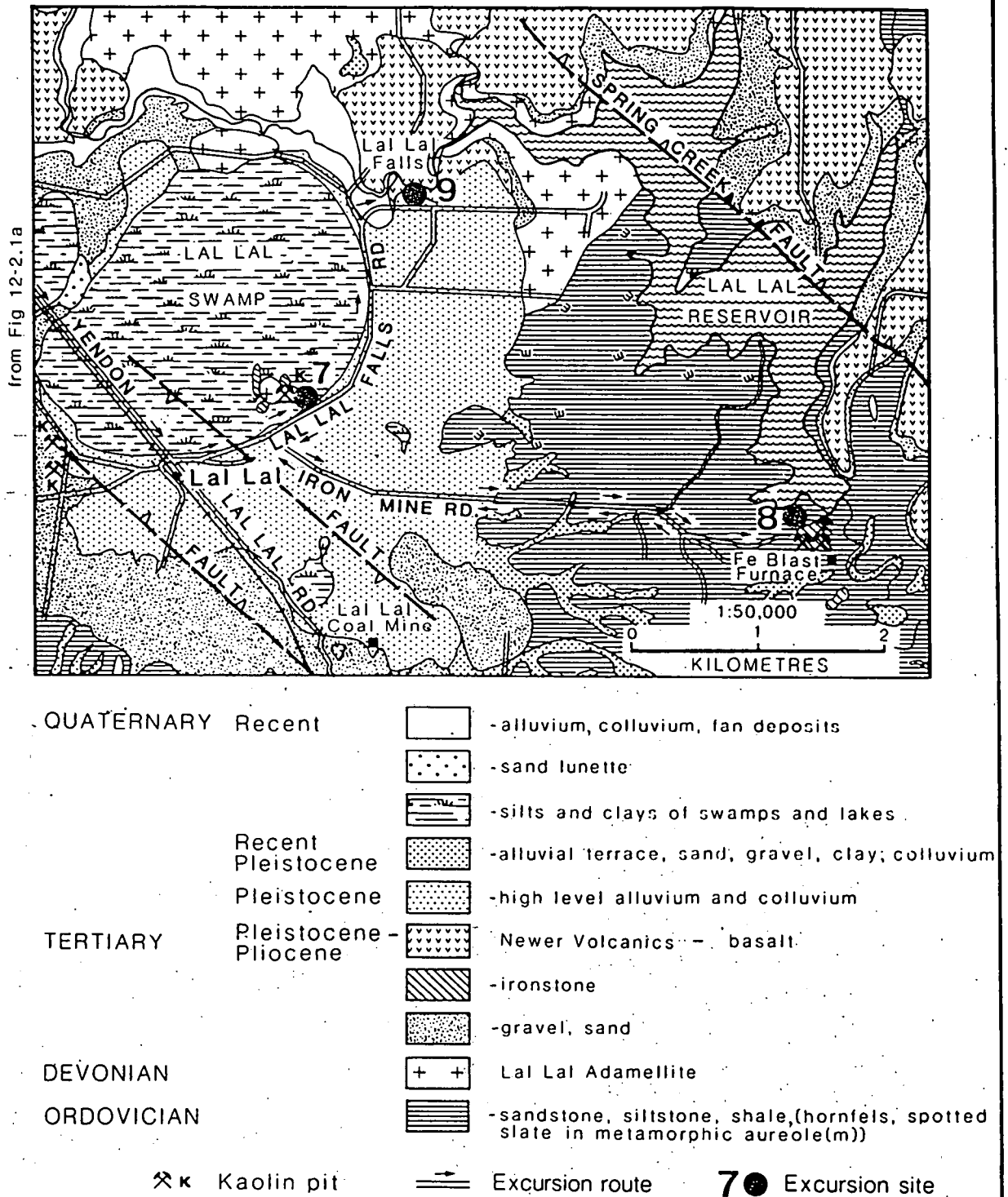


Figure 1. Geology of the Lal Lal area (Day et al. 1988)

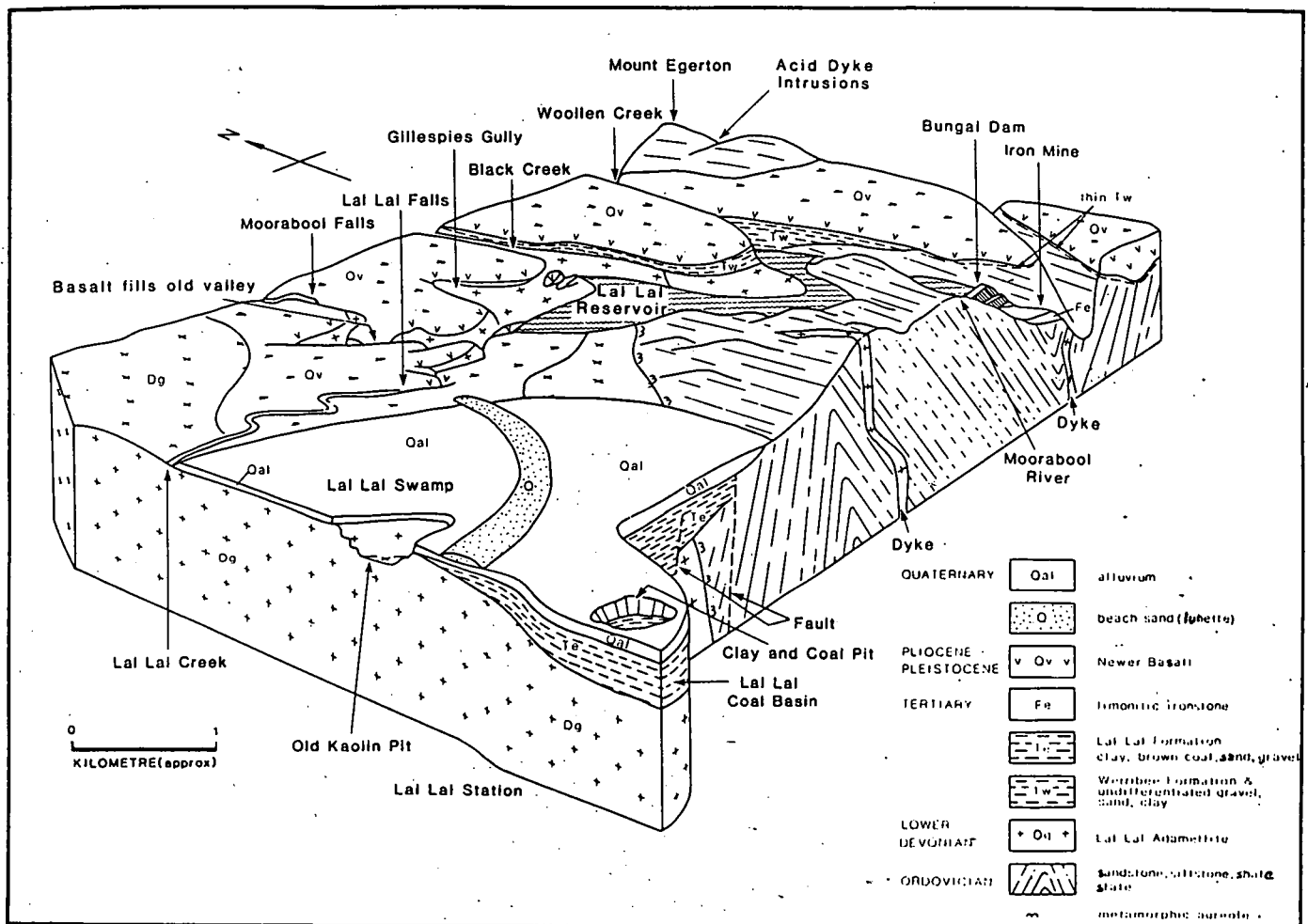


Figure 2. Block diagram of the Lal Lal area

**ENGLISH CHINA CLAY (KAOLIN AUST. / JUPITER MINING)
LAL LAL KAOLIN PIT**

- The kaolin mined at this site is a residual clay formed by the insitu weathering of a granodiorite. The granodiorite is part of the Gong Gong - Lal Lal pluton, of Devonian age.
- The high quality kaolin reserve has a dimension of 800 metres by 200 metres and averages 20 metres thick.
- The deposit is adjacent to basalt which caps most of the Lal Lal Swamp, and part of the kaolin reserve.
- 10,000 cubic metres produced in 1990
- Medium to coarse grained granodiorite. Biotite forms 10-15% of the original rock and is totally broken down in the high quality kaolin.
- Other deposits in the area at Yendon, Warrenheip & Dunnstowen. All have a similar setting, with the kaolin found in the low-lying area, with granodiorite outcropping along the ridges.
- Typical profiles as follows:

Non-basalt area

Peaty soil
orange-brown plastic clay
pale-grey clay, qtz pebbles
kaolin

Basalt Area

Peaty soil
orange-brown plastic clay
orange-brown weathered basalt
dense green basalt
kaolin

- Aplite dyke cuts through the pit. It is fine grained, mainly quartz, some feldspar and mica.
- Palaeochannels delineated by drilling. Now basalt filled. The kaolin is situated on the palaeoridges beneath the alluvium.
- Major problems in getting permission to mine. Long delays in obtaining planning permission, council and resident opposition. Major EIS required. Now severe restrictions are placed on the company.

BUNGAL BOG-IRON DEPOSITS (Fig. 3)

- Small quantities of low-grade iron ore were mined in this area between 1875 and 1902.
- The deposits consist of siliceous limonite of variable grade occurring in beds 1 to 4 metres thick. The largest deposit covers 6 hectares. It unconformably overlies the Ordovician.
- **Theories of formation:**
 - dissected remnants of a basalt-dammed area
 - laterite (ferricrete) formed by deep weathering of Ordovician
 - Tertiary bog-iron formed by chemical deposition of limonite
 - local ferruginisation of Tertiary clay beds
- The ore was smelted at nearby blast furnace, one of the first iron ore smelters in Australia. Iron sent to Ballarat for use in gates, fences, mine skips, and parts of railway locomotives.

LAL LAL DYKE

- Near vertical (85°) and narrow (1-2m), the dyke intrudes the Ordovician.
- Virtually quartz-free, high-grade kaolin (98% pure aluminium silicate), but is iron stained in parts.
- Larger dykes of the same setting occur around Ballarat, particularly in the Mt Egerton area. These dykes generally strike north-south parallel to the regional bedrock. The deepest recorded intersection was at 586 metres in the Sebastopol Plateau No. 1 shaft.
- This particular deposit is currently mined by Mr Martin Stielow under a Miner's Right Claim.

LAL LAL FALLS

The Plio-Pleistocene Newer Volcanics unit at the reserve is approximately 35m thick, and comprises two separate flows. Yates (1954) examined the unit in detail and concluded that it resulted from two separate lava flows from the north. The lava probably issued from a vent at Springbank and flowed southwards down the valley of the ancestral Western Moorabool River.

Within the reserve the boundary between the two flows is apparent on the southern cliff. Both flows exhibit columnar jointing, with the columns in the upper flow being narrower than in the bottom flow. A thin weathered horizon between the two flows indicates a short time interval between the two extrusions.

The basalt of the lower flow is a dark grey, fine-grained, dense material, which appears very uniform throughout the flow. Microscopic examination (Yates, 1954) reveals its composition to be feldspar-rich, olivine-deficient, and containing abundant iron.

The base of the upper flow is vesicular and exhibits remnant flow textures. Above this it is coarser grained, light grey, dense and uniform. Petrology is described by Yates as a typical olivine-rich basalt.

FURTHER READING

- BARAGWANATH, W. 1923 The Ballarat goldfields. *Victoria. Geological Survey Memoirs* 14
- BARAGWANATH, W. 1953 The Ballarat goldfield. In EDWARDS, A.B. *Geology of Australian ore deposits*. Melbourne: Fifth Empire, Mining and Metallurgical Congress
- KING, R.L. 1985 Ballarat 1: 250,000 geological map, explanatory notes. *Victoria. Geological Survey Report* no. 75
- ROBERTS, P.S. 1984 Explanatory notes on Bacchus Marsh and Ballan 1: 50,000 geological maps. *Victoria. Geological Survey Report* no., 76
- YATES, H. 1954 The basalts and granitic rocks of the Ballarat district. *Proceedings of the Royal Society of Victoria* vol. 66:63-102



M. STIELOW ENTERPRISES PTY LTD

EVEREST MINERALS

Tel. No. : 03-687 6482
Mob. No. : 018 315 843
Fax No. : 03-687 6482

TECHNICAL INFORMATION SHEET

KAOLIN-CHINA WHITE

DESCRIPTION:

A HIGH GRADE CHINA CLAY
EXCELLENT COLOUR, LOW IRON CONTENT

CHEMICAL ANALYSIS:

Silica	SiO_2	46.4%
Alumina	Al_2O_3	38.0%
Titania	TiO_2	0.3%
Ferric Oxide	Fe_2O_3	0.3%
Lime	CaO	0.2%
Magnesia	MgO	0.2%
Soda	Na_2O	0.2%
Potash	K_2O	0.3%
Loss on Ignition		13.6%
Specific Surface		24,000 cm^2/g
Oil Absorption (rub out)		48 ml/100g
Reflectance (457 mu)		89 at 1000°C

TYPICAL APPLICATION:

PAPER FILLING AND COATING, CERAMICS,
ADHESIVES, PAINT, RUBBER, PORCELAIN,
INSECTICIDES, COSMETICS,
PHARMACEUTICALS ETC.ETC.

SIZING:

Residue + 75 microns	0.5%
MPD	0.9 microns

All information is given in good faith but no guarantee of accuracy is made nor can we anticipate every possible application of our product. Our product is therefore sold without warranty express or implied and on the condition that the purchaser relies on his own ability to determine the suitability of the product for a particular purpose. Statements concerning the possible use of our product are not intended as recommendation for use. No liability is accepted for infringement of any patents.



ORIGINS OF THE FALLS

The origin of the Lal Lal Falls has been described by Yates (c.1945), from which the following summary is taken:

1. In Pliocene times, during the period of volcanism around the Ballarat district, the first lava flow to reach the reserve flowed down the ancestral valley of the Western Moorabool River. The flow displaced the drainage of the Western Moorabool River to the east.
2. A second lava flow followed after a brief interval, and a contemporaneous flow from the north west flowed down the ancestral valley of the Lal Lal Creek. The effect of these flows was to fill the landscape so that a lake formed at the site of the present day Lal Lal Swamp.
3. The sand brought down by the Lal Lal Creek into the swamp eventually choked the drainage, and the Lal Lal Creek was diverted along the northern boundary of the lake and was captured by a small tributary of the Moorabool.
4. The Moorabool flowed over the edge of the basalt flow at a point about 500 metres southeast of the confluence of the two streams. At this point, where cascades had formed, the erosive power of the river had increased by the addition of the Lal Lal Creek. A waterfall developed due to the columnar jointing of the basalt flows, and began to recede upstream.
5. At the point of confluence, two distinct waterfalls developed - the Lal Lal Falls, and the Moorabool Falls. Both have since receded upstream, to their present positions.

PITTONG

ENGLISH CHINA CLAYS INTERNATIONAL (KAOLIN AUST) PITTONG CLAY PIT

- Residual deposit formed by the weathering of a granite. The kaolin is refined on-site. Around 70% of the product is used in paper manufacture. The remainder mostly finds a market as fillers for plastic, rubber and fibreglass manufacture.
- Information will be given on-site.

INTRODUCTION

ECC International is the worlds largest producer of white pigments for the paper industry. Kaolin Australia Pty Ltd., is a subsidiary of ECC and produces kaolin for markets within the Pacific region.

DEPOSITS

The Pittong mine was first worked in 1972 when the plant opened and until 1988 was the only source of raw material. It now produces 80% of the total plant requirement, the remainder coming from a second pit located at Lal Lal some 56 kms east of the Pittong plant.

Both deposits yield high purity kaolinite derived from deeply weathered primary granodiorites. The depth of alteration ranges between 15 and 50 metres with an average depth of around 30 metres. Recoveries of kaolinite are variable and can range between 10 and 50 wt%. Altered feldspar is classified as either fine, medium or coarse grained clay types, the latter generally yields the highest recoveries. Free iron oxides and oxyhydroxides are found in both deposits and depending on concentration, can result in a wide range of colour variations.

MINING

At Pittong, overburden depth varies between 2 and 3.5 metres. Elevating scrapers are used for both stripping and mining. Ore stockpiles ranging between 3000 and 6000M³ are built in and around at the mine site. Stockpiles are sampled and tested before being trucked to the processing site. Areas to be mined are identified using computer software which utilizes borehole information. Any single property such as brightness, particle size or rheology or a combination of properties can be plotted in the form of a contour map at any predetermined thickness or depth.

At Lal Lal overburden depths vary between 5 and 6 metres. The mine is worked in 3 metre benches and crude clay is extracted by excavator directly into trucks. A drilling programme has been undertaken to identify ore quality and provides the information base for mine development.

Stockpiles are blended to produce products with different properties (see table 1). Stockpile blends are specified by the laboratory. Crude clay is fed into a feed hopper by front end loader. From the hopper it is belt fed into a trommel. Water, dispersant and alkali are added and sufficient energy provided by the trommel to produce a stabilized clay suspension. Coarse sand immediately separates and is rake classified into a stockpile to dewater. Dewatered sand is transported by front end loader to a waste stockpile. Fine sand separates at the hydrocyclone stage and is stored separately.

Final clay sizing is achieved by a combination of hydrocyclones, centrifugation, residue attrition and recombination.

COLOUR BENEFICATION

Clays used as white pigments particularly in the paper and paint industry are tightly controlled in terms of both brightness and shade. This control is achieved by a combination of wet blending and reductive bleaching. Free iron oxides and oxyhydroxides present in crude clay are bleached to reduce Fe(III) to Fe(II). The latter is soluble and can be stabilized and removed with the aqueous phase.

DEWATERING

Following a pH adjustment the sized, beneficiated clay slurry is transferred into large, raked, thickening tanks. When sufficient water has been removed thickened slurry is screened then heat exchanged to ca. 30 deg. C to increase pressing efficiency. Six Charlestown leaf presses provide a continuous feed of pressed clay to the drying plant.

DRYING

Presscake at 65 wt% solids is mixed with 99 wt% solids powder in a twin shaft paddle mixer to produce a 75 wt% solids feed to an extruder. Powder for feed back is generated by Aritor mill into a cyclone. A rotary valve transfers powder from the cyclone into the paddle mixer. Extruded clay is fed by oscillating conveyor to an apron dryer. A 10mm diameter pellet at a moisture of 10 ± 2 wt% is produced and conveyed to bulk storage or to the second Aritor mill.

Powder products are produced by drying pelletised clay to <1.0 wt% moisture in a second Attritor mill. Two bulk powder silos provide storage for pneumatically transported powder. Export markets are serviced with clay in IBC's or 25kg paper sacks.

QUALITY

Process control and product quality is monitored at all stages through the wet and drying processes. The company is actively pursuing ISO 9002 registration.

USES

Kaolin Australia currently produces ca. 60,000 tonnes of hydrous clay products. Approximately half of this output is exported to countries throughout the Pacific region. The major user of china clay is the paper industry with other users being the paint, ceramics, rubber and plastics industries.

	Eckacote	Pittong Filler	Eckalite 120
<hr/>			
Chemical analysis (wt%)			
SiO ₂	46.0	47.0	52.0
Al ₂ O ₃	38.0	38.0	32.0
Fe ₂ O ₃	0.58	0.65	0.83
TiO ₂	0.60	0.70	0.82
CaO	0.03	0.03	0.02
MgO	0.01	0.01	0.05
K ₂ O	0.14	0.20	0.61
Na ₂ O	0.13	0.10	0.10
LOI	14.0	13.3	11.4
<hr/>			
Product form	Pellet or Powder	Pellet or Powder	Powder
<hr/>			
Particle size distribution			
Plus 53 microns	0.05 max	0.05 max	0.05 max
Plus 10 microns	1.0 max	7.0 ± 2	25
Minus 2 microns	83.0 ± 3	70.0 ± 3	45
<hr/>			
Other properties			
Moisture content (wt%)	10% or 1%	10% or 1%	1% max.
150 Brightness (457nm)	84 ± 1	80 ± 1	80 ± 1
Surface area (BET m ² /g)	18	16	11
pH at 10% solids	5 ± 0.5	5 ± 0.05	5 ± 0.05
<hr/>			

NB Where limits are not indicated values are typical.

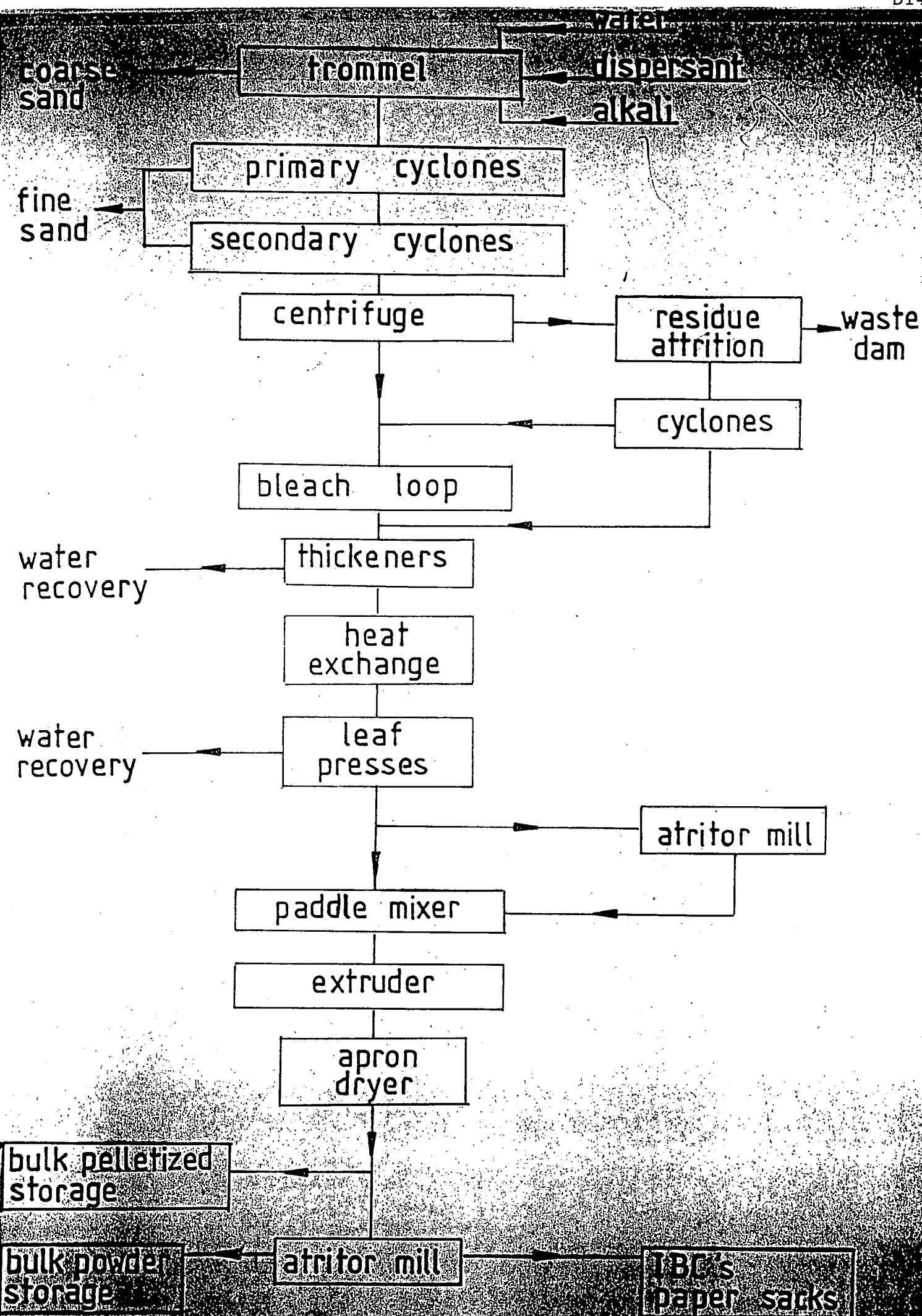




Plate D1. Lal Lal Kaolin Pit (Kaolin Aust. Pty Ltd) Peaty and clay soil overlying kaolinized granodiorite mined and processed for paper-coating and filler-grade kaolin. Feb. 1991.

Neg. No. 39506



D16

Plate D2. Lal Lal Dyke Kaolin Deposit, 25 km southeast of Ballarat. Shed covers head frame to underground kaolin workings operated by M. Stielow Enterprises Pty Ltd for filler and ceramic grade kaolin. Neg. No. 39507



Plate D3. Pittong Kaolin Deposit (Kaolin Aust Pty Ltd). Kaolinized granodiorite which is mined by scraper and beneficiated on site to produce kaolin for the paper industry and for ceramics and general fillers. Feb. 1991.

Neg. No. 39508